Overview: Recent advances on the understanding of the Northern Eurasian environments and of the urban air quality in China - Pan Eurasian Experiment (PEEX) program perspective

Hanna K. Lappalainen[1,2], Tuukka Petäjä[1,2], Timo Vihma[3], Jouni Räisänen[1], Alexander Baklanov[4], Sergey Chalov[5], Igor Esau[6], Ekaterina Ezhova[1], Matti Leppäranta[1], Dmitry Pozdnyakov[7,46], Jukka Pumpanen [8], Meinrat O. Andreae[9,42,43], Mikhail Arshinov[10], Eija Asmi[3], Jianhui Bai[11,44], Igor Bashmachnikov[7], Boris Belan[10], Federico Bianchi[1], Boris Biskaborn[12], Michael Boy[1], Jaana Bäck[13], Bin Cheng[3], Natalia Ye Chubarova[5], Jonathan Duplissy[1,45], Egor Dyukarev[14], Konstantinos Eleftheriadis[15], Martin Forsius[16], Martin Heimann[17], Sirkku Juhola[20], Vladimir Konovalov[18], Igor Konovalov[19], Pavel Konstantinov[5,33], Kajar Koster[13], Elena Lapsina [21], Anna Lintunen[1,13], Alexander Mahura[1], Risto Makkonen[3], Svetlana Malkhazova[5], Ivan Mammarella[1], Stefano Mammola[22,23], Stephany Mazon[1], Outi Meinander[3], Eugene Mikhailov[24, 25], Victoria Miles[6], Stanislav Myslenko[5], Dmitry Orlov[5], Jean-Daniel Paris[26], Roberta Pirazzini[3], Olga Popovicheva[27], Jouni Pulliainen[3], Kimmo Rautiainen[3], Torsten Sachs[28], Vladimir Shevchenko[29], Andrey Skorokhod[30], Andreas Stohl[31], Elli Suhonen[1], Erik S. Thomson [32], Marina Tsidilina[39], Veli-Pekka Tynkkynen [34], Petteri Uotila[1], Aki Virkkula[3], Nadezhda Voropay[35], Tobias Wolf[6], Sayaka Yasunaka [36], Jiahua Zhang[37], Yubao Qiu[37], Aijun Ding[38], Huadong Guo [37], Valery Bondur[39], Nikolay Kasimov[5], Sergej Zilitinkevich (ǂ)[1,2,3], Veli-Matti Kerminen[1] and Markku Kulmala[1,2,39,40,41]

[1]   Institute for Atmospheric and Earth System Research / Physics, Faculty of Science, University of Helsinki, Finland

[2]   Tyumen State University, Department of Cryosphere, 625003 Tyumen, Russia

[3]   Finnish Meteorological Institute, 00101 Helsinki, Finland

[4]   World Meteorological Organization, WMO, Geneva, Switzerland

[5]   Faculty of Geography, Lomonosov Moscow State University, Lenin Hills, 119991, Moscow, Russia

[6]   Nansen Environmental and Remote Sensing Center/Bjerknes Centre for Climate Research, Bergen, Norway

[7]   Nansen International Environmental and Remote Sensing Centre", Nansen Centre, NIERSC, St. Petersburg, Russia

[8]   Department of Environmental and Biological Sciences, PO Box 1627 (Address: Yliopistonranta 1 E), FI-70211 Kuopio, Finland

[9]   Max Planck Institute for Chemistry, Mainz, Germany

[10]   V.E. Zuev Institute of Atmospheric Optics (IAO) SB RAS, Tomsk, 634055, Russia

[11]   LAGEO, Institute of Atmospheric Physics, Chinese Academy of Sciences (IAP-CAS), Beijing, 100029, PR, China

[12]   Alfred Wegener Institute, Helmholtz Centre for Polar and Marine Research, Potsdam, Germany

[13]   Institute for Atmospheric and Earth System Research /Forest Sciences, University of Helsinki, Helsinki, Finland

38 [14] Institute of Monitoring of Climatic and Ecological Systems SB RAS, Tomsk, 634055, Russia; Yugra

39   State University, Khanty-Mansiysk, 628012, Russia

40 [15] ERL, Institute of Nuclear and Radiological Science & Technology, Energy & Safety, NCSR

41   Demokritos, Attiki, Greece

42 [16] Finnish Environment Institute SYKE, Latokartanonkaari 11, 00790 Helsinki, Finland

43 [17] Max-Planck-Institute for Biogeochemistry, Jena, Germany

44 [18] Institute of Geography RAS, Moscow, Russia

45 [19] Institute of Applied Physics, Nizhny Novgorod, Russia

46 [20] Faculty of Biological and Environmental Sciences, University of Helsinki, Helsinki, Finland

47 [21] Yugra State University, Khanty-Mansiysk, 634012, Russia

48 [22]   Finnish Museum of Natural History (LUOMUS), University of Helsinki, Helsinki, 00100, Finland

49 [23]   Molecular Ecology Group (MEG), Water Research Institute (IRSA), National Research Council of Italy

50   (CNR), Verbania Pallanza, 28922, Italy

51 [24] St. Petersburg State University, 7/9 Universitetskaya nab, St. Petersburg, 199034, Russia

52 [25] Multiphase Chemistry and Biogeochemistry Departments, Max Planck Institute for Chemistry, 55020

53   Mainz, Germany

54 [26] Laboratoire des Sciences du Climat et de l'Environnement, IPSL CEA-CNRS-UVSQ, 91190 Gif-sur-

55   Yvette, France

56 [27] Institute of Nuclear Physics, Lomonosov Moscow State University, Moscow, Russia

57 [28] GFZ German Research Centre for Geosciences, Telegrafenberg, Potsdam, Germany

58 [29] Shirshov Institute of Oceanology, Russian Academy of Sciences, Moscow, Russia

59 [30] A.M. Obukhov Institute of Atmospheric Physics, Moscow, Russia

60 [31] Department of Meteorology and Geophysics, University of Vienna, Vienna, Austria

61 [32] Department of Chemistry & Molecular Biology, University of Gothenburg, Göteborg, 41296, Sweden

62 [33] Peoples' Friendship University of Russia (RUDN), Laboratory of sSart technologies for sustainable

63   development of urban environment under global changes, Moscow, Russian Federation

64 [34] Aleksanteri Institute, University of Helsinki, Helsinki, Finland

65 [35] V B Sochava Institute of Geography SB RAS, Irkutsk, 664033, Russia; Institute of Monitoring of

66   Climatic and Ecological Systems SB RAS, Tomsk, 634055, Russia

67 [36] Japan Agency for Marine-Earth Science and Technology (JAMSTEC), Yokosuka, Japan

68 [37] Aerospace Information Research Institute, Chinese Academy of Sciences, Beijing, 100094, China

69 [38] Joint International Laboratory of Atmospheric and Earth System sciences (JirLATEST), Nanjing

70   University, Nanjing, China

71 [39] Institute for Scientific Research of Aerospace Monitoring "AEROCOSMOS", Moscow, 105064, Russia

72 [40] Aerosol and Haze Laboratory, Beijing Advanced Innovation Center for Soft Matter Sciences and

73   Engineering, Beijing University of Chemical Technology (BUCT), Beijing, China

74 [41] Guangzhou Institute of Geography, Guangzhou Academy of Sciences, Guangzhou, China

75 [42] Department of Geology and Geophysics, King Saud University, Riyadh, Saudi Arabia

76   [43]   Scripps Institution of Oceanography, UCSD, La Jolla, CA, USA

77   [44]   Interdisciplinary Scientific and Educational School of M.V.Lomonosov Moscow State

78   University «Future Planet and Global Environmental Change, Russia

79   [45]   Helsinki Institute of Physics, University of Helsinki, 00014 Helsinki, Finland

80   [46]   St. State Petersburg University (St. Petersburg State University, 7/9 Universitetskaya nab. St. Petersburg,

81   199034. Russia

83   **Corresponding author(s):** Hanna Lappalainen, hanna.k.lappalainen@helsinki.fi, Veli-Matti Kerminen, veli-

84   matti.kerminen@helsinki.fi

86   **Keywords**

87   Grand Challenges, climate change, land-atmosphere interactions and feedbacks, biogeochemical cycles,

88   Arctic Ocean, Northern Eurasia, China, Arctic marine ecosystem, atmospheric composition, air quality,

89   Arctic greening, land use change, permafrost, Pan-Eurasian Experiment (PEEX), Global Earth Observatory,

90   Digital Earth, Silk Road Economic Belt, Arctic societies, energy policy, boreal region, science diplomacy

92   **ABSTRACT**

93   The Pan-Eurasian Experiment (PEEX) Science Plan, released in 2015, addressed a need for a holistic system

94   understanding and outlined the most urgent research needs for the rapidly changing Artic-boreal region. Air

95   quality in China, together with the long-range transport of atmospheric pollutants, was also indicated as one

96   of the most crucial topics of the research agenda. These two geographical regions, the Northern Eurasian

97   Arctic-boreal region and China, especially the megacities in China, were indentified as a "PEEX region". It

98   is also important to recognize that the PEEX geographical region is an area where science-based policy

99   actions would have significant impacts on the global climate. This paper summarizes results obtained during

100   the last five years in the Northern Eurasian region, together with recent observations on the air quality in the

101   urban environments in China, in the context of the PEEX program. The main regions of interest are the

102   Russian Arctic, Northern Eurasian boreal forests (Siberia) and peatlands, and the megacities in China. We

103   frame our analysis against research themes introduced in the PEEX Sceince Plan in 2015. We summarize

104   recent progress towards an enhanced holistic understanding of the land – atmosphere – ocean systems

105   feedbacks. We conclude that although the scientific knowledge in these regions has increased, the new

106   results are in many cases insufficient and there are still gaps in our understanding of large-scale climate-

107   Earth surface interactions and feedbacks. This arises from limitations in research infrastructures, especially

108   the lack of coordinated, continuous and comprehensive in situ observations of the study region as well as

109   integrative data analyses, hindering a comprehensive system analysis. The fast-changing environment and

110   ecosystem changes driven by climate change, socio-economic activities like the China Silk Road Initiative,

111   and the global trends like urbanization further complicate such analyses. We recognize new topics with an

112   increasing importance in the near future, especially "the enhancing biological sequestration capacity of

113   greenhouse gases into forests and soils to mitigate the climate change" and the "socio-economic

114   development to tackle air quality issues".

115

Contents

115

116   Contents

117   Table of contents

118   ABSTRACT

119   1. INTRODUCTION

120   2.   RESULTS

121   2.1. LAND ECOSYSTEMS

122   2.1.1 Changing land ecosystem processes (Q1)

123   *High-latitude photosynthetic productivity*

124   *Vegetation changes*

125   *New methodologies determining Earth surface characteristics*

126   2.1.2 Thawing permafrost (Q2)

127   *Observations of ground temperature evolution*

128   *Changing GHG fluxes and VOCs due to permafrost thaw*

129   2.1.3 Ecosystem structural change (Q3)

130   *Changes in microbial activity*

131   *Effects of forest fires on soils*

132   2.2. ATMOSPHERIC SYSTEM

133   2.2.1   Atmospheric composition and chemistry (Q4)

134   *Boreal forests carbon balance*

135   *Arctic methane (CH_4) balance*

136   *Northern Eurasian carbon monoxide (CO)*

137   *Northern Eurasian Ozone (O_3)*

138   *Sources and properties of atmospheric aerosols in boreal and Arctic environments*

139   *Black carbon and dust in the atmosphere and snow*

140   *Methodological and model developments related to atmospheric chemistry and physics*

141   2.2.2 Urban air quality and megacities (Q5)

142   *Air quality in China – recent observations*

143   2.2.3 Weather and atmospheric circulation (Q6)

144   *Cold and warm episodes*

145   *Cyclone density dynamics and atmosphere-ocean interaction*

146   *Circulation effect on temperature*

147   *Cloudiness in Arctic*

148   *Boundary layer dynamics and urban heat islands*

149   2.3   ARCTIC-BOREAL AQUATIC SYSTEM

150   2.3.1 Changing water systems, snow, sea ice and ocean sediments (Q7)

151   *Sea ice and thermodynamics with atmospheric and ocean dynamics*

152   *Snow depth/mass and sea ice thickness*

153 *Ocean floor and Sediments: composition and fluxes*

154 2.3.2 Marine ecology (Q8)

155 *Living marine organisms weaken or even subdue CO_2 accumulation*

156 *Organic carbon in lakes*

157 *Lake ice cover*

158 *Lake Baikal and Selenga River delta*

159 *Asian water lakes*

160 2.4   SOCIETY

161 2.4.1. Anthropogenic impact (Q10)

162 *Mitigation*

163 2.4.2 Environmental impact (Q11)

164 *Reindeer (Rangifer tarandus L.) grazing and ground vegetation structure and biomass*

165 2.4.3 Natural hazards (Q12)

166 *Naturally-determined diseases*

167 *UV variations*

168 3. SYNTHESIS AND FUTURE PROSPECTS

169 3.1 Future research needs from the system perspectives

170 3.2 Feedback mechanisms under changing climate, cryosphere conditions and urbanization

171 3.3 Climate scenarios for the Arctic-boreal region

172 ACKNOWLEDGEMENTS

173 REFERENCES

174

175

176

177 1. INTRODUCTION

178 Earth system is facing major challenges, including climate change, biodiversity loss, ocean acidification,

179 epidemics and energy demand on a global scale (Ripple et al., 2017). These "Grand Challenges" are highly

180 connected and interlinked. This creates a need for an approach of a multidisciplinary scientific program,

181 which could deliver science-based messages to fast-tracked policy making (Kulmala et al., 2015). The recent

182 estimates based on observed atmospheric concentrations of CO_2

183 (ftp://aftp.cmdl.noaa.gov/products/trends/co2/co2_mm_mlo.txt) and business-as-usual scenario show that

184 humankind should find solutions to answer the Grand Challenges (IPCC, 2021). Deep understanding of the

185 feedbacks and interactions between the land, atmosphere and ocean domains, and accounting for social

186 aspects in the regions of substantial changes, are needed for effective technical solutions, mitigation and

187 adaption policy actions. The northern regions (> 45°N), together with the arctic coastal zone and Siberian

188 region in Russia, are among the most critical areas for the global climate (Smith 2011; Kulmala et al., 2015;

189 Kasimov et al., 2015).

190

191 The idea of the Pan-Eurasian Experiment (PEEX) (www.atm.helsinki.fi/peex), originating from a group of

192 Finnish and Russian scientists and research organizations in 2012, is a bottom-up research and capacity

193 building program concentrating on the sustainable development of the Arctic-boreal regions of the Northern

194 Eurasia under changing climate and socio-economic megatrends (Kulmala et al., 2015, Lappalainen et al.,

195 2016). The program was laid on four interconnected parts, namely research agenda, research infrastructures,

196 capacity building and societal impacts (Lappalainen et al., 2014; Kulmala et al., 2016a, Lappalainen et al.,

197 2017, Kulmala 2018). In addition to a strong involvement of the Russian partners, the PEEX China

198 collaboration was established in 2013. China has a strong economic interest in Arctic regions (Tillman et al.

199 2018). Furthermore, China is already facing extensive environmental and air pollution challenges and has

200 major interests toward finding technical solutions for environmental monitoring of the Silk Road Economic

201 Belt Program (SREB) initiated by the President XI Jinping in 2013 (Kulmala 2018, Lappalainen et al., 2018,

202 Dave and Kobayashi, 2018). The PEEX program is an umbrella for several bilateral scientific projects and

203 activities in Russia (e.g. Chalov et al., 2015, 2018; Esau et al., 2016; Alekseychik et al., 2017; Bobylev et

204 al., 2018; Malkhazova et al., 2018; Kukkonen et al., 2020; Ezhova et al., 2018b; Ziltinkevich et al., 2019;

205 Petäjä et al., 2020 submitted; ; Bondur et al, 2019 a,b,c,d,e,f; Yuanhuizi He et al, 2020), whereas in China

206 the primary focus is on the development of atmospheric in-situ stations and advanced air quality monitoring

207 in megacity environments (e.g. Ding et al., 2016 b; Yao et al., 2018; Ying et al., 2020; Wang et al., 2020).

208 Furthermore, PEEX is closely collaborating with the Digital Belt and Road (DBAR) Program coordinated by

209 the Institute for Digital Earth and Remote Sensing (RADI). The PEEX collaboration with DBAR is driven by

210 a need for a novel in-situ station network and ground-based data as a complementary information for the

211 remote sensing in the Silk Road economic region. Long-term development of a "Station Measuring the

212 Earth Surface and Atmosphere Relations" (SMEAR) concept could provide baselines for this (Hari et al.
213 2016; Kulmala 2015, Kulmala 2018; Lappalainen et al., 2018).

214

215 The PEEX program is motivated by the need for obtaining scientific information that combines research in
216 the Arctic and boreal environments, and for understanding large-scale feedbacks and interactions operating
217 in land-atmosphere-ocean systems (Kulmala et al., 2004; Kulmala et al., 2016a; Vihma et al., 2019) and
218 large-scale weather impacts related to the Arctic amplification (e.g. Coumou et al., 2014; Vihma et al.,
219 2020). One of the scientific backbones of PEEX is the previously coordinated research frameworks and their
220 synthesis. For example, the latest comprehensive overview on the interactions between the atmosphere,
221 cryosphere and ecosystems at northern high latitudes was performed by the Nordic Center of Excellence in
222 "Cryosphere-atmosphere interactions in a changing Arctic climate", CRAICC) community (Boy et al.,
223 2019). The PEEX program can upscale the CRAICC results into a wider geographical context.

224

225 Climate change, as a main driver of environmental changes in the Northern Eurasian Arctic-boreal region
226 and China, sets environmental boundaries for the future socio-economic activities of these regions in general.
227 The harsh climate of this region puts a pressure on the ecosystems and living conditions of the local people
228 (e.g. IPCC, 2019). PEEX introduced fifteen large-scale research questions, which would help us to fill the
229 key gaps in our holistic understanding of land-atmosphere interactions and their connections to societies
230 living in the northern Eurasian region (Kulmala et al., 2015; Lappalainen et al., 2018). This approach also
231 sets the framework of the current paper. Here we introduce the recent research progress in the large-scale
232 scientific themes relevant to the PEEX region. The PEEX study region consists of the Northern Eurasian
233 Arctic and boreal (taiga) environments, thus the major geographical part of the environments is located in the
234 Russian territory. China was added to the study area in 2013 as it was seen as locally and globally
235 consequential region for climate change, air quality and long-term transport of atmospheric pollutants
236 (Kulmala et al., 2015 a,b; Lappalainen et al., 2016, 2018).

237 Here we introduce the scientific results from PEEX scientific output, review the main results from PEEX
238 scientific papers and present an analysis of the key gaps in the current scientific understanding. We use the
239 PEEX research agenda structure (Kulmala et al. 2016, Lappalainen et al. 2018) as a reference and mirror new
240 rising themes and results against this plan. For the literature material, we used the following sources for
241 demonstrating the results: (i) individual inputs sent by the PEEX research community, (ii) contents of the
242 scientific papers published in Atmospheric Chemistry and Physics (ACP) PEEX special issue in 2016-2019
243 (www.atmos-chem-phys.net/special_issue395.html) and (iii) scientific outputs from PEEX-labeled projects
244 (www.atm.helsinki.fi/peex/index.php/projects) and other relevant results reported by the PEEX partners. For
245 the individual input, we asked the PEEX research community to identify the main published papers in peer
246 reviewed journals for each question out of their own work and to connect the work with one of the 15
247 science questions introduced in the PEEX science plan. Based on the abstracts we listed "addressed research
248 themes" over last 5 years per PEEX key topical areas (Table 1), which we review in more detail in section 2.

249 The results are first discussed with a holistic approach and then we categorize the advances through a set of

250 identified feedbacks and interactions within the Arctic boreal environment. We follow up with a discussion

251 on the need for a future research infrastructure to be able to provide relevant data and underline the future

252 socio-economics development of the region setting the boundaries for proposed new science-based concepts

253 and technical solutions.

254 **2. RESULTS**

255 In the PEEX Science Plan, we indicated four main thematic research domains: the land system, the

256 atmospheric system, the water system and the society with 15 thematic research areas and related large-scale

257 research questions (Q) presented in Table 1 (Lappalainen et al., 2015), also indicated in the structure of the

258 "Table of Contents". This is the framework we re-visited and utilized in the synthesis of new results of the

259 PEEX community brought together in this paper. Furthermore, we synthetized the results and discuss their

260 contribution to the large - scale feedbacks and interactions in the Arctic context in the sections below.

261

262 2.1. LAND ECOSYSTEMS

263

264 2.1.1 Changing land ecosystem processes (Q1)

265

266 *High-latitude photosynthetic productivity*

267

268 High-latitude terrestrial ecosystems are crucial to the global climate system and its regulation by vegetation.

269 These ecosystems are typically temperature limited, and thus also considered especially sensitive to climate

270 warming. Better understanding of an inter-annual and seasonal dynamics and resilience of the photosynthetic

271 activity of forest vegetation as a whole is needed for the quantification of photosynthesis, or gross primary

272 production (GPP), and for analyzing the carbon balance of the boreal forests. The carbon sink and source

273 dynamics of the boreal forests have been intensively studied during the last five years at the SMEAR

274 (Stations Measuring Atmosphere Ecosystem Relations) II station in Finland (Hari and Kulmala 2005; Hari et

275 al., 2009). Recent results show that the Norway spruce and Scots pine ecosystems are rather resilient to a

276 short-term weather variability (Matkala et al., 2020). Overall, the analyses by Kulmala et al. (2019) and

277 Matkala et al. (2020) on subarctic Scots pine and Norway spruce stands at the northern timberline in Finland

278 serve as examples of the canopy scale dynamics, showing that these ecosystems are generally weak carbon

279 sinks but have a clear annual variation. Kulmala et al. (2019) observed that there is a difference between tree

280 canopy photosynthesis compared to forest floor photosynthesis which starts to increase after the snowmelt.

281 Thus, the models for photosynthesis should also address the snow cover period in order to better capture the

282 seasonal dynamics of photosynthesis of the Northern forests (Kulmala et al., 2019).

283

284 The abundance of tree species, stand biomass, increasing tree growth and coverage of broadleaf species may

285 also affect biogenic volatile organic compound (BVOC) emissions from the forest floor and impact the total

BVOC emissions from northern soils. At least the stand type has been shown to affect BVOCs fluxes from the forest floor in a hemi boreal-boreal region (Mäki et al., 2019). As a whole, BVOCs emitted by boreal evergreen trees are connected to the photosynthetic activity with a strong seasonality and have a crucial role in atmospheric aerosol formation processes over the boreal forest zone. BVOC emissions have low rates during photosynthetically inactive winter and increasing rates towards summer (Aalto et al., 2015). High emission peaks caused by enhanced monoterpene synthesis were found in spring periods simultaneously with the photosynthetic spring recovery (Aalto et al., 2015). This suggests that monoterpene emissions may have a protective functional role for the foliage during the spring recovery state, and that these emission peaks may contribute to atmospheric chemistry in the boreal forest in springtime. Vanhatalo et al. (2018) studied the interplay between needle monoterpene synthase activities, its endogenous storage pools and needle emissions in two consecutive years at a boreal forest in Finland. They found no direct correlation between monoterpene emissions and enzyme activity or the storage pool size. Monoterpene synthase activity of needles was different depending on seasonality and needle ontogenesis. However, the pool of stored monoterpenes did not change with the needle age (Vanhatalo et al., 2018). Also, clear annual patterns of primary biological aerosol particles have been measured from a boreal forest, with late spring and autumn being the seasons of a dominant occurrence. Increased levels of free amino acids and bacteria were observed during the pollen season in the SMEAR II station in Finland, whereas the highest levels for fungi were observed in autumn (Helin et al., 2017).

Extensive measurements of Scots pine photosynthesis and modelling resulted in optimized predictions of the daily behavior and annual patterns of photosynthesis in a subarctic forest (Hari et al., 2017). The study connected theoretically the fundamental concepts affecting photosynthesis with the main environmental drivers (air temperature and light), and the theory gained strong support through empirical testing. Understanding stomatal regulation is fundamental in predicting the impact of changing environmental conditions on photosynthetic productivity. Lintunen et al. (2020) showed that the canopy conductance and soil-to-leaf hydraulic conductance are strongly coupled, and that both soil temperature and soil water content influence the canopy conductance through changes in the belowground hydraulic conductance. In particular, the finding that the soil temperature strongly influences the belowground hydraulic conductance in mature, boreal trees may help to better understand tree behavior and photosynthetic productivity in cold environments. The plant photosynthetic rate is concurrently limited by stomatal and non-stomatal limitations, and recent modelling (Hölttä et al., 2017) and empirical (Salmon et al., 2020) studies suggest that stomatal and non-stomatal controls are coordinated to maximize leaf photosynthesis, i.e. non-stomatal limitations to photosynthesis increase with a decreasing leaf water potential and/or increasing leaf sugar concentration. This new approach allows including the effects of non-stomatal limitations in models of tree gas-exchange (Fig. 1).

Due to climate warming, it seems that trees in high-latitudes have been progressively decreasing their regional growth coherence in the last decades (Shestakova et al., 2019). Shestakova et al. (2019) showed

324   results that unequivocally linked a substantial decrease in the temporal coherence of forest productivity in

325   boreal ecosystems to a less temperature-limited growth that is concurrent with regional warming trends. This

326   emerging pattern points, for example, to an increasing dependence of the carbon balance on local drivers

327   and the role of forests as carbon sinks in the northern Ural region.

328

329   Vegetation gross primary production (GPP) is the largest CO_2 flux of the carbon cycle in terrestrial

330   ecosystems and impacts all of the carbon cycle variables (Beer et al., 2010). Ecosystem models usually

331   overestimate GPP under drought and during spring, late fall and winter (Ma et al., 2015). Several new

332   methodological improvements for a better quantification and scaling of GPP have been reported (Zhang et

333   al., 2018; Pulliainen et al., 2017; Kooijmans et al., 2019). The GPP, measuring photosynthesis, is crucially

334   important for the global carbon cycle and its accurate estimation is essential for ecosystem monitoring and

335   simulation. Pulliainen et al. (2017) introduced a new proxy indicator for spring recovery from *in situ* flux

336   data on CO_2 exchange. This made it possible to quantify the relation between spring recovery and carbon

337   uptake, and to assess changes in the springtime carbon exchange, demonstrating a major increase in the CO_2

338   sink. Zhang et al. (2018) introduced a new water-stress factor that effectively mitigates the overestimation of

339   GPP under drought conditions, while Bai et al. (2018 a,b) developed a method for quantifying the

340   evapotranspiration of crops by using a remote sensing-based two-leaf canopy conductance model. These

341   methods can provide novel insights into the quantification of GPP under different conditions and, in general,

342   into the impacts of biosphere-atmosphere relations on a larger scale.

343

344   Methods for satellite-based remote sensing of photosynthesis have been developed recently based on solar-

345   induced chlorophyll fluorescence signal, such as the OCO-2 product that has an improved spatial resolution,

346   data acquisition and retrieval precision, as compared with earlier satellite missions with solar-induced

347   chlorophyll fluorescence (SIF) capability, which allows for validation of the data directly against ground and

348   airborne measurements (Sun et al., 2017). Interpretation of the solar-induced chlorophyll fluorescence signal

349   has also been improved by many *in situ* studies. For example, Liu et al. (2019a, 2019b) simulated SIF in

350   realistic 3D birch stand reconstructed from terrestrial laser scanning data and found a large contribution of

351   the understory layer to the remote sensing signal.

352

353   *Vegetation changes*

354

355   The normalized difference vegetation index (NDVI) is used for detecting large-scale changes in vegetation

356   productivity. In the past decades, these changes include an increasing NDVI, called "greening", taking place

357   in the tundra regions and a decreasing NDVI, called "browning", in the Northern forest regions (Miles and

358   Esau, 2016). A deeper analysis behind these changes are needed. For example, in Northern West Siberia only

359   18% of the total area had statistically significant changes in productivity either towards greening or

360   browning, and having these opposite trends for different species within the same bioclimatic zone. The

361   observed complexity of the patterns and trends in the vegetation productivity underlines the need for new

362   studies on how forest types and different species are responding to climate and environmental changes in the

363   Northern environments (Miles and Esau, 2016). Also understanding the variations in small-scale plant

364   communities, seasonality and biogeochemical properties are needed for modeling the functioning of the

365   arctic tundra in global carbon cycling. Also the rapid development of the leaf area index (LAI, leaf area per

366   ground area, m^2 m^2) during the short growing season and the yearly climatic variation address the

367   importance of optimal timing of the satellite data images when it is compared with the field verification data

368   in the Arctic region (Juutinen et al., 2017).

369

370   Bondur and Vorobyev (2015) analyzed the vegetation indices and complex spectral transformations derived

371   from processed long-term satellite data (1973-2013) for areas around the cities of Arkhangelsk and

372   Zapolyarny (Murmansk oblast). They demonstrated that these areas are subject to a peak anthropogenic

373   impact associated with specific industrial facilities, leading to changes in landscapes and depletion of natural

374   ecosystems, consequently leading to the decline in the quality of life and health conditions (Bondur and

375   Vorobyev, 2015). Region-wide changes in the vegetation cover and changes in and around several urbanized

376   areas in Siberia reveal robust indications of an accelerated greening near the older urban areas. Many

377   Siberian cities have turned greener while their surroundings have been dominated by wider browning. The

378   observed urban greening could be associated not only with a special tending of within-city green areas but

379   also with urban heat islands and succession of more productive shrub and tree species growing on warmer

380   sandy soils (Koronatova and Milyaeva 2011, Sizov and Lobotrosova 2016). Tundra and forest-tundra biomes

381   are sensitive to mean summer temperatures, which increases production and greening. Taiga biomes are

382   sensitive to precipitation and soil moisture with increased production in wet summer (Miles et al., 2019).

383

384   *New methodologies determining Earth surface characteristics*

385

386   Earth surface characteristics are fundamental knowledge to the understanding and quantification land-

387   atmosphere processes. The methods for determining Earth surface characteristics from satellites are

388   improving. As an example, a method for recognition of the Earth surface types according to space images

389   using an object-oriented classification was developed. The classification relies on Markov stochastic

390   segmentation for object extraction and supervised classification of the objects (Gurchenkov et al., 2017).

391   Furthermore, a prototype algorithm for hemispheric scale detection of autumn soil freezing using space-

392   borne L-band passive microwave observations was developed (Rautiainen et al., 2016) and is currently an

393   operative soil freeze and thaw product that delivers freely available data (*ftp://litdb.fmi.fi/outgoing/SMOS-*

394   *FTService*/). The CryoGrid 3 land surface model provides improved descriptions of possible pathways of ice-

395   wedge polygon evolution and describes better the complex processes affecting ice-rich permafrost

396   landscapes (Nitzbon et al., 2019). In addition, there are new observations for validating satellite observations

397   and permafrost models. Boike et al. (2016) introduced a new, 16-year permafrost and meteorology data set

398   from the Samoylov Island Arctic research site, north-eastern Siberia. Terentieva et al. (2016) introduced

399   maps used as a baseline for validation of coarse-resolution land cover products and wetland data sets at high

400   latitudes. Other examples of available data for the model validation are "BC emissions from agricultural

401   burns and grass fires in Siberia" by Konovalov et al. (2018) and permafrost records at the Lena River delta"

402   by Boike et al. (2016).

403

404   Tundra ecosystems are under pressure and intensifying permafrost thawing, plant growth and ecosystem

405   carbon exchange under the changing climate. The heterogeneity of Arctic landscapes is an extra challenge

406   for environmental monitoring. For example, remote sensing methods are not able to capture variations in

407   moss biomass, which is dominating the plant biomass and controlling soil properties in the Artic. The

408   general accuracy of landscape level predictions in the land cover type (LCT) is good, but the spatial

409   extrapolation of the vegetation and soil properties relevant for the regional ecosystem and global climate

410   models still needs to improved (Mikola et al., 2018). Furthermore, for the future, we need to have a land

411   characterization, in order to perform quantification and assessment of the ecosystem services at different

412   scales using integrative techniques and integrated field observations together with remote sensing and

413   modelling at the landscape scale (Burkhard et al., 2009, Fu and Forsius, 2015). At smaller scales, the isotopic

414   composition of carbon and oxygen in peat can be used for the climate reconstruction (Granath et al., 2018).

415

416   2.1.2 Thawing permafrost (Q2)

417

418   *Observations of ground temperature evolution*

419

420   Permafrost regions of the Northern Eurasia are warming along with the climate (IPCC, 2019). During the

421   Global Terrestrial Network for Permafrost reference decade, 2007 - 2016, the temperature at the depth of

422   zero annual amplitude increased by 0.39 ± 0.15 °C in the continuous permafrost zone and by 0.20 ± 0.10 °C

423   in the discontinuous permafrost zone. At the same time, the mountain permafrost warmed by 0.19 ± 0.05 °C.

424   The global average of the permafrost temperature increased by 0.29 ± 0.12 °C (Biskaborn et al., 2019). The

425   observed trend in the continuous permafrost zone follows the air temperature trend in the Northern

426   Hemisphere.

427

428   The changes in the permafrost region affects climate, hydrology and ecology from local to global scales

429   (Arneth et al., 2010; Hinzman et al., 2005). Several local studies focused on differences introduced by

430   vegetation, soil and hydrological characteristics at the same site (Göckede et al., 2017, 2019). Göckede et al.

431   (2017, 2019) presented findings on shifts in energy fluxes from paired ecosystem observations in northeast

432   Siberia comprising a drained and a corresponding control site. Drainage disturbance triggered a suite of

433   secondary shifts in ecosystem properties, including alterations in vegetation community structure, which in

434   turn influenced changes in snow cover dynamics and surface energy budget. First, the drainage reduced heat

435   transfer into deeper soil layers, which may have led to shallower thaw depths. Second, the vegetation change

436   due to the drainage led to an albedo increase, which decreased the total energy income, or net radiation, into

437   the system. Third, the drainage reduced water content available for evapotranspiration, which resulted in a

438   reduced latent heat flux and increased sensible heat flux, transferring more energy back to the atmosphere.

439   The reported affects led to surface and permafrost cooling (Göckede et al., 2019).

440

441   Kukkonen et al. (2020) compared temperature data from several shallow boreholes in the Nadym region,

442   Siberia, and predicted permafrost evolution for different climate scenarios. The Nadym area represents a

443   typical site located in the discontinuous permafrost zone. Kukkonen et al. (2020) found that the permafrost

444   thawed most rapidly in low-porosity soils, whereas high-porosity soils in the top layer (e.g., peatland)

445   retarded thawing considerably. Similarly, the depth of a seasonally frozen layer and the temperature regime

446   of peat soils in the oligotrophic bog in the southern taiga zone of Western Siberia showed significant

447   differences between the sites with high and low levels of bog waters (Kiselev et al., 2019). Both Kukkonen et

448   al. (2020) and Kiselev et al. (2019) results are in line with previous conclusions on the importance of

449   volumetric water content and unfrozen water content for soil thermal properties governing heat transfer and

450   phase change processes (Romanovsky and Osterkamp, 2000). Locally, the sites with a thin snow cover (e.g.,

451   hill tops) demonstrated a higher resistance to the thawing (Williams and Smith, 1989; Kukkonen et al.,

452   2020). To follow-up on the development of permafrost thaw in different soil types require continuous and

453   comprehensive observations during the coming decades.

454

455   *Changing GHG fluxes and VOCs due to permafrost thaw*

456

457   Biogenic GHG emissions are strongly connected with permafrost conditions and changes in other related

458   environmental conditions, such as soil temperature and moisture conditions. Here we discuss recent results

459   on the observed emissions from these permafrost perspectives and, later in section 2.2.1, address the

460   connections between GHG fluxes and the other environmental factors, like deforestation and forest fires.

461

462   During the permafrost thaw, even small changes in the soil carbon cycle can turn a terrestrial ecosystem from

463   a sink into a source (Schuur et al., 2008). Based on regional *in situ* observations of CO_2 fluxes, Natali et al.

464   (2019) estimated a winter-time carbon loss of 1 662 TgC per year, which is more than predicted by the

465   process models estimates. Furthermore, Natalie et al. (2019) found that even if the soil CO_2 loss were

466   enhanced due to winter warming, the growing season might start earlier and onset the carbon uptake under

467   warming climate conditions. For a better understanding of these connections and both spatial and temporal

468   dynamics of the Arctic carbon cycle, we need more observations from permafrost ecosystems. Additional

469   flux measurements are urgently needed to understand the variation between the current measurements and,

470   especially extended measurements on the CH_4 emissions to better quantify their role in the carbon balance.

471   For example, a new data assimilation system estimates an Arctic carbon sink of -67 g C m^{-2} yr^{-1}, but this

472   value is associated with very high uncertainties. Furthermore, these estimates do not include methane, which

473   is even more difficult to evaluate (López-Blanco et al., 2019). Based on the field flux measurements, the

474   Carbon Cycle Report 2018 (Schuur et al., 2018) estimated that the Eurasian boreal wetland is a source of 14

Tg CH_4 per year. On the other hand, Kirschke et al. (2013) estimations, based on atmospheric

measurements, ends up to the value of 9 Tg CH_4 per year. Locally, methane fluxes measured in 2005-2013

showed significant year-to-year variations. Interestingly, the observed variability in North America,

specifically in the Hudson Bay lowlands, appears to have been driven partly by the soil temperature, while in

the Western Siberian lowlands the variability was dependent on the soil moisture (Thompson et al., 2017).

The comparison of high-resolution modelling of atmospheric CH_4 to CH_4 observations already in 2012 from

the East Siberian Arctic Shelf (ESAS), a potentially large CH_4 source, confirms that methane releases are

highly variable and inhomogeneous (Berchet et al., 2016).

Long-term flux measurements provide insight into the carbon sink - source dynamics. The flux

measurements from the moist tussock tundra in the north-eastern Siberia indicated that drainage influences

the carbon cycle and that the tundra is changing to a weaker CO_2 sink and CH_4 source. Another relevant

observation was that the time outside the growing season influences the carbon balance of ecosystem

processes, especially during the zero-curtain period (Kittler et al. 2017). This is in line with similar studies in

Alaska (Commane et al., 2017; Euskirchen et al., 2017). Therefore, the autumn temperature was identified as

a major driving factor describing the differences between the annual GHG fluxes. Notably, however, the

seasonal amplitudes of CO_2 concentrations in Siberia were found to be significantly higher than those in the

North American continent, likely due to the more intense biological activity here (Timokhina et al., 2015a).

A recent study showed that the Siberian carbon cycle is a major contributor to the Northern Hemisphere

amplitude of CO_2 variation (Lin et al., 2020).

Observations from non-permafrost sites may give us a clue on the future dynamics of fluxes, as the

permafrost is thawing. The chamber measurements of CH_4 and CO_2 fluxes from a non-permafrost site in the

Siberian peatland in August, 2015, showed that the highest values of methane fluxes were obtained in burnt

wet birch forest and the lowest ones in seasonally waterlogged forests (Glagolev et al., 2018). The fluxes can

vary even between different sites of a bog, as measured by Dyukarev et al. (2019). The net ecosystem

exchange (NEE), ecosystem respiration (ER) and gross primary production (GPP), based on the measured

CO_2 fluxes at a ridge-hollow complex bog and a model for ridge and hollow sites at oligotrophic bog in

Middle Taiga Zone of West Siberia, showed that a two-year-average NEE at the hollow site was 1.7 times

higher than at the ridge site (Dyukarev et al., 2019). The ecosystem processes are influenced by drying in

tundra ecosystems. Kwon et al. (2019) reported from Alaska that drying in the tundra ecosystems increased

contributions of modern soil carbon to the ecosystem respiration but, at the same time, decreased

contributions of old soil carbon. These changes were attributed mainly to modified soil temperatures at

different soil layers due to the altered thermal properties of organic soils following drainage. Furthermore,

the drainage lowered CH_4 fluxes by a factor of 20 during the growing season, with post drainage changes in

microbial communities, soil temperatures, and plant communities also affecting the flux reduction in an

Arctic wetland ecosystem (Kwon et al., 2017).

513   Voigt et al. (2016) reported that, under warming conditions, the vegetated tundra in north-eastern European

514   Russia shifted from a GHG sink to a source. The positive warming response was dominated by CO_2;

515   however, N_2O emissions were also significant. N_2O was emitted not only from bare peat, already identified

516   as a strong source, but also from vast vegetated peat areas not emitting N_2O under current climate conditions.

517   These results can be explained by the dynamics between the temperature, nitrogen assimilation by plants and

518   soil microbial activity, having a strong impact on the future GHG balance in Arctic (Voigt et al., 2016; Gil et

519   al., 2017). Studying N_2O emissions from a typical permafrost peatland in Finnish Lapland, it was concluded

520   that about 25% of the Arctic territory are areas that potentially emit nitrous oxide (Voigt et al., 2017). It

521   seems that there is positive feedback mechanism between the permafrost thawing and moisture regime.

522   Predicting the response of soils to climate change or land use is central to understanding and managing N_2O

523   emissions. According to recent results, the N_2O flux can be predicted by models that incorporate soil nitrate

524   concentration (NO_3-), water content and temperature (Pärn et al., 2018).

525

526   In addition to CO_2 and CH_4, thawing or collapsing of arctic permafrost can release volatile organic

527   compounds (VOCs). Li et al. (2020a) examined the release of VOCs from thawing permafrost peatland soils

528   sampled from Finnish Lapland in laboratory. The average VOC fluxes were four times as high as those from

529   the active layer, and mainly attributed to direct release of old, trapped gases from the permafrost. These

530   results demonstrate a potential for substantive VOC releases from thawing permafrost and suggests that

531   future global warming could stimulate VOC emissions from the Arctic permafrost.

532

533   2.1.3 Ecosystem structural change (Q3)

534

535   *Changes in microbial activity*

536

537   Climate change is likely to cause an increased appearance of trees on open peatlands, but we do not know

538   how this vegetation change will influence the below-ground microbiology and composition. Changes along

539   bog ecotones at three Russian peatland complexes suggest that tree encroachment may reduce the trophic

540   level of *Testate Amoeba* communities and reduce the contribution of mixotrophic *Testate Amoebae* to

541   primary production. Thus, it seems that increased tree recruitment on open peatlands will have important

542   consequences for both microbial biodiversity and microbial-mediated ecosystem processes (Payne et al.,

543   2016). We also need to understand better the dynamics affecting the bacteria, fungi and other related species

544   in the ground air layer. Recent studies by Korneykova and Evdokimova (2018) and Korneikova et al. (2018

545   a, 2018b) showed the influences of anthropogenic sources (Copper-Nickel Plant) and acidic soils in Russian

546   northern taiga and tundra on the portion of the airborne fungi, and on the structure of algological and

547   mycological complexes (Korneikova et al., 2018 a, 2018b). New methods were reported on how to improve

548   soil conditions, developed on all kinds of materials made or exposed by human activity that otherwise would

549   not occur at the Earth's surface, referred as "Techno sol engineering" (Slukovskaya et al., 2019), and how to

550   monitor climate change impacts on the functional state of bogs by using *Sphagnum* mosses (Preis et al.,

551   2018).

552

553   *Effects of forest fires on soils*

554

555   Forest fires, a significant environmental factor in the Northern Eurasian region, change soil chemical and

556   physical properties and may influence greenhouse gas fluxes and emissions of BVOCs. Recent results

557   indicate that a slower post-fire litter decomposition has a clear impact on the recovery of soil organic matter

558   following forest fires in northern boreal coniferous forests due to accumulated soil organic matter. The soil

559   recovery is related to slow litter composition and reduced enzymatic and microbial activity (Köster et al.,

560   2016).

561

562   Post-fire studies on the long-term evolution of the structure and functioning of bacterial communities are

563   sparse. Sun et al. (2016) showed that the major drivers influencing bacterial community are the soil

564   temperature, pH and moisture. Furthermore, Köster et al. (2015) analyzed long-term effects of fire on soil

565   CO_2, CH_4 and N_2O fluxes in pine forest stands in the Finnish Lapland, and discussed the role of microbial

566   bio mass in this context. They did not detect significant effects of fires on CO_2 emissions or N_2O fluxes, but

567   there were long-lasting strengthening of the CH_4 sink by the soil. Interestingly, Köster et al. (2018) did not

568   find a similar kind of long-term effect on the $CH4$ sink dynamics in studies carried out in Siberia.

569

570   Forest wildfires also regulate the BVOC emissions from boreal forest floors by changing the ground

571   vegetation. Total BVOC emissions from a forest floor were found to decrease after a forest fire and then to

572   increase again along with the succession of forests (Zhang-Turpeinen et al., 2020). For a comparison, Bai et

573   al. (2017) showed that biomass burning resulted in increased BVOC emission fluxes and ozone

574   concentration above canopy in a subtropical forest in China.

575

576   2.2. ATMOSPHERIC SYSTEM

577

578   Concerning critical atmospheric processes and large-scale climate implications, we concentrate here on

579   greenhouse gases and aerosol particles over Northern Eurasia and Arctic, urban air quality, and issues related

580   to the weather and atmospheric circulation. We summarize the recent measurements on the atmospheric

581   composition relevant to sink and source dynamics in Siberia, on the sources and properties of atmospheric

582   aerosols in Arctic-boreal environments, including black carbon and dust in the atmosphere and snow, and on

583   the methodological and model developments related to atmospheric chemistry and physics (Q4, section

584   2.2.1). Furthermore, we introduce new results and observations on atmospheric pollution in rural, suburban

585   and mega city environments in China and Russia (Q5, section 2.2.2). We briefly show some recent results

586   related to synoptic-scale weather in Artic-boreal regions, focusing on cold and warm episodes, cyclone

587 density and atmosphere-ocean interaction, effects of circulation on temperature and moisture, cloudiness in

588 the Arctic, and boundary layer dynamics (Q6, section 2.2.3).

589

590   2.2.1   Atmospheric composition and chemistry (Q4)

591

592 *Boreal forests carbon balance*

593

594 As already discussed in section 2.1.1, boreal forests as a carbon sink and the related role of forestation have

595 been under international debate. It seems that early snowmelt increases springtime carbon uptake of the

596 boreal forests of Eurasia and North America and shows a major advance in the CO_2 sink (Pulliainen et al.,

597 2017). A scenario of a complete global deforestation by Scott et al. (2018), combining radiative forcing to

598 CO_2, surface albedo and short-lived climate forcers (SLCFs), suggests that global deforestation could cause a

599 0.8 K warming after 100 years, with SLCFs contributing 8% of the effect. However, deforestation as

600 projected by the RCP8.5 scenario leads to zero net radiative forcing from SLCF, primarily due to

601 nonlinearities in the aerosol indirect effect. Tuovinen et al. (2019) showed that methane fluxes vary strongly

602 with a wind direction in a tundra ecosystem having heterogeneous vegetation. By combining very high-

603 spatial-resolution satellite imagery and footprint modelling, they were able to estimate the relation between

604 the main land cover types and ecosystem-level measurements. CH_4 emissions originated mainly from wet fen

605 and graminoid tundra patches, whereas the areas of bare soil and lichen acted as strong CH_4 sinks (Tuovinen

606 et al. 2019. Tsuruta et al. (2017) reported posterior mean global total emissions of 516 ± 51 Tg CH_4 yr^{-1} during

607 2000-2012, which indicates that these emissions had increased by 18 Tg CH_4 yr^{-1} from the period 2001-2006

608 to the period 2007-2012. This increase can be explained by increased emissions from the temperate region in

609 South America and from the temperate region and tropics in Asia.

610

611 Analysis of the trends and the diurnal, weekly and seasonal cycles of CO_2 and CH_4 mixing ratios derived

612 from the long-term data of the "Japan–Russia Siberian Tall Tower Inland Observation Network" showed that

613 the frequency of identified events of elevated concentration differs for CO_2 and CH_4 and may reach up to

614 20% of days in some months (Belikov et al., 2019). These observations made it possible to reduce

615 uncertainties in the biosphere surface CO_2 uptake (Kim et al., 2017). Although the CO_2 uptake in boreal

616 Eurasia estimated by Kim et al. (2017) was about 30% lower than that obtained without the assimilation of

617 Siberian observation data, Siberia still remains a key contributor to the terrestrial CO_2 sink in the Northern

618 Hemisphere.

619

620 There are tendencies of a significant growth or suppression of soil CO_2 fluxes across different types of

621 human impacts, such as forest fires, trampling, settlements, reindeer grazing and clearcuts on cryogenic

622 ecosystems in Russia (Karelin et al., 2017). For example, Ivanhov et al. (2019) analyzed CO_2 measurements

623 during 2010-2017 and reported CO_2 concentration increases of 20 ppm in Tiksi at a coast of Laptev Sea and

624 of 15 ppm at the Cape Baranov station. They also detected that wildfires in Siberia can lead to a parallel

625   increase of the CO_2 concentration at the Russian Arctic. Furthermore, the measurements showed that the

626   atmospheric CO_2 concentration increased on average by 2.0 ppm yr^{-1} during 2006-2013 in central Siberia,

627   with a large inter-annual variations. The highest increase were found in 2010 and 2012 (3.6 and 4.3 ppm yr^{-1}

628   , respectively), when large wildfires released huge amounts of CO_2 in Siberia (Timokhina et al., 2015b).

629   Repeated wildfires in boreal forests can combust a portion of the thick organic soil layer characteristic for

630   this ecosystem, and change the forests from a carbon sink into a carbon source (Walker et al., 2019). A study

631   on a fire chronosequence of the central Siberian permafrost soil showed that soils affected by fires over

632   decades act as CO_2 sources, and that the CO_2 emissions from these soils increased with an increasing time

633   since the last fire (Köster et al., 2018). However, there were no similar effects on CH_4 emissions, with soils

634   acting as a CH_4 sink without any connection to forest fires. In addition to CO_2, wildfires also release large

635   amounts of other trace gases and aerosols. Emission factors of several trace gases and aerosols from Siberian

636   fires measured from the Trans-Siberian railway were reported by Vasileva et al. (2017). The impact of

637   Siberian fires as elevated aerosol concentrations was at times observed to extend up on the Arctic coast

638   (Asmi et al., 2016).

639

640   *Arctic methane (CH_4) balance*

641   Deep understanding on the dynamics of methane emissions in the Arctic is needed for identifying and

642   quantifying GHG-related feedbacks and global methane cycle (Dean et al., 2018). During the winter,

643   methane originates mostly from anthropogenic sources, while on smaller scales also emissions from the

644   oceans, including the Eastern Siberian Arctic Shelf (ESAS), can play an important role. During the warm

645   season, the balance is dominated by emissions from wetlands and freshwater bodies. Thonat et al. (2017)

646   employed the CHIMERE model for an assessment of the methane cycle in Arctic. They reported that all

647   methane sources, except biomass burning, contributed to measurements at six study sites. That study

648   emphasizes the importance of a joint model-measurements approach for studies of complex phenomena at

649   large spatial scales. Accounting for OH oxidation and soil uptake, two important sinks of methane, improved

650   the agreement between observed and modelled methane concentrations (Thonat et al., 2017). Peltola et al.

651   (2019) up-scaled CH_4 fluxes measured at 25 northern wetland sites and showed three different maps of

652   wetland distribution with the annual methane emissions varying from 31to 38 $Tg(CH_4)$ yr^{-1}. (For the monthly

653   up scaled CH_4 flux data products see *doi.org/10.5281/zenodo.2560163*). Multiple sources, together with

654   different spatiotemporal dynamics and magnitudes, are influencing the total Arctic CH_4 budget and addresses

655   the need for the further improved assessments (Peltola et al., 2019; Thonat et al., 2017).

656

657   *Northern Eurasian carbon monoxide (CO)*

658   Analysis of long-term trends in the atmospheric composition in remote Northern Eurasia (1998–2016)

659   showed that the total column carbon monoxide (CO) amount has been stabilized or increased in summer and

660   autumn months (Rakitin et al., 2018). The changes in the global photochemical system, especially changes in

661   the ratio between the sources and sinks of minor atmospheric chemical species, could explain these trends

662   (Skorokhod et al., 2017). A comparative study (1998–2014) on the atmospheric total column CO amount in

663 background and polluted regions of Eurasia indicated that this amount has decreased remarkably in the

664 Moscow urban environments (3.73%±0.39% per year) compared to the background regions (0.9–1.7% per

665 year) (Wang et al., 2018a).

666

667 *Northern Eurasian Ozone (O₃)*

668 Atmospheric measurements of ozone, its precursors and other pollutants over Siberia are important for the

669 atmospheric chemistry modelling, satellite product validation and comparisons between Siberia and other

670 regions of the Northern Hemisphere. Isoprene and monoterpenes together with nitrogen oxides impact

671 tropospheric O_3 formation and lead to an increase in the daytime ozone-forming potential (OFP) in urban

672 environments. Bai et al. (2021) showed that O_3 may respond either positively or negatively to isoprene and

673 monoterpene emissions depending on the level of solar radiation and atmospheric loadings of trace gases and

674 aerosol particles. It was demonstrated that monoterpenes have a major contribution to tropospheric O_3

675 formation, especially in cities in Siberia having high atmospheric NOx concentration (10-20 ppb) and

676 daytime temperatures (>25 °C) (Berezina et al., 2019). In contrast, isoprene is dominating the O_3 formation

677 and the increasing OFP in the cities in Far East. The isoprene-derived OFP can originate from deciduous

678 vegetation growing in city environments or nearby regions, or from an anthropogenic isoprene source. The

679 monoterpene-derived OFP was found to be the lowest in medium-size cities and the highest in small cities

680 (Berezina et al., 2019). The total contribution of benzene and toluene to photochemical O_3 production was

681 found to be up to 60–70% in urbanized environments, indicating anthropogenic pollutant sources

682 (Skorokhod et al., 2017). In addition to atmospheric chemistry, the connection between stratospheric O_3, UV

683 radiation and health effects needs to be addressed in the populated urban environments of Siberia. Chubarova

684 et al. (2019b) estimated that the wintertime O_3 depletion in northern regions of Siberia is not critical, but the

685 much larger O_3 reductions observed in the early spring can lead to dangerous levels of erythema UV

686 radiation (see also section 2.4.3 Natural Hazards and UV variation) .

687

688 *Sources and properties of atmospheric aerosols in boreal and Arctic environments*

689

690 Atmospheric new particle formation (NPF) is the largest contributor to the number concentration of aerosol

691 particles in the global troposphere. During the past couple of decades, NPF has been measured in more than

692 10 boreal forest sites (Kerminen et al., 2018). The annual frequency of NPF event days varies between about

693 10 and 30% in the boreal forest zone, being the highest in the western part of this region and lowest in the

694 northern edge and Siberian part of it. Similar high nucleation frequencies were found at two very remote

695 sites in boreal North America (Andreae et al., 2019). In contrast, annual NPF event frequencies below 2%

696 were reported from central Siberia (Wiedensohler et al., 2019). Similarly, in the northern Siberia on the

697 Arctic coast, NPF events were mainly connected with marine and coastal air masses and rarely observed in

698 continental air masses (Asmi et al., 2016). Seasonally, NPF tend to be most frequent during spring, even

699 though high NPF event frequencies can also be observed during summer or autumn. Winter-time NPF is rare

700 throughout the boreal forest region. In the Arctic, NPF appears to be a major aerosol particle source from

701   spring to summer, after which this source collapses during autumn and is practically absent over the whole

702   winter (Freud et al., 2017). 20 years of NPF observations in a boreal forest at the SMEAR II station in

703   Finland show higher frequency of NPF events under clear-sky conditions in comparison to cloudy conditions

704   (Dada et al. 2017). Also oxidized organic vapors showed a higher concentration during the clear-sky NPF

705   event days, whereas the condensation sinks and some trace gases had higher concentrations during the

706   nonevent days.

707

708   The overall importance of atmospheric NPF in boreal and Arctic areas depends on the growth of freshly-

709   formed particles to cloud condensation nuclei. In the boreal forest environment, both observations and model

710   simulations indicate that the particle growth is tied strongly with the oxidation products of biogenic volatile

711   organic compounds originating from forest ecosystems (Paasonen et al., 2018; Östrom et al., 2017). The

712   important compound group in this respect are monoterpenes, even though also sesquiterpenes were found to

713   have high secondary organic aerosol yields in boreal forest environments (Hellén et al., 2018). The observed

714   particle growth rates were found to increase with an increasing particle size and to be highest in summer

715   (Paasonen et al., 2018). The chemistry of new particle growth in the Arctic atmosphere is not well

716   characterized, even though available observations suggest that this growth is associated mainly with biogenic

717   emissions from high-latitude marine areas (Giamarelou et al., 2016; Heintzenberg et al., 2017; Kecorius et

718   al., 2019).

719

720   Wildfires are an important source of particulate pollutants on a global scale and are affecting both air quality

721   and climate (Andreae, 2019; Bondur et al., 2020). Satellite observations indicate that the annual burned area

722   by wildfires in Russia decreased by a factor of 2.6 during 2005–2016 owing to early detection and

723   suppression of fire sources, whereas in Ukraine the relative size of burned-out areas increased by a factor of

724   6–9 from 2010–2013 to 2014–2016 (Bondur et al., 2017; 2019d). For Siberia, Ponomarev et al. (2016)

725   reported strong increases in both number and burned areas based on satellite data, with burned areas

726   doubling from 2005 to 2016. While biomass burning emissions have been measured widely over Russia

727   (Bondur, 2016; Bondur and Ginzburg, 2016; Bondur et al., 2019d), there is still a need for further

728   information on the atmospheric composition of wildfire emissions and related emission ratios from the

729   Siberian region. Fire experiments provide important information on the emission and aging characteristics of

730   smoke aerosols (e.g. Kalogridis et al., 2018).

731

732   Luoma et al. (2019) presented a detailed trend analysis for aerosol optical properties at the SMEAR II station

733   in Finland. They found a statistically significantly decreasing trend for the scattering coefficient, and even a

734   stronger decreasing trend for the absorption coefficient during 2006 – 2017. These trends are very likely

735   indicative of decreasing influence of anthropogenic emissions, with the contribution from emissions

736   containing black carbon decreasing even faster.

737

738 Measurements of carbonaceous aerosols over central Siberia during 2010-2012 showed that in fall and

739 winter, high concentrations of such aerosols were caused by long-range transport from the cities located in

740 southern and southwestern regions of Siberia (Mikhailov et al., 2015a). In spring and summer, pollution

741 levels were high due to regional forest fires and agricultural burning in the Russian-Kazakh region. The

742 variability of the background concentration of organic aerosols correlated with the air temperature in

743 summer, implying that biogenic sources dominated the formation of organic particles at that time of the year

744 (Mikhailov et al., 2015b). Based on a five-year study by Mikhailov et al. (2017), it seems that the

745 atmospheric pollution originating from the biomass burning and anthropogenic emissions is

746 significantly affecting the Siberian region. However, in summer precipitation is removing the

747 pollutants from the air and leading to relatively clean atmospheric conditions in this region.

748

749 At circumpolar sites over the Arctic, aerosol optical properties were found to vary both seasonally and

750 spatially (Schmeisser et al., 2018). Arctic haze aerosols in late winter and spring are characterized by

751 increased concentrations of sulfate, whereas in summer rich organic chemistry seems to be associated with

752 vegetation, local urban and shipping sources as well as secondary aerosol formation influenced by emissions

753 from low latitude Siberia (Popovicheva et al., 2019a). In a longer perspective, Arctic observations show large

754 decreases in both sulfate and black carbon concentrations since the early 1980s (Breider et al., 2017).

755

756 Observations on the elemental composition of surface aerosols on the coastal Kandalaksha Bay of the White

757 Sea were indicative of the dominance of biogenic aerosol particles during summer time, with heavy metal

758 concentrations in aerosols being at Arctic background levels (Starodymova et al., 2016). Increases in Ni and

759 Cu concentrations were observed in air masses arriving from the western part of the Kola Peninsula

760 indicative of emissions from the smelters in that region.

761

762 *Black carbon and dust in the atmosphere and snow*

763

764 Black carbon (BC) is a potentially large contributor to climate forcing in the Arctic region, however, the

765 assessment of its pollution is hampered by the lack of aerosol studies in Northern Siberia (Popovicheva et al.,

766 2019). The spatial variability of Arctic BC was studied using a harmonized dataset from six circumpolar

767 Arctic observatories (Backman et al., 2017). These data suggested a significant spatial and seasonal

768 variability (Schmeisser et al., 2018), addressing a need for more year-round data. BC observations (Sep 2014

769 – Sep 2016) at the Hydrometeorological Observatory Tiksi at a coast of the Laptev Sea showed a seasonal

770 variation, with the highest concentrations (up to 450 ng/m^3) from January to March and the lowest ones

771 (about 20 ng/m^3) in June and September. During winter, stagnant weather and stable atmospheric

772 stratification resulted in the accumulation of pollution, depending also on the wind direction and air mass

773 transport (Popovicheva et al., 2019a).

774

775   For Arctic, important sources of BC include industrial regions of Northern Europe, gas flares of the oil fields

776   in the North Sea and Siberia, and Siberian biomass burning (Shevchenko et al., 2015; Konovalov et al.,

777   2018). In 2012, for example, approximately a quarter of the biogenic BC emissions from Siberia after fire

778   season were transported into the Arctic (Konovalov et al., 2018). Popovicheva et al. (2017a) analyzed the BC

779   origins over the Russian Arctic seas together with simulated BC concentrations. Concentrations were

780   observed to be high (100-400 ng m^{-3}) over the Kara Strait, Kara Sea and Kola Peninsula, and extremely high

781   (about 1000 ng m^{-3}) over the White Sea. It seems that the gas-flaring emissions from the Yamal-Khanty-

782   Mansiysk and Nenets-Komi regions affected the measurements made over the Kara Strait (northerly 70 °N)

783   region, while the Near Arkhangelsk (White Sea) region was connected to the biomass burning in mid-

784   latitudes. Combustion in Central and Eastern Europe were also identified as important BC sources.

785

786   Atmospheric aging promotes an internal mixing of BC with other aerosol constituents, leading to enhanced

787   light absorption and radiative forcing. *In situ* observations at Arctic stations demonstrated an absorption

788   enhancement due to the internal mixing of BC, which is a systematic effect and should be considered for

789   quantifying the aerosol radiative forcing in this region (Zanatta et al., 2018).

790

791   Regional modelling of the Arctic aerosol pollution showed that long-range transported anthropogenic

792   emissions and biomass burning are the main contributors to direct aerosol radiative effects in the region

793   (Marelle et al., 2018). However, a scenario for 2050 indicates that shipping emissions in the Arctic Ocean

794   could become the main source of surface aerosol and local flaring as a major source of BC, as the flaring

795   already is a major source of BC in northwestern Russia. Kühn et al. (2020) assessed the effects of different

796   BC mitigation measures on Arctic climate and showed that reducing BC emissions by the Arctic Council

797   member states can reduce BC deposition by about 30 % compared to the current situation. A full execution

798   of recommendation by the Arctic Council member and observer countries could reduce the annual global

799   premature deaths due to PM by ~9 % by 2030 (Kühn et al. 2020). Evangeliou et al. (2018) estimated the

800   origin of elemental carbon (EC) in snow and showed that for western Siberia where gas flaring emissions is a

801   major contributor, the model underestimation was significant. Furthermore, the model was evaluated by

802   independent BC measurements in snow over the Arctic showed and, again, the model underestimated BC

803   concentrations, especially in spring.

804

805   Climatically significant cryosphere effects of light-absorbing, high-latitude dust can be similar to the albedo

806   and melt effects of BC (Peltoniemi et al., 2015; Svensson et al., 2016, 2018; Meinander et al. 2020a, 2020b).

807   Iceland is the most significant source for European Arctic dust and plays a role in the cryosphere-

808   atmosphere-biosphere interactions and feedbacks (Boy et al., 2019; Dragosics et al., 2016, Dagsson-

809   Waldhauserova and Meinander, 2019). Dust storms from technogenic mining industry tailing dumps on the

810   Kola Peninsula are also an important source of local atmospheric pollution for neighbor cities, e.g., Apatity

811   and Kirovsk (Amosov et al., 2020). Besides regional-scale dust storms from deserts in Kazakhstan, also

812   Mongolia and China are significant sources of aerosol pollution for these regions and for the Northern Asia.

813

Methodological and model developments related to atmospheric chemistry and physics

815

816 Several methods to characterize the atmospheric chemistry were introduced or improved. Motivated by the

817 ability of atmospheric ion measurements to identify new particle formation (NPF) events in the atmosphere

818 (Leino et al., 2016), a new classification method for atmospheric NPF was developed (Dada et al., 2018).

819 The new method uses both ion and aerosol particle number concentration measurements in the size ranges of

820 2-4 nm and 7-25 nm, respectively, is complementary to the traditional event analysis, and can also be used as

821 an automatic way of determining new particle formation events from large data sets. Zaidan et al. (2018b)

822 used a mutual information approach for a variety of simultaneously monitored ambient variables, including

823 trace gas and aerosol particle concentrations and several meteorological variables, in order to identify key

824 factors contributing to atmospheric NPF. This method can be used in the atmospheric studies also to discover

825 other interesting phenomena and relevant variables. The NPF is directly observed by monitoring the time

826 evolution of ambient aerosol particle size distributions. A new machine learning-based approach, a Bayesian

827 neural network (BNN) classifier, points out the potential of these methods and suggest further exploration in

828 this direction (Zaidan et al., 2018a).

829

830 The condensation sink, being proportional to the surface area of an aerosol population, is one of the major

831 parameters controlling NPF. A simple model for the time evolution of the condensation sink in the

832 atmosphere for intermediate Knudsen numbers was developed to describe the coupled dynamics of the

833 condensing vapor and the condensation sink (Ezhova et al., 2018a). The model gives reasonable predictions

834 of condensation sink dynamics during periods of particle growth by condensation in the atmosphere. A new

835 empirical relation between the atmospheric cloud condensation nuclei (CCN) concentration and aerosol

836 optical properties was derived (Shen et al., 2019), making it possible to estimate CCN concentrations at sites

837 with continuous observations of aerosol optical properties.

838

839 Empirical models of solar radiation were developed and used for calibrations of solar radiometers (Bai,

840 2019). This method can be used to calibrate all kinds of solar radiometers. A solar radiation model combined

841 with ceilometer and pyranometer measurements was used to classify clouds at SMEAR II (Ylivinkka et al.,

842 2020) It opens new possibilities for studies of aerosol-cloud interactions.

843

844 Che et al. (2016) made an inter-comparison of three satellite (AATSR Level 2) aerosol optical depth (AOD)

845 products (SU, ADV and ORAC) over China. The SU algorithm performs very well over sites with different

846 surface conditions in mainland China from March to October, but slightly underestimates AOD over barren

847 or sparsely vegetated surfaces in western China. The ADV product has the same precision and error

848 distribution as the SU product. The main limits of the ADV algorithm are underestimation and applicability.

849 The ORAC algorithm has the ability to retrieve AOD at different ranges, including high values of AOD, but

850 its stability deceases significantly with an increasing AOD, especially when AOD > 1.0 (see also section

851 2.2.2 Urban air quality and megacities).

852

853 One of the major problems for both interpretation of satellite data and applications of empirical models of

854 solar radiation is related to elevated aerosol layers in the atmosphere. It was demonstrated that their origin

855 can be attributed at a higher confidence when back trajectories are combined with lidar and radiosonde

856 profiles (Nikandrova et al., 2018).

857

858 Black carbon measurement methods have progressed. A representative value for the multiple scattering

859 enhancement factor, a fundamental quantity correcting atmospheric black carbon measurement using an

860 aethalometer, was derived for the first time in the Arctic environment (Backman et al., 2017). By analyzing

861 BC measurements made with an Aethalometer in Nanjing, Virkkula et al. (2015) showed that the

862 compensation parameter of a widely-used data processing method depends both on single-scattering albedo

863 and backscatter fraction of the aerosol (see also section 2.2.2 Urban air quality and megacities). The

864 multiple-scattering correction factor of quartz filters and the effect of filtering particles mixed in snow was

865 estimated by Svensson et al. (2019) who applied the method for analyzing light absorption and BC in snow

866 samples taken from the Finnish Lapland and the Indian Himalayas.

867

868 Measurement of atmospheric sub-10 nm particle number concentrations has been of substantial interest

869 recently. A new high flow differential mobility particle sizer (HF-DMPS) was built, calibrated and operated

870 in field conditions for one month (Kangasluoma et al. 2018). The counting uncertainties of the HFDMPS

871 were reduced by about 50% as compared to the traditional DMPS. The HFDMPS detected about two times

872 more particles than the DMPS in the size range of 3–10 nm. Below 3 nm, the HF-DMPS is currently limited

873 by the inability of diethylene glycol to condense on biogenic particles. For collecting BVOC samples, a

874 novel collection method offering portability and improved selectivity and capacity was developed. A solid-

875 phase microextraction (SPME) Arrow sampling (Barreira et al. 2018) can be used for static and dynamic

876 collection of BVOCs in the field conditions. A significant improvement on sampling capacity was observed

877 with the new SPME Arrow system over SPME fibers. A fully automated online dynamic in-tube extraction

878 (ITEX)–gas chromatography/mass spectrometry (GC/MS) method was introduced for continuous and

879 quantitative monitoring of volatile organic compounds in air (Lan et al. 2019). The stability and suitability of

880 the developed system was validated with a measurement campaign, and the ITEX method provided 2–3

881 magnitudes lower quantitation limits than established methods. Parshintsev et al. (2015) introduced a new,

882 fast analysis method for the desorption atmospheric pressure photoionization high-resolution (Orbitrap) mass

883 spectrometry (DAPPI-HRMS). The DAPPI results agreed with the aerosol particle number measured with an

884 established method and was found to detect different compounds and giving complementary information

885 about the aerosol samples.

886

Fragmentation of molecular clusters inside mass spectrometers is a significant uncertainty-source in many chemical applications. A novel model, capable of quantitatively predicting the extent of fragmentation of sulfuric acid clusters was developed (Passananti et al. 2019). The fragmentation cannot be described in terms of rate constants under equilibrium conditions, because clusters accelerate under electric fields (Zapadinsky et al. 2019). A model describing an energy transfer to the cluster internal modes caused by collisions with residual carrier gas molecules was developed. The model can be used to interpret experimental measurements done with atmospheric pressure interface mass spectrometers.

Recently, a new atmospheric observation site equipped with state-of-the-art atmospheric aerosol instrumentation was deployed in Beijing, China (Liu et al. 2020). At the Beijing University of Chemical and Technology (BUCT), the Aerosol and Haze Laboratory (AHL) was established in 2018 - 2019, providing novel insights into air pollution in a comprehensive manner. The station hosts comprehensive instrumentation to concentrations of atmospheric trace gases, aerosol particle size distributions and mass concentrations, particle chemical composition on the levels from molecules, clusters and nanometer to micrometer sized aerosol particles. For example, the first results showed increased cluster mode particle number concentrations during NPF events, whereas during haze days accumulation mode particle number concentrations were high (Zhou et al., 2020). The observations have enabled to quatify number emission factors and underlined the importance of traffic (Kontkanen et al. 2020). Daytime sulfuric acid concentrations in Beijing were typically around $4.9 \times 10^6 \, \text{cm}^{-3}$ (Lu et al. 2019). During these measurements, an evidence was found on significant nighttime sulphuric acid production, yielding gaseous sulphuric acid concentrations of 1.0 to $3.0 \times 10^6 \, \text{cm}^{-3}$ (Guo et al., 2021). For further results, see also section 2.2.2 Urban air quality and megacities.

Besides Beijing, measurements have been performed in several other locations inside the PEEX area. We used novel instrumentation to measure new particle formation and its precursors at the background Fonovaya station in the Tomsk region (Russia, Siberia), at the Värriö subarctic research station (Finland), in Ny-Ålesund (Svalbard, Norway) and on the German icebreaker, the Polarstern, during the MOSAIC project. As an example, the first results from Fonovaya station are shown in Fig. 2. Thanks to these deployments, in the next years we will be able to understand the identity of NPF precursors in those remote places. This will help us to elucidate the human impact on aerosol formation and thereby on aerosol-cloud interactions at high latitudes. In Siberia, we will finally understand why new particle formation occurs infrequently, and hopefully also identify the human role in this phenomenon. In the Arctic, we will understand the marine influence on NPF and will find out the detailed mechanism that leads to the formation of small clusters that which initiate NPF.

923   Model developments were made at several scales. Aerosol-radiation and aerosol-cloud interactions are
924   among the main sources of uncertainties in climate models, and detailed information on anthropogenic
925   aerosol number emissions is needed to improve this situation. Anthropogenic aerosol number emissions in
926   current large-scale models are usually converted from corresponding mass emissions in pre-compiled
927   emission inventories using very simplistic methods. In the global aerosol-climate model ECHAM-HAM, the
928   anthropogenic particle number emissions, converted originally from the AeroCom mass emissions, were
929   replaced with recently-formulated number emissions from the Greenhouse Gas and Air Pollution Interactions
930   and Synergies (GAINS) model (Xausa et al., 2018). However, revisions are still needed in the new particle
931   formation and growth schemes currently applied in global modeling frameworks.
932
933   For regional and urban scales, a fully integrated /online coupled meteorology-chemistry-aerosol model
934   Enviro-HIRLAM was developed (Baklanov et al., 2017) and tested for several applications in Europe,
935   Russian Arctic and China (Shanghai) (Mahura et al., 2018, 2019). Key issues for seamless integrated
936   chemistry–meteorology modeling for Earth System prediction were analyzed and formulated (Baklanov et
937   al., 2018), highlighting the scientific issues and emerging challenges that require proper consideration to
938   improve the reliability and usability of these models for three main application areas: air quality,
939   meteorology, and climate modeling. Baklanov et al. (2018) also presents a synthesis of scientific progress in
940   the form of answers to nine key questions, and provides recommendations for future research directions and
941   priorities in the development, application, and evaluation of online coupled models.
942
943   2.2.2 Urban air quality and megacities (Q5)
944
945   The rapid urbanization and growing number of megacities and urban aglomerations requires new types of
946   research and services that make the best use of science and available technology. There are urgent needs for
947   examining what the rising number of megacities means for air pollution and local climate, and what effects
948   these changes have on global climate (Baklanov et al., 2016). Such integrated studies and services should
949   assist cities in facing hazards, such as storm surge, flooding, heat waves and air pollution episodes,
950   especially in changing climates (WMO, 2019). We discuss here the recent observation on the atmospheric
951   pollution in China and Russia.
952
953   *Air quality in China – recent observations*
954
955   China is one of the regions with highest concentrations of fine $PM_{2.5}$ in the world (Wang et al., 2017a). This
956   has serious consequences on air pollution and the associated visibility reduction (haze) and adverse health
957   effects (Zhao et al., 2017). The number of haze days in China has been growing during the recent decades,
958   but detailed understanding of the factors governing the occurrence of haze is still not clear (Wang et al.,
959   2019). Both NO_2 and SO_2 concentrations showed increasing trends during the 2004-2012 period, and these
960   trends could be linked to increased power plant and traffic missions (Wang et al., 2019). A key feature of

haze formation seems to be an increased inorganic fraction of the aerosol, suggesting that the reduction of nitrate, sulfate and their precursor gases would improve air quality and visibility in China (Wang et al., 2019). In northern China, $PM_{2.5}$ concentrations declined over the period 2013–2017, and approximately half of the inter-annual variability in this region was attributed to atmospheric circulation changes (Li et al., 2020b). The maximum daily 8-h average O_3 concentrations increased over most of northern China during the same time period, with again large influences due to atmospheric circulation on daily basis (Liu et al., 2019b).

Compared with most other urban environments investigated so far, measurements in urban China demonstrated a relatively frequent occurrence of atmospheric new particle formation (NPF), and the observed NPF events were typically characterized by high particle formation rates and strongly size-dependent growth of newly-formed particles (Kulmala et al., 2016b; Wang et al., 2017b; Chu et al., 2019). Since the first reported sub-3 nm particle measurements in China a few years ago (Xiao et al., 2015), new insight into the formation pathways of molecular clusters and their growth have been obtained, including the relative roles of gaseous sulfuric acid, amines, ammonia and organic vapors in these processes (Yao et al., 2018; Yan et al., 2021). While high pre-existing particle loadings appear to suppress NPF during severe haze periods in Chinese megacities, it is unclear how NPF is possible at all under less but still quite polluted conditions typical for these environments (Kulmala et al., 2017). Overall, the available observations suggest NPF to be a major source of aerosol particles in urban China, with potentially large effects on haze formation (Kulmala et al., 2021) and cloud properties (Chu et al., 2019).

Urban measurements of particle number size distributions give deep understanding into the sources and atmospheric processing of fine particles. The longest urban continuous record is from the SORPES station in the Yangtze River Delta (Qi et al., 2015), covering almost a decade of measurements, whereas the broadest size range (1.5 nm – 1 μm) was measured in the winter Beijing atmosphere (Zhou et al., 2020). The latter study found clear differences in particle sources in different size ranges: NPF was in general the largest source of clusters and nucleation mode (<25 nm) particles, while traffic contributed to all the size ranges and dominated both cluster and nucleation modes on haze days. Aitken mode (25–100 nm) particles originated mainly from local emissions, with additional contributions from regional and transported pollution as well as from the growth of nucleation mode particles. Regional and transported pollution were identified as the main source of accumulation mode (>100 nm) particles.

Air pollution and chemical transformation, including annual and seasonal variations of the concentrations of atmospheric constituents, were analyzed for North China for the period 2005–2015 (Bai et al., 2018a). A photochemical link that related the production of fine PM and O_3 to VOCs was detected, and this mechanism was found to be prominent in summer. An intensive measurement campaign (SORPES station, Yangtze River Delta) was carried out to investigate sulfate formation and associated nitrogen chemistry (Xie et al., 2015). That study highlighted the effect of NOx in enhancing the atmospheric oxidizing capacity, and

999   indicated a potentially very important impact of increasing NO concentrations on particulate pollution

1000   formation and regional climate change in East Asia. In Changzhou, a highly-populated city in the Yangtze

1001   River Delta, primary organic aerosol concentrations outweighed secondary ones, indicating an important role

1002   of local anthropogenic emissions in aerosol pollution (Ye et al., 2017). The measurement also showed the

1003   abundance of organic nitrogen compounds in water-soluble organic aerosol, suggesting that these

1004   compounds are likely associated with traffic emissions.

1005

1006   Aerosol impacts on warm cloud properties were investigated over three major urban clusters in Eastern

1007   China and East China Sea using multi-sensor satellite observations (Liu et al., 2017, 2018). In addition to the

1008   amount of aerosol, evidence was provided that aerosol types and environmental conditions need to be

1009   considered to understand the relationship between cloud properties and aerosols. Aerosol-cloud interactions

1010   were found to be more complex and of greater uncertainty over land than over ocean.

1011

1012   The atmospheric boundary layer (ABL), and especially its dynamic behavior, is central to the evolution of

1013   near-surface air pollution. Using atmospheric observations combined with theoretical arguments, Petäjä et al.

1014   (2016) proposed a feedback mechanism connecting ABL properties with PM. According to such mechanism,

1015   high concentrations of PM enhance the stability of an urban boundary layer (BL) decreasing its height, thus

1016   causing further accumulation of pollution inside BL. Ding et al. (2016a) and Wang et al. (2018b)

1017   demonstrated an important role of BC aerosols in this feedback using model simulations combined with

1018   observations. A tight connection between the BL height and pollutant concentration, and indications of the

1019   presence of the above feedback mechanism, was also found based on comprehensive observations made on a

1020   325-m tower in Beijing (Wang et al., 2020). In order to understand these feedbacks, Kulmala (2018) and

1021   Hari et al. (2016) emphasized the crucial role of continuous, comprehensive measurements on a network of

1022   flagship stations in tackling the air pollution problem in urban China and megacities elsewhere in the world.

1023   They also introduced a so-called "Stations for Measuring Atmospheric and Earth surface Relations"

1024   (SMEAR) concept, which consists of integrated atmospheric and ecosystem observations allowing the

1025   analysis of Earth surface – atmosphere feedbacks and interactions. The first SMEAR-type station in China,

1026   the SORPES station located in the Yangtze River Delta, has been operating since 2011 (Ding et al., 2016b).

1027

1028   *Anthropogenic emissions and environmental pollution in Russia*

1029

1030   In the complex situation of the plurality of emissions, an important research task remains in the Moscow

1031   megacity environment for the assessment of the air quality and potential sources through aerosol

1032   composition analyses. Moscow aerosol pollution has been studied using a special AeroRadCity-2018

1033   experiment (Chubarova et al., 2019) and satellite data with the application of new MAIAC/MODIS aerosol

1034   algorithm with a 1-km resolution (Zhdanova et al., 2020). An advanced source apportionment for this

1035   environment was performed using combined Fourier-transform infrared spectroscopy data and statistical

1036   principal component analysis (Popovicheva et al., 2020b). The main principal component loadings revealed

1037 the source impacts of transport, biomass burning, biogenic, dust and secondary aerosol in spring.

1038 Identification of biomass burning-affected periods discriminated the daily aerosol composition change with

1039 respect to air mass transport and number of fires detected in the surrounding areas. Measurements of

1040 particulate BC were conducted at an urban background site (Meteorological Observatory of MSU) during the

1041 spring period of 2017-2018 (Popovicheva et al., 2020c). The mean BC concentrations displayed significant

1042 diurnal variations, with a poorly prominent morning peak and minimum at daytime. BC mass concentrations

1043 were higher at nighttime due the shallow boundary layer and intensive diesel traffic. The aerosol optical

1044 thickness (AOT) over Moscow showed a pronounced seasonal cycle, with a summer maximum and winter

1045 minimum (Chubarova et al., 2016a). It was found that during 2001–2014, the monthly-mean values of AOT

1046 declined by 1–5% per year, and this decline was attributed to decreased emissions of aerosols and their

1047 precursors.

1048

1049 In general, the atmospheric environment over remote areas of Siberia and Northern Asia is relatively clean

1050 compared with other surrounding regions of Asia and Eastern Europe (Baklanov et al., 2013). However, air

1051 pollution from Siberian industrial centers poses significant environmental threats. For Siberian cities (e.g.,

1052 Norilsk, Barnaul, Novokuznetsk), the air quality is among the worst in the Russian and European cities.

1053 Similar to Arctic cities, stable atmospheric stratification and temperature inversions dominate for more than

1054 half a year. This leads to pollution accumulation near the surface, which influences ecosystems and people.

1055 Moreover, not only severe climatic conditions, but also manmade impacts on the environment in industrial

1056 areas and large cities have intensified. The impacts manifest themselves as the pollution of environment, land

1057 use changes, hydrodynamic regimes and local climate. Ultimately, these impacts feed back to people,

1058 affecting their health and well-being.

1059

1060 The Russian part of the Barents Euro-Arctic region includes severe emission 'hot spots' for air pollutants.

1061 The Kola Peninsula, despite the presence of areas with undisturbed nature in the eastern part, is the most

1062 industrially developed and urbanized region in the Russian Arctic. The main polluters are the smelters of the

1063 Severonickel (Monchegorsk, central part of the peninsula) and the Pechenganickel (Nickel and Zapolyarnyi

1064 near the Russian-Norwegian border) enterprises. For comparison, emissions of SO_2 from the Nickel smelter

1065 alone are 5-6 times larger than the total Norwegian emissions (NILU, 2013). In 2015 the Norilsk Nickel in

1066 Siberia - the biggest mining and the metallurgical complex - emitted about 1.9 million tons of SO_2 (GGO,

1067 2016). With the nickel factory (located in the southern part of the city), copper factory (just to its north) and

1068 metallurgical plant (12 km to the east), the city of Norilsk is influenced by heavy industry no matter which

1069 way the wind blows. The Blacksmith Institute declared in 2007 that Norilsk is one of the top 10 worst-

1070 polluted places in the world. The impacts of emissions are manifested as deterioration of forest ecosystems

1071 and acidification of soils and surface waters (Derome and Lukina, 2011), even at considerable distances from

1072 the smelters. Heavy metals and alkaline pollutants contaminate areas around the sources of pollution within a

1073 few hundred kilometres, while acid sulphates can be transported over long distances (Mahura et al., 2018).

1074

A recent analysis on the total deposition and loading on the population in North-Western Russia and Scandinavian countries caused by the continuous sulfur emissions from the Cu-Ni smelters in Murmansk indicates the dominance of wet deposition, especially in winter time (Mahura et al., 2018). North-Western Russia is influenced more by the Severonikel emissions compared with countries in the Scandinavian Peninsula. The cities of the Murmansk region (Kola Peninsula) are under highest impacts. On a yearly scale, the individual loadings on population are at the largest level (up to 120 kg/person) in the Murmansk region, much lower (15 kg/person) in northern Norway, and the smallest (< 5 kg/person) in eastern Finland, Karelia Republic and Arkhangelsk region. Distinct seasonal variability was identified, with the lowest contribution during summer and the highest contribution during winter-spring in Russia, during spring in Norway, and during autumn in Finland and Sweden.

The annual yearbook "The State of Atmospheric Pollution in Cities on the Territory of Russia" for 2018 (Roshydromet and GGO, 2019) sates the highest atmospheric emissions of PM were observed in Siberian and Ural cities. In Novokuznetsk and Omsk, the observed PM was the highest (> 30 000 tons per year) while emissions from other cities such as Angarsk and Chelyabinsk were lower (< 20 000 tons per year). Note that in the 2015-2019 yearbooks, emissions from only stationary sources were provided due to revisions (approved and implemented in November 2019 by the Russian Ministry of Natural Resources and Ecology, MNRE) of methods applied for estimation of emissions into the atmosphere from mobile sources. Depending on a source type, different methods to calculate emissions are applied (MNRE, 2019). For the gaseous compounds, such as SO_2, the maximum emissions included very high from Siberian cities (e.g. Norilsk, Novosibirsk, Novokuznetsk, Omsk, Ufa, Irkutsk, Angarsk) and from North-West Russia cities (Zapolyarny, Nickel, Monchegorsk). High NO_2 emissions were observed in Novosibirsk, Omsk, Angarsk and Chelyabinsk. The CO integral urban emissions depend on a city size. These varied from less than 10 Gg yr^{-1} (for small regional centers like Vladimir, Kursk, Samara) to 406 and 804 Gg yr^{-1} for large metropolitan areas such as St. Petersburg and Moscow. As a whole, an analysis of spatio-temporal variation of trace gases in the boundary layer over Russian cities indicated significant emission variations between the urban environments and remote sites (Elansky et al., 2016).

Cities, being not isolated systems, may distribute as much pollution to the surrounding areas as they receive it from outside them or from remote regions. The analysis of the transboundary atmospheric transport between Russian Siberia and bordering countries (e.g. China, Kazakhstan, and Mongolia) is part of a mutual risk assessment for urban areas/ cities and their surroundings. For example, the city of Ulaanbaatar (Mongolia) suffers from high levels of pollution due to excessive airborne particulate matter emanating from coal combustion mixed with traffic emissions and resuspended soil dust, resulting in variable chemical source profiles (Gunchin et al., 2019). Long-range transport from remote sources might be an additional contributor. Moreover, there are indications that such transport of biomass burning emissions from Siberia could lead to pollution episodes and impact on surface ozone as far as in western North America (Jaffe et al., 2004).

1113   2.2.3 Weather and atmospheric circulation (Q6)

1114

1115   The observed evolution of weather and climate represents the combined effects of external forcing (changes

1116   in the concentrations of greenhouse gases and aerosols etc.) and internal variability, related to a large extent

1117   to the atmospheric circulation. It is also affected by local factors, particularly urban heat islands in cities.

1118   Here we discuss these interconnected processes, focusing on cold and warm episodes, cyclone density and

1119   atmosphere-ocean interactions, effects of circulation on temperature and moisture, cloudiness in the Arctic,

1120   and boundary layer dynamics relevant to the Arctic-boreal region.

1121   *Cold and warm episodes*

1122   The Arctic warming, as well as the Arctic amplification, have been associated with changes in atmospheric

1123   large-scale circulation together affecting the European winter temperatures. In large parts of Europe, severe

1124   cold (warm) winter events are significantly correlated with warm (cold) Arctic episodes (Vihma et al., 2020).

1125   Air mass trajectory analysis revealed that air masses associated with extreme cold (warm) events typically

1126   originate from over continents (sea areas). Despite Arctic and European-wide warming, winter cooling has

1127   occurred in northeastern Europe in cases of air masses arriving from the southeast (Vihma et al., 2020).

1128

1129   *Cyclone density dynamics and atmosphere-ocean interaction*

1130   Transporting large amounts of heat and moisture from mid-latitudes to the central Arctic, synoptic-scale

1131   cyclones are vital for the Arctic climate system. Recent findings, based on atmospheric reanalysis, above all

1132   the global ERA-Interim reanalysis available from 1 January 1979 to 31 August 2019, are summarized below.

1133   During 1979–2016 in winter (Dec, Jan, Feb), the cyclone density increased in the areas around Svalbard and

1134   in northwestern Barents Sea, but decreased in southeastern Barents Sea (Wickström et al., 2020). This is

1135   related to a shift to more meridional winter storm tracks in the Norwegian, Barents and Greenland Seas. The

1136   shift is favored by a positive trend in the Scandinavian Pattern and, in the areas north of Svalbard, by a

1137   significant increase in the Eddy Growth Rate (Wickström et al., 2020).

1138

1139   Numerical model simulations of the storm activity in the White, Baltic and Barents Seas were analyzed for

1140   the period 1979-2015 (Myslenkov et al., 2018). A high interannual variability in the storm number was

1141   observed for all studied seas. No significant trends in the storm number during the period 1979-2015 were

1142   found in the studied sea areas. On average, the connection with global atmospheric circulation is stronger for

1143   the Baltic Sea than for the other two seas. Also, the future changes of wind wave climate were analyzed.

1144   According to the RCP8.5 scenario, in the second part of the 21st century the number of storm events will rise

1145   in the Baltic and Barents Seas.

1146

1147   In the Bjerknes compensation, changes in atmospheric heat transport co-occur with opposing changes in

1148   ocean heat transport. Observations and model simulations indicate a central role for ocean-atmosphere heat

1149 exchange in the Barents Sea area in maintaining this compensation in the Arctic (Bashmachnikov et al., 2018

1150 a, 2018b).

1151

1152 *Circulation effect on temperature*

1153 The effect of atmospheric circulation on temperature trends in years 1979-2018 was studied by Räisänen

1154 (2019, 2021) using a trajectory-based method. He found that the circulation trends had reduced the annual

1155 mean warming during this period in western and central Siberia locally by over 1°C, with a much larger

1156 cooling effect in autumn and winter (Fig. 3). His findings also confirmed a circulation-induced amplification

1157 of warming over the Barents and Kara seas particularly in winter. Yet, in most areas the circulation-related

1158 temperature trends have varied strongly from month to month, leaving only a relatively small effect on the

1159 annual mean temperature trends. The residual warming obtained after subtracting the circulation effect

1160 therefore tends to have a smoother seasonal cycle than the observed temperature trends, in better agreement

1161 with the multi-model mean trends in the CMIP5 simulations (Taylor et al., 2012).

1162

1163 *Circulation effect on moisture*

1164 The effects of large-scale circulation on moisture, cloud and longwave radiation occur mostly via the impact

1165 of horizontal moisture transport (Nygård et al., 2019). Evaporation is typically not efficient enough to shape

1166 those distributions, and much of the moisture evaporated in the Arctic is transported southward (Nygård et

1167 al., 2019). Strong moisture transport events avail a large part of the northwards moisture transport. The

1168 meridional net transport is only a small part of the water vapor exchange between the Arctic and mid-

1169 latitudes (Naakka et al., 2019). When a high-pressure pattern across the Arctic Ocean from Siberia to North

1170 America is lacking, the amounts of moisture, clouds and downward longwave radiation are anomalously

1171 high near the North Pole (Nygård et al., 2019). Using vertically-integrated water vapor as a metric, the Arctic

1172 (north of 70°N) has experienced a robust moistening trend since 1979, and in absolute numbers this trend is

1173 the smallest in March and the largest in August (Rinke et al., 2019). However, the relative trends are the

1174 largest in winter. Although different atmospheric reanalysis are consistent in spatiotemporal trend patterns,

1175 they scatter in the trend magnitudes.

1176

1177 Analysis of moisture and aridity estimated using the web-GIS "CLIMATE" and the ECMWF ERA-Interim

1178 reanalysis data for Southern Siberia (50-65 °N, 60-120 °E) from 1979 to 2010 with a 0.75° × 0.75° grid

1179 resolution showed that the mountain regions of Eastern Siberia have been come more arid each month during

1180 the last 30 years (Ryazanova and Voropay, 2017). In Western Siberia, aridity increased in May and

1181 decreased in June, while in the other months positive and negative trends were found. The greatest

1182 differences in the trends of the aridity index, air temperature and precipitation were observed in July.

1183

1184 *Cloudiness in Arctic*

1185

1186 The climatology and inter-annual variability of Arctic cloudiness remains a wildcard in regional climate

1187 change projections. Both climate models and satellite data products need *in situ* observations for calibration

1188 and validation. Chernokulsky et al. (2017) and Chernokulsky and Esau (2019) collected and processed

1189 manual cloud observations from meteorological stations in the PEEX area. The cloud records in the Arctic

1190 are available since the end of the 19th century. Since 1936, cloud observations representatively cover the

1191 Eurasian Arctic. This permits reconstructions of cloud type and cloud cover climatologies as well as studies

1192 of inter-decadal variability of cloudiness. A problem of a special interest is related to the co-variability of the

1193 total could cover and sea ice concentration or extent. Both clouds and sea ice affect the surface heat balance

1194 through surface albedo, but their feedback mechanisms, dynamical impacts and climate sensitivities are

1195 different. Chernokulsky et al. (2017) found that the annual-mean total cloud cover (TCO) decreases during

1196 warmer climate periods with a lower sea ice concentration, but increases over sea ice in the Barents Sea as

1197 more moisture is transported into the Arctic at higher temperatures. Furthermore, the increasing TCO

1198 reduces the deficit of the surface heat, and the intra- and inter-annual variability of TCO over solid ice is

1199 higher than that over open water (Chernokulsky et al. 2017). Long-term cloud climatological analysis based

1200 on meteorological observations of the total and low cloud cover and cloud types from the Barents Sea to the

1201 Chukchi Sea showed that significant transitions between cloud types has been taken place, especially the

1202 low-level stratus and stratocumulus types have been transformed to convective cloud types (Chernokulsky

1203 and Esau, 2019). Chernokulsky and Esau (2019) addressed that their results are relevant for understanding

1204 Arctic cloud processes and feedbacks, and that new knowledge is needed to connect the changes in the

1205 Arctic radiation balance with the Arctic cloud cover—cloud type climatology.

1206

1207 *Boundary layer dynamics and urban heat islands*

1208

1209 On the background of accelerated and amplified Arctic warming, anthropogenic heat release and metabolism

1210 of cities add up to persistent warm temperature anomalies in urbanized areas (Fig. 4). Indeed, if the climate

1211 change forcing approaches 2 W m^{-2}, the urban heat forcing could be 10-100 W m^{-2} (Konstantinov et al.,

1212 2018). The urban heating trapped in shallow planetary boundary layers is potent to rise the local

1213 temperatures by 1 to 10 $^{\circ}$C or even more. This local climate phenomenon is known as the urban heat island

1214 (UHI) (Esau et al., 2020). A series of *in situ* and satellite UHI studies in the northern cities revealed strong

1215 and persistent warm temperature anomalies in almost all of 28 northern West Siberian cities (Miles and Esau,

1216 2017), in 5 cities covered by the UHIARC network (Konstantinov et al., 2019; Varentsov et al., 2018a) and

1217 in 57 Scandinavian cities (Miles and Esau, 2020). The mean wintertime temperature anomalies, the UHI

1218 intensity, varied from 0.8 K to1.4 K and had extreme intensities of up to 7 K during cold anticyclone weather

1219 conditions. The complete dataset of surface UHI intensity derived from MODIS LST data products is freely

1220 available and published in Miles (2020). Such a UHI-induced strong mediation of cold temperature spells

1221 might cause significant socio-economic and environmental impacts in the cities (Konstantinov et al. 2018,

1222 Fig. 4). A survey of other UHI studies in 11 Arctic cities and towns confirmed that even relatively small

cities at high latitudes may exhibit intensive UHIs. A recent analysis confirms the important role of the surrounding temperature in explaining spatial-temporal variation of the UHI intensity (Miles and Esau, 2017). The major contribution to the UHI was revealed for water, sparse vegetation, grassland and scrubland. The mechanisms and pathways of the UHI maintenance requires an involvement of numerical experiments with turbulence-resolving models to advance the understanding of the local climate features (Urban Heat Islands - UHIARC dataset see http://urbanreanalysis.ru/uhi arc.html). We would need a denser meteorological network, especially high quality temperature data, to better understand the urban climatology and the thawing processes in urban soils and to better assess climatic trends relevant to Arctic societies and welfare (Konstantinov et al. 2018).

Urban climate anomalies may cause more extreme weather and climate phenomena in densely populated megacities. The Moscow agglomeration – the largest megacity in the boreal continental climate within the PEEX domain – demonstrates profound effect of interactions between the UHI and urban winds, known as a cross-over effect (Varentsov et al. 2018b). The UHI creates an urban heat "dome" with near-surface air inflow into the urban central districts and air outflow at higher levels in the atmosphere. The air uplift in the urban dome is connected to the increase in summer rainfall at the lee side and over the central urban districts. Stable atmospheric stratification over rural area is strengthen by the downwind air motions coming from the urban region.

Atmospheric boundary layer over the Arctic Ocean has been studied on the basis of tethersonde sounding observations over sea ice (Palo et al., 2017) and research aircraft observations over the open ocean and sea ice (Suomi et al., 2016). Palo et al. (2017) found that in spring and summer, the occurrence and properties of temperature inversions were controlled by the surface melt and warm air advection rather than surface net radiation. During snow/ice melt, temperature inversions were frequently surface-based, and equally strong as winter inversions over the Arctic Ocean. To better understand atmospheric boundary layer processes in the Arctic, Suomi et al. (2016) developed a method to measure wind gusts from a research aircraft. It allows wind gust observations at altitudes not reached by traditional weather mast observations. The observed gust factors strongly depended on the surface roughness, which differed for sea ice and the open ocean.

2.3   ARCTIC-BOREAL AQUATIC SYSTEM

We discuss the recent results on Arctic sea ice dynamics and thermodynamics, snow depth and sea ice thickness, sea ice research supporting navigation, and rare elements in snow and the ocean sediments, especially from the perspective of improvements in the observation and modelling methods (Q7, section 3.3.1). We introduce new results on the Arctic marine ecosystem and focus on the primary production and carbon cycle (Q8, section 3.3.2.). In section 3.3.3 for the Artic – boreal lakes and rivers, we discuss the browning of lakes and lake sediment with a special attention on the Selenga River system of Lake Baikal (Q9).

2.3.1 Changing water systems, snow, sea ice and ocean sediments (Q7)

Sea ice and thermodynamics with atmospheric and ocean dynamics

Referring to the earlier discussion in section 2.2.3 on atmospheric circulation, we address here how the sea ice dynamics closely interacts with the atmospheric and ocean dynamics. A rapid decrease in the Arctic Ocean ice cover, particularly in the Barents and Kara Seas, has been taking place since the late 1970s simultaneously with the cooling of winters in central Eurasia (McCusker et al., 2016). This unexpected winter cooling is related to increasing northeasterly winds over the southeastern flank of an anomalous high that has developed over the northwestern coast of Russia (McCusker et al., 2016; Mori et al., 2019, Räisänen 2021). However, the causality between the atmospheric circulation changes and the Arctic sea ice decrease is debated. Observations suggests a strong correlation between these two, but climate model simulations forced by reduced ice cover produce much weaker circulation changes than observed, resulting in only weak cooling in central Eurasia (Mori et al., 2014, 2019; McCusker et al., 2016). This suggests that either most models are underestimating the sensitivity of the atmospheric circulation to sea ice decrease, supported by Romanowsky et al. (2019), or that the circulation change has not been primarily caused by the decreasing sea ice. In the latter case, the correlation between the reduced ice cover and atmospheric circulation would mainly reflect the effect of circulation on sea ice. In support of this, Blackport et al. (2019) showed that a reduced sea ice coincides with an anomalous heat flux from the atmosphere to the ocean, and that on the sub-seasonal time scale, anomalies in atmospheric circulation tend to precede rather than follow those in sea ice. Thus, while the reduced sea ice might partly explain the observed changes in atmospheric circulation (Mori et al., 2019), the effect of circulation on sea ice appears to be stronger than the effect of sea ice on circulation.

Considering atmosphere-ice interactions, Jakobson et al. (2019) studied the linkages between sea ice concentration (SIC), atmospheric stratification, surface roughness and wind speed at the 10-m height (W10) and 850-hPa level (W850). In all the seasons except summer, a reduction in SIC favored reduced atmospheric stratification and aerodynamic surface roughness, which resulted in a stronger W10. The effect was the strongest in autumn, and positive trends in W10 and its ratio to W850 typically occurred in regions with the strongest negative trends in SIC. The relationships were stronger on inter-annual than on sub-seasonal time scales. Large-scale atmospheric circulation, characterized, e.g., by the Dipole Anomaly (DA), has also contributed to sea ice dynamics. A positive polarity in DA has contributed to the recent rapid loss of summer sea ice in the Pacific part of the Arctic Ocean by bringing warmer air masses from the south and transporting more ice towards the north enhancing the ice-albedo feedback (Lei et al., 2016). Another example of ice dynamics affecting the ice-albedo feedback was the weakened Transpolar Drift Stream in summer 2013. It reduced sea ice transport out of the Arctic Ocean, and restrained ice melt because of the low

1298 air temperatures, weakened albedo feedback, and a relative small oceanic heat flux in the central Arctic (Lei

1299 et al., 2018).

1300 Solar radiation, being the main forcing factor for a sea ice melt in summer, is difficult to parameterize in

1301 thermodynamic models. This is due to the large variability in the optical properties of sea ice in space and

1302 time. A two-stream model provides a time-efficient parameterization of the apparent optical properties

1303 (AOPs) for ponded sea ice, accounting for both absorption and scattering, and has a potential to be

1304 implemented into sea-ice thermodynamic models to explain the role of melt ponds in the summer decay of

1305 Arctic sea ice (Lu et al. 2016). This model was used to investigate the role of solar radiation in the Arctic sea

1306 ice during the melting season considering layers of melt ponds, underlying sea ice, and ocean beneath the

1307 ice. It was found that the energy absorption profiles depend strongly on the incident irradiance and ice

1308 scattering, but only weakly on the pond depth. It seems that the incident solar energy is largely absorbed by

1309 the melt pond rather than by the underlying sea ice (Lu et al., 2018a). The model was further applied to

1310 investigate the influence of a surface ice lid on the optical properties of a melt pond. The thickness of the ice

1311 lid determines the amount of solar energy absorbed. Visual inspections on the color of refreezing melt ponds

1312 also help to judge the significance of the influence of the ice lid. This will allow for an accurate estimation

1313 on the role of surface ice lid during field investigations on the optical properties of melt ponds (Lu et al.,

1314 2018a). The modelled pond color agrees with field observations from the Arctic sea ice in summer. The

1315 analysis of pond color is a new potential method to obtain ice thickness in summer, however, more validation

1316 data and improvements to the radiative transfer model would be needed (Lu et al., 2018b).

1317

1318 *Snow depth/mass and sea ice thickness*

1319 Snowpack on sea ice has a crucial role in insulating the sea ice from the colder atmosphere, accordingly

1320 reducing sea ice growth in winter, effectively reflecting the incoming solar radiation, reducing sea ice melt in

1321 spring and summer and contributing to its formation. The replacement of snow fall by rain strongly enhances

1322 the ice-albedo feedback in the Arctic Ocean (Dou et al., 2019). Shalina and Sandven (2018) refined the

1323 description of snow depth on sea ice in the central Arctic, providing new snow depth data for the Arctic

1324 marginal seas. High autumn and winter precipitation and thinning Arctic sea ice make snow-ice formation

1325 prevalent in the Atlantic sector of the Arctic (Merkouriadi et al., 2017).

1326

1327 Advance has been made in applying thermistor string based autonomous high-resolution Snow and Ice Mass

1328 Balance (IMB) Array (SIMBA) buoys to measure snow depth and ice thickness (Figs. 5 and 6.). SIMBA has

1329 a lower cost, allowing deployment in large numbers (Lei et al., 2015). The determination of snow depth and

1330 ice thickness from SIMBA temperature profiles has so far been largely a manual process. A SIMBA-

1331 algorithm was developed to process SIMBA data automatically (Liao et al., 2018), assuming a fixed snow-

1332 ice interface. Snow-ice formation results in snow-ice interface moving upward. The SIMBA-algorithm was

1333 further developed to tackle the moving interfaces (Cheng et al., 2020). The developed SIMBA-algorithm

1334 works well in cold condition for lakes and Polar Oceans. For Polar Oceans, the snow and ice are close to

1335   isothermal during summer, which prevents the identification of interfaces on the basis of the temperature

1336   gradient. Under such conditions, thermodynamic modelling yields valuable information on snow depth and

1337   ice thickness (Tian et al., 2017).

1338   A challenge in sea ice thermodynamic modelling is the uncertainty in the magnitude of the oceanic heat flux

1339   at the ice base, especially for land-fast sea ice. Yang et al. (2015) applied a one-dimensional thermodynamic

1340   model to investigate impact factors on land-fast sea ice in the East Siberian Sea. The modelled snow cover

1341   was less than 10 cm, having a small influence on the ice thickness, but surface albedo and oceanic heat

1342   fluxes were critical.

1343

1344   Also in the terrestrial Arctic and boreal zone, there is a need for a better efficiency and coverage of an *in-situ*

1345   snow observation network. Snow cover and snow mass are fundamental parameters for global energy and

1346   water cycles, and the changes in the regional snowpack have societal impacts like on amount of drinking

1347   water or capacity for the hydropower generation (Bormann et al., 2018). Snow depth data in the Arctic

1348   region are available from the synoptic weather stations and snow mass data are systematically collected from

1349   the snow courses, as demonstrated in Extended Data (fig. 2) by Pulliainen et al. (2020). The use of automatic

1350   and cost-effective measurements together with harmonized snow measurement practices is the way forward.

1351   A survey on a harmonized snow monitoring in Europe demonstrated that crucial parameters for operational

1352   services, such as parameters characterizing precipitating and suspended snow, are measured by 74% of the

1353   European snow network contributors (COST Action ES1404), but the parameters characterizing the snow

1354   microstructural properties, electromagnetic properties and composition are currently measured by only 41%,

1355   26% and 13%, respectively, of the network contributors (Pirazzini et al., 2018). The observations at the

1356   continental scale, so far, demonstrate a widespread snow-cover retreat since the 1970's across the Northern

1357   Hemisphere, particularly in the Arctic (Derksen et al., 2012; Bormann et al., 2018). On the contrary, the

1358   results from the mountains are mixed and there is no consistent picture of what is happening at the regional

1359   scale (Bormann et al., 2018). Pulliainen et al. (2020) provided new insight into the seasonal snow mass and

1360   its trend by using a bias-corrected GlobSnow 3.0 estimates. Pulliainen et al. (2020) is now able to

1361   demonstrate different continental trends based on the 39-year satellite record: a decrease in North America, a

1362   negligible trend in Eurasia, and a high regional variability in both areas.

1363   *Sea ice research supporting navigation*

1364

1365   Recent research has addressed emerging opportunities for Arctic navigation and the importance of

1366   operational sea ice analysis. Lei et al. (2015) showed trends along the Arctic Northeast Passage (NEP) and

1367   demonstrated an increase in the spatially-averaged length of the open period (the ice concentration less than

1368   50%) from 84 days in the 1980's to 114 days in the 2000s. The summer sea ice along the High-Latitude Sea

1369   Route (HSR) north of the eastern Arctic islands has decreased during the last decade, with the ice-free period

1370   reaching 42 days in 2012. The HSR avoids shallow waters along the coast, which easier the access to for

1371   deeper-draft vessels (Lei et al., 2015). Considering operational sea ice analyses for the Bohai Sea, work has

been done to combine thermodynamic modelling and Earth Observation (EO) data from synthetic aperture radar (SAR) and microwave radiometers (Karvonen et al., 2017). The SAR-based discrimination between sea ice and open-water works well, and areas of thinner and thicker ice can be distinguished. However, a larger comprehensive training dataset is needed to set up an operational algorithm for the estimation of sea ice concentration and for the weighting scheme for sea ice thickness (Karvonen et al., 2017).

Multi-decadal Arctic sea-ice state estimates are important for the strategic planning of Arctic navigation. These estimates are usually based on climate models with a thermodynamic-dynamic sea-ice models. An up-to-date assessment of large-scale sea-ice models was with the aid of sea-ice models as a climate model component, a comprehensive review was carried out by Leppäranta et al. (2020). Specifically, Uotila et al. (2015) found that a model with the subgrid-scale sea-ice thickness distribution reproduces more realistic sea ice and upper ocean, due to better captured spring evolution, than a model with just single sea-ice thickness category. In terms of validity of initial conditions for multi-decadal predictions, Uotila et al. (2019) analyzed a set of ocean reanalysis products, including Arctic sea ice, and found that the multi-model set mean is a useful product as a state estimate. This finding increases confidence toward the use of the combination of ocean reanalysis for both initialization of multi-decadal predictions and analysis of multi-decadal variability.

Ocean floor and Sediments: composition and fluxes

A significant content of illite and muscovite among layer silicates in most of the ice-rafted sediments samples taken from selected Arctic regions suggests that sources of the sedimentary material are mainly mineralogically similar to modern bottom sediments of the East Siberian and Chukchi seas, as well as presumably sediments of the eastern Laptev Sea. A significant kaolinite fraction in the samples from the North Pole area can be caused by the influx of ice-rafted fine-grained sedimentary material from the Beaufort or Chukchi seas, where kaolinite is supplied from the Bering Sea. The samples contained variable proportions of erosion products of both mafic and felsic magmatic rocks and/or sufficiently mature sedimentary rocks (Maslov et al., 2018a).

Quantification of CH_4 sources is fundamental information for the climate change mitigation (Fletcher and Schaefer 2019). Methane stored in ocean floor reservoirs can reach the atmosphere in the form of bubbles or dissolved in water. Methane hydrates could destabilize with rising temperatures, further increasing greenhouse gas emissions in a warming climate. Subsea permafrost and hydrates in the East Siberian Arctic Shelf (ESAS) are acting as a substantial carbon pool, and source of methane to the atmosphere. Annual methane emissions of the region varies from 0.0 to 4.5 Tg CH_4 yr^{-1} estimated by Berchet et al. (2016). Yasunaka et al. (2018) estimated the monthly air-sea CO_2 fluxes in the Arctic Ocean and adjacent seas located north of 60 degrees N for the period 1997 2014 and ended up to a net annual Arctic Ocean CO_2 uptake of 180 ± 130 Tg C per year.

1410 The Zeppelin Observatory data for 2014 suggest that the CH_4 fluxes from the Svalbard continental platform

1411 are smaller than 0.2 Tg yr^{-1}. All estimates are in the lower range of values reported earlier (Pisso et al.,

1412 2016). Platt et al. (2018) reported a potential region with high ocean-atmosphere CH_4 flux located north of

1413 Svalbard, but addressed that at the time of the measurements the meteorological conditions were unique,

1414 including a short episode of the highly sensitive to emissions over an active seep site without a sensitivity to

1415 land-based emissions.

1416

1417 *River runoff affecting the hydrological processes at coastal marine environments*

1418

1419 The Arctic Ocean, including the Hudson Bay, receives 55.6 % of its river inflow from Russia, mostly via 19

1420 large rivers (Shiklomanov and Shiklomanov, 2003). This freshwater inflow of approximately 2920 km^3 per

1421 year (Shiklomanov, 2008) is associated with large sediment and heat transports, which together affect the

1422 hydrography, marine climate and ecosystems across the Siberian shelf seas (Magritsky et al., 2018). A major

1423 part of seasonal and interannual variations in the river runoff is anthropogenic, due to regulation in large

1424 reservoirs (Georgiadi et al., 2016). In addition, Magritsky et al. (2018) detected an increased runoff trend of

1425 5-10 %, compared to a reference period of 1936 to 1975, in most of the major Russian rivers discharging into

1426 the Arctic Ocean. This trend is mostly due to a climate-induced increase since the second half of 1980's

1427 (Magritsky et al., 2018). However, due to gaps in the monitoring programs, these estimates have a large

1428 uncertainty: focusing on river discharges from the six largest Eurasian rivers to the Arctic Ocean, estimates

1429 of the increase range from 7% (Peterson et al., 2002) to 1.5 % (Shiklomanov and Lammers, 2009).

1430

1431 Permafrost thawing has resulted in releases of old carbon storages, but so far there is no clear evidence on

1432 the impact of permafrost thawing on the net emissions of CO_2 and CH_4 to the atmosphere (IPCC, 2019). A

1433 potential explanation of no or weak net increase is that a fraction of the released methane has been taken by

1434 rivers instead of emitted to the atmosphere. Increased amounts of organic carbon in rivers impact the

1435 regional and global biochemical and methane cycles (Shakhova et al., 2007; Wild et al., 2019). With the

1436 accelerating permafrost thaw, also the atmospheric emissions are expected to increase, in particular for CO_2

1437 but also for CH_4. Expected future changes in river ice regime are consistent with the expected changes in the

1438 duration of the cold season and accumulated negative air temperatures. Significant changes are expected for

1439 the rivers in the Kola Peninsula and the lower reaches of the rivers Northern Dvina and Pechora, whereas the

1440 lowest changes are expected for the central parts of Eastern Siberia (Agafonova et al., 2017). Due to

1441 anthropogenic activities (above all industry, municipal services, and filling of reservoirs), water withdrawal

1442 from Russian Arctic rivers and related groundwater systems is approximately 20.6 km^3 per year, and it is

1443 expected to increase to 37 km^3 per year by 2025 to 2030 (Magritsky et al., 2018). Features of these changes

1444 at the marine margin of the Lena River delta are different compared to changes in the delta head area.

1445

1446 The hydrological representativeness of a glacier is a new characteristic, and of practical importance for

1447 basin-wide tasks of hydrology and glaciology. For its evaluation, it is proposed to replace the seasonal air

1448   temperatures with the glacier summer mass balance (BS) or to include BS in the multiple regression

1449   equations for calculating the runoff of rivers fed by melting of snow and ice. This method can be

1450   recommended for at least of some glaciers in the existing network of the World Glacier Monitoring Service

1451   (WGMS) (Konovalov et al., 2019).

1452

1453   2.3.2 Marine ecology (Q8)

1454

1455   *Living marine organisms weaken or even subdue CO_2 accumulation*

1456   The important climatological role of the world's oceans is to reduce the CO_2 accumulation into the

1457   atmosphere through its absorption. This mechanism is ordinarily viable as the partial pressure of dissolved

1458 CO_2 in marine surface waters is less than the content of CO_2 in the overlying atmosphere. Due to the organic

1459   pump, a net draw down of atmospheric CO_2 into the ocean is put into effect. It proceeds in the process of

1460   sinking of particulate organic carbon of algal origin: organically bound CO_2 is released through

1461   remineralization and further accumulated in the deep ocean. In contrast, owing to the processes of carbonate

1462   counter pump, $CaCO_3$ is exported downward and, at depth, dissolves causing a net release of CO_2 to the

1463   atmosphere (Balch et al., 2016). However, there are living marine organisms that are able to weaken or even

1464   subdue CO_2 accumulation, at least within their habitat. Among this group of marine organisms, the leading

1465   role belongs to coccolithophores. Among marine bio systems, coccolithophores (class Primnesiophycea) are

1466   most productive calcifying algae (Taylor et al., 2017). They both produce particulate inorganic carbon (in the

1467   form of calcite) and promote the increase of CO_2 partial pressure (pCO_2) in the ambient marine surface

1468   waters. Thus, the biological activity of coccolithophores can exercise a direct influence on both the CO_2 flux

1469   exchange at the atmosphere-ocean interface and the marine carbonate chemistry system (CCS). The rain

1470   ratio, i.e. the ratio of particulate inorganic carbon to organic carbon, determines the intensity and direction of

1471 CO_2 flux at the atmosphere-ocean interface. In the case of coccolithophores, the rain ratio is above unity

1472   within their habitat area, which potentially can have climatic consequences but also drive alterations in

1473   marine CCSs (Balch 2018).

1474

1475   *Emiliania huxleyi* is the most widespread coccolithophorid algal species in Earth's oceans, which, in light of

1476   the above, naturally explains why this is one of the best-studied marine algae. Of all other coccolithophores,

1477   *E. huxleyi* is probably the most successful in forming extensive blooms in world-wide marine waters ranging

1478   from oligotrophic to eutrophic. Unlike diatoms and dinoflagellates, this alga is phenomenally immune to

1479   both light-limitation and very high light intensities. As high levels of incident light/irradiances enhance

1480   calcification (which is predominantly a light-dependent reaction), it is supposed that the calcification

1481   machinery enables *E. huxleyi* cells to resist photodamage through dissipating excess energy. This specialty is

1482   important in case of nutrient-depleted waters, especially in combination with the high affinity of *E. huxleyi*

1483   for nutrients including nitrogen but especially phosphorous. The property of both mixothropic nutrition, and

1484   resistance, at least partial, to zooplankton grazing and virus attacks (due to cell's coverage by calcite

1485   scales/coccoliths) contribute to this alga ability to sustain a variety of unfavorable conditions and retain

1486 steadfastly its ecological niche (Godrijan et al, 2020). Thus, the elaborate biology of *E. huxleyi* cells imparts

1487 to them the intrinsic and rather rare property of pursuing growth-maximizing and loss-minimizing life

1488 strategies. This property reveals itself through multiple manifestations, two of which are vastness and

1489 sustainability of *E. huxleyi* bloom areas. A typical bloom surface is not less than thousands of square

1490 kilometers, but in many marine environments it is far larger (Kondrik et al., 2018b). For example, in some

1491 years, the value of S in the North and Norwegian Sea can be well above $100\,000\ km^2$, in the Bering Sea

1492 maximum bloom area (S) values were registered at $250\,000\ km^2$, particularly large *E. huxleyi* bloom areas

1493 (up to $380\,000\ km^2$) were observed in the Barents Sea (Kondrik et al., 2017). Within the subpolar and polar

1494 zones of the Northern Hemisphere, in the waters around the Great Britain, in the North, Norwegian,

1495 Labrador, Greenland, Barents, and Bering seas *E. huxleyi* blooms occur annually although with largely

1496 varying intensity (Pozdnyakov et al., 2017). The duration of blooms in the Northern Atlantic and the Barents

1497 Sea is on average about three-four weeks. The moment of onset of the *E. huxleyi* bloom area maximum shifts

1498 from June-July to September-October for the seas located at the temperate, subpolar and polar latitudes of

1499 the Northern Hemisphere, respectively. This sequence mimics the flow pattern of the Golf Stream. In the

1500 Bering Sea, the temporal pattern of S variations reveals two periods (1998-2001 and 2018-2020) of

1501 extraordinary intense *E. huxleyi* outbursts. It is hypothesized that this phenomenon was driven by massive

1502 advection of Fe-depleted North Pacific waters due to a significant weakening of the Alaskan Current. The

1503 latter is supposed to be a teleconnected aftermath of exceptionally strong El Niño events in 1996-1997 and

1504 2017, respectively (Pozdnyakov et al., 2020).

1505

1506 Satellite-borne estimations made during 1998-2018 showed that *E. huxleyi* outbursts resulted in a release of

1507 inorganic carbon (PIC) in the form of $CaCO_3$ in surface waters in amounts ranging from ~10 to several

1508 hundreds of kilotons. In the Barents Sea, the released PIC content varied between ~100 kt and 250-300 kt,

1509 whereas in the Bering Sea, during the two periods of exceptional activity, the PIC content was as high as 500

1510 kt (Kondrik et al., 2017). There is ample evidence that the release of PIC was accompanied by a significant

1511 increase in CO_2 partial pressure ($\Delta p CO_2$) within the bloom area: between 1998 and 2016, the mean and

1512 maximum values of the ratio $\Delta p CO_2 / (\Delta p CO_2)_{background}$, varied in the ranges of ~ (20-40)%, and ~(30- 60)%,

1513 respectively. The highest numbers were registered in the Bering and Barents seas (Kondrik et al., 2018a;

1514 2019). Also, there is space borne evidence for the atmospheric columnar ΔCO_2 enhancement $(\Delta CO_2)_{atm}$ over

1515 *E. huxleyi* blooms: numerous case studies in the aforementioned North Atlantic seas as well as in the Barents

1516 and Black seas proved that $(\Delta CO_2)_{atm}$ could reach 2-3 ppm (Kondrik et al., 2019; Morozov et al., 2019).

1517

1518 Notwithstanding the remarkable ability of *E. huxleyi* to grow under conditions unfavorable for algae of other

1519 functional groups (e.g. diatoms, flagellates, cyanobacteria), a highly irregular pattern of the registered two-

1520 decadal (1998-present) time series of S, PIC, and $\Delta p CO_2$ are indicative of susceptibility of this alga outbursts

1521 to environmental conditions (Nissen et al., 2018; Kazakov et al., 2019; Silkin et al., 2019). Statistical

1522 prioritization of non-biogenic forcing factors (FFs) shows that the latter are sea- and time-period specific

1523 (Pozdnyakov et al., 2019). Thus, in the Barents Sea, sea water temperature (SWT) is the highest-ranked FF,

1524   followed by PAR (photosynthetic active radiation). In the Bering Sea, beyond the aforementioned periods

1525   (1998-2001 and 2018-present), sea surface salinity (SSS) is the FFs leader, with PAR as a runner up,

1526   whereas SWT is only third in the row. Although these assessments are done without explicitly considered

1527   nutrients concentrations (NCs), implicitly NCs were among the FFs. Indeed, arguably, variations in SWT,

1528   SSS, CHL, MLD, and surface current speed/advection (tested as FFs) indirectly account for the variations in

1529   NCs as well in such CCSs parameters as alkalinity and basicity (Durairaj et al., 2015; Pozdnyakov et al.,

1530   2019, and references therein).

1531

1532   In the long run, the steady accumulation of CO_2 into the atmosphere should closely be considered (Rivero-

1533   Calle et al., 2015). The action of a rising atmospheric CO_2 concentration is expected to proceed through a

1534   number of direct and indirect interactions (Fig. 7), both of which should ultimately cause alterations in the

1535   rain ratio. An increase in the atmospheric CO_2 concentration leads to the rising of the global temperature, and

1536   further to the strengthening of stratification, intensification of irradiance within the euphotic zone and cutting

1537   of nutrient fluxes from below. Although increases in CO_2 fluxes to the surface ocean cause a reduction of pH

1538   and CO_3^{2-} levels in water, the large pool of HCO_3^- remains to support the calcification machinery. Thus, it

1539   will lead to the establishment of environmental conditions unfavorable for non-calcifying phytoplankton

1540   (NCP), but beneficial (or at least endurable) for coccolithophores in general and *E. huxleyi* specifically. The

1541   reduction of NCP and uncontested growth of *E. huxleyi* drives a further reduction of dissolved CO_2

1542   consumption by other groups of phytoplankton, increase in $p$$CO_2$ in the surface ocean and intensification of

1543 CO_2 fluxes into the atmosphere. Concurrently, through a system of feedback interactions, alterations in the

1544   rain ratio are bound to affect the carbon fluxes at the water-atmosphere interface. Therefore, the scenario of

1545   further increases atmospheric CO_2 concentration in the future, in all probability, implies a vaster proliferation

1546   of *E. huxleyi* in the world's oceans.

1547

1548   In combination with statistic-based-mathematical models of *E. huxley* blooms (Pozdnyakov et al., 2019), the

1549   available IPCC climate models permit mid-term projections of the forthcoming changes (Gnatiuk et al.,

1550   2020). However, our knowledge on the reciprocal influence of climate change and both the structure and

1551   functioning of marine ecosystems (even at the level of primary producers!) is still insufficient to confidently

1552   prognose the future dynamics of the *E. huxleyi* phenomenon. More studies are required even to fully

1553   understand the mechanism of intracellular light-dependent reaction of calcification, its dependency on both

1554   seawater carbonate chemistry and environmental FFs (Vihma et al., 2019). Creation of respective

1555   multidecadal databases (as in Kazakov et al., 2019) as well as further delivery of satellite and *in*

1556   *situ*/shipborne/laboratory data are necessary to improve our capacity to assess with certainty the

1557   climatological and ecological role of *E. huxleyi* blooms on regional and global scales (Fig. 7).

1558

1559   2.3.3 Lakes and rivers (Q9)

1560   *Organic carbon in lakes*

1561

Spatial variability, an essential characteristic of lake ecosystems, has often been neglected in field research and monitoring. The detected spatial "noise" strongly suggests that besides vertical variation also the horizontal variation should be considered in the ecosystem monitoring and, most importantly when the role of dissolved organic carbon (DOC) on the CO_2 flux is estimated (Manasypov et al., 2015; Leppäranta et al., 2018). In natural waters with an increasing level of colored dissolved organic matter (CDOM) concentration, the water color is shifted towards brown. The key "permanent" landscape variables, the coverage by lakes and peatland in the catchment area can be strongly correlated with lake elevation above the sea level. A high lake coverage indicates a low CDOM concentration, while a high peat coverage indicates the opposite (Arvola et al., 2016). For example in Finland, recent results from inland water studies have not shown any overall, consistent large-scale changes in CDOM concentrations over the last 101-year period (Arvola et al., 2017). Rather, CDOM changes in individual lakes have been related to changes in land use in the drainage basin. Manasypov et al. (2015) reported results from Siberian lakes, representing a discontinuous permafrost zone, and addressed that although the concentration of most elements in the lakes are lowest in spring, the maximal water coverage of land made it as an significant reservoir of DOC. The soluble metals in the water column that can be easily mobilized to the hydrological network.

In very shallow freezing lakes, the volume liquid water is much reduced due to ice growth, and rejection of nutrients and pollutants in the ice growth causes major enrichment of the water body. This has major implications to the ecosystem of these lakes (Yang et al., 2016; Song et al., 2019). Freezing rejects some 80-90 % of the impurities in freshwater lakes. On the other hand, ice cover accumulates atmospheric deposition over several months but releases them into the water body within one month's melting phase. Rejection of nutrients and pollutants in lake ice growth causes major enrichment of the water body in shallow lakes and notable increases in nutrient concentrations in a shallow lake during seasonal ice growth (Fang et al., 2015).

Lake carbon balance

Arctic and boreal lakes are an important natural source of CH_4 into the atmosphere (Bastviken et al, 2011). Methane is produced mainly in the bottom sediments and/or hypolimnion, where most of the anaerobic decomposition of organic matter take place, and then is either oxidized to CO_2 in the water column or emitted to the atmosphere. At Kuivajärvi, a typical meso humid lake located in Southern Finland, it was found that 91% of available CH_4 was oxidized in the active CH_4 oxidation zone during hypolimnetic hypoxia (Saarela et al., 2020). In warm springs, the early onset of thermal stratification with cold and well-oxygenated hypolimnion delays the period of hypolimnetic hypoxia and thus limiting the production of methane. At Kuivajärvi measured CO_2 fluxes (F-CO2) showed that the lake acted as net source of carbon during two open-water periods (Mammarella et al., 2015). During daytime, with typically high wind speeds, shear-induced water turbulence controls the water-air gas transfer efficiency, thus enhancing the vertical diffusive fluxes across the water-air interface. However, during calm nighttime conditions, buoyancy-driven turbulent mixing, associated with penetrative cooling of surface water, controls the gas exchange, and simple

1600   wind speed-based transfer velocity models strongly underestimate F- CO_2 (Mammarella et al., 2015). Kiuru

1601   et al. (2018) developed a model simulating CO_2 dynamics of a boreal lake in warming climate. The

1602   simulations for 2070-2099 showed a 20–35% increase in the CO_2 flux from the lake compared to the

1603   reference period of 1980–2009.

1604

1605   *Lake ice cover*

1606   Wei et al. (2016) studied the Lake Inari (67.14 N, 25.73 E), Finnish Lapland, in winters 1980/1981 -

1607   2012/2013, and observed an increasing trend in the air temperature during the freezing season, associated

1608   with an increasing trend in the water precipitation during winter. Low temperatures with less precipitation

1609   lea to the formation of columnar ice, while strong winds together with heavy snowfall favored granular ice

1610   formation. Karetnikov et al., (2017) analyzed long-term ice conditions in Lake Ladoga, Russia, for the period

1611   of 1913–2015 and showed that the mean freezing and breakup dates were November 26 and May 15,

1612   respectively, and that the annual frequency of complete freeze over of the lake was 0.83.The period from

1613   1990 to present was much milder than the preceding years. The annual increase in the ice concentration

1614   depended on the accumulated freezing-degree-days (AFDD) and the hypsographic curve, while the ice

1615   thickness increased with the square root of AFDD.

1616

1617   An analysis of a Siberian thermokarst lake located in the Lena River Delta, characterized as a floating ice

1618   lake, showed that the temporal dynamics and magnitude of heat fluxes and surface energy balance closures

1619   are substantially different depending on lake surface conditions (Franz et al., 2018). Sensible heat and latent

1620   heat fluxes, modelled using available heat bulk transfer models (Woolmay et al, 2015; Verburg and

1621   Antenucci, 2010; Andreas et al, 2002), tend to underestimate the measured fluxes and show less variability

1622   over freezing ice cover, melting ice in Spring, as well as over open water in Summer. However, the

1623   performance of these models depends also on the accuracy of meteorological and hydrological input

1624   parameters, which should be carefully measured especially during challenging winter conditions.

1625

1626   The seasonal lake ice cover is a sensitive indicator of climate variations in the Arctic (Kirillin et al., 2012;

1627   Leppäranta, 2015). To work more on this question, Lake Kilpisjärvi (surface 37.1 km2, max depth 57 m), a

1628   tundra lake in northern Finland, has been under an intensive ice-related field programs in recent years. The

1629   research covered the whole year but was focused on the melting period in May–June. The heat budget over

1630   the ice season was dominated by the radiation balance. Turbulent fluxes were significant before the freeze-up

1631   in fall, but in the ice season they were small. The evolution of ice thickness served as a very good

1632   approximation to the total surface heat flux (Leppäranta et al., 2017) (Fig. 8). In the melting stage, solar

1633   radiation, the strongest forcing of the water body beneath ice cover, breaks the stability and initiates

1634   convective turbulent mixing. This brings heat from the deeper water to ice, enhancing melting at the ice

1635   bottom (Kirillin et al., 2018). Thus, the common assumption of the heat flux from the water to ice to be due

1636   to molecular conduction does not hold in the melting stage but it is much higher. The ice–water interaction

1637   under lake ice has not been well covered in earlier studies of ice growth and melting.

1638

1639 The ice melting process was studied in detail in Lake Kilpisjärvi. The melting progressed in the upper and

1640 lower surfaces and in the interior, with proportions depending on the solar flux and optical properties of the

1641 ice, and were therefore case-dependent. About one-third of the solar flux that penetrated the ice returned to

1642 ice bottom, providing heat for melting. This was consistent with the under-ice results by Kirillin et al. (2018).

1643 In 2013 a rapid ice breakage event completed the ice breakup in a short time interval, with final breakage at

1644 the ice porosity 40-50%. A lake ice melting model should include the thickness and porosity of ice, with

1645 porosity connected to an ice strength criterion (Leppäranta et al., 2019).

1646

1647 *Lake Baikal and Selenga River delta*

1648 The Selenga River, the main tributary of Lake Baikal, has a catchment area of 450 000 km^2 in the boundary

1649 region between Northern Mongolia and Southern Siberia. This area is well known by its climate, land use

1650 and dynamic socioeconomic changes which might have negative impacts on the ecosystems of Lake Baikal

1651 and thus was selected as PEEX field laboratory within PEEX subprogram Selenga-Baikal Network

1652 (www.atm.helsinki.fi/peex/index.php/baikal-selenga-network-basenet. In the recent past, hydroclimatic

1653 development together with land use changes led to a contaminant influx from mining areas and urban

1654 settlements increased. Additional hydrological modifications due to the construction of dams and

1655 abstractions/water diversions from the Selenga's Mongolian tributaries could lead to additional alterations

1656 (Karthe et al., 2017b). In addition to Selenga River, a key issue for an improved understanding of regional

1657 impacts of the environmental change is to disentangle the influence of climate change from that of other

1658 pressures within the catchment (Lychagin et al., 2017). The PEEX subprogram Selenga-Baikal Network

1659 aims at integrated field-based and modeling knowledge to develop basin-wide conceptual framework of

1660 riverine fluxes (Kasimov et al., 2017a; Karthe et al., 2019).

1661

1662 As a PEEX field laboratory, regional large-scale assessments made it possible to predict the comprehensive

1663 nature of hydrological and geochemical changes driven by climatic processes and human impacts. Heavy

1664 metals in water and sediments (Kasimov et al., 2020a, 2020b) and fish communities (Kaus et al., 2017) were

1665 measured since 2011 in over 50 locations around the catchment. The mining zones are potential hotspots for

1666 increasing metal loads to downstream river systems. Several metals (Al, Cd, Fe, Mn, Pb and V) are exported

1667 from mining sites to the downstream river system, as shown by net increasing mass flows. Based on a novel

1668 partitioning coefficient approach (Table. 2), contrasting patterns with domination of both particulate and

1669 dissolved phases in different parts of the basin were found. Such heterogeneity in the metal partitioning is

1670 likely to be found in many large river systems.

1671

1672 Multi-scale modeling ranged from the basin wide (Malsy et al., 2017; Frolova et al., 2017) to specific sub-

1673 regions, such as particular segments of the river system (Kaus et al., 2017; Thorslund et al., 2017; Garmaev

1674 et al., 2019) or its delta (Chalov et al., 2017a, 2017b; Shinkareva et al., 2019), and identified reactions of

1675 hydrogeochemical pathways on climate change. The mean flow reduction in the Selenga River was 3-5%

1676   during 2020's to 2030's and 4-25% during 2080's to 2090's, being a crucial driver of ongoing and future

1677   hydrogeochemical changes. Increases in temperatures with permafrost thaw and the expansion of

1678   agricultural, mining and urbanization processes may induce up to a 6% increase in the particulate modes and

1679   3% in the dissolved modes of some metals in the river system (Chalov et al., 2018). Possible changes in the

1680   number or magnitude of high-flow events, caused by climatic or other anthropogenic factors, could influence

1681   the total sediment deposition, which was primarily found to occur during relatively short high-flow events.

1682   Such potential changes have important implications to the possible spreading of polluted sediments (Pietron

1683   et al., 2015) and their storage in the Selenga River Delta, which is an important wetland region forming the

1684   geochemical barrier which mitigate pollution of Lake Baikal by riverine fluxes (Voropay and Kichigina,

1685   2018, Chalov et al., 2015). The Selenga delta region sequester various metals bound to Selenga River

1686   sediments (Chalov et al., 2015, Pietroń et al., 2018). The water shortage decreases the processes of

1687   suspended sediment retention in the delta. The seasonal hydrogeochemical patterns are explained by wetland

1688   inundation during floods and channel erosion or Baikal wind surge during low flow periods (Chalov et al.,

1689   2017a, 2017b).

1690

1691   *Asian water lakes*

1692

1693   The largest internal drainage basins in the world are located in Central Asia, with a limited availability of

1694   both surface and groundwater (Karthe et al., 2017a). Since the twentieth century, water resources of this

1695   region have been over exploited and, for example, from small Mongolian headwater streams to the mighty

1696   Aral Sea, surface waters have been partially desiccated. It seems that the implementation of the Integrated

1697   Water Resources Management and water-food-energy nexus approaches would lead to a more

1698   environmental-friendly future (Karthe et al., 2017). The lake-rich Qinghai-Tibet Plateau (QTP) has recently

1699   been identified as the Third Pole of the Earth. Due to its high elevation and unique climate, QTP affects the

1700   global and local climate and played an important role on the Central and Southern Asian water cycle (Zhang

1701   et al., 2018). Lake-atmosphere interactions have been quantified over open-water periods, yet little is known

1702   about the lake ice thermodynamics and heat and mass balance during the ice-covered season. A modelling

1703   study for a thermokarst lake in the QTP was performed (Huang et al., 2019a). Strong diurnal cycles were

1704   seen for all surface heat fluxes. The ice mass balance was dominated by the growth and melt at the base, but

1705   the surface sublimation was also crucial for the ice loss, accounting for up to 40% of the maximum ice

1706   thickness and 41% of the lake water loss during the ice-covered period. The strong penetration of solar

1707   radiative flux is the dominant contributor to the high value of upward sensible heat flux at ice bottom,

1708   resulting in a relatively thin ice cover compared with equivalent high-latitude climate.

1709

1710   2.4   SOCIETY

1711

1712   The anthropogenic impact has been addressed as one of the PEEX themes for the society system. The

1713   discussion on the mitigation and adaptation, including urban infrastructure design and risk assessment, are

1714   addressed in this context (Q10, section 2.4.1). The social transformations are discussed in terms how local

1715   reindeer grazing interacts with the environment (Q11 section 2.4.2). The adaptive capacity of the Northern

1716   societies depends on their environment, demographic structure and economic capacity, and the

1717   environmental hazards and environmental health under chancing climate are the key research areas in this

1718   context (Q12 section 2.4.3.).

1719

1720   2.4.1. Anthropogenic impact (Q10)

1721

1722   *Mitigation*

1723   Artic climate change generates a need for long-term planning and development of new socio-economic

1724   infrastructures, such as dams, bridges, roads and transnational and regional energy networks. For this task,

1725   new climate-based forecasting tools, cost and operational risk estimates as well as other methods and tools

1726   for an infrastructure and urban design are needed. As an example, engineering calculations for maximal

1727   discharges were provided for the Nadym River in Russia (Shevnina et al., 2017). Badina (2018) introduced a

1728   method for the natural risk assessment by using indices based on socioeconomic potential data and spatial

1729   distribution of natural hazards. This method has been tested and used to identify the most vulnerable

1730   municipalities in South Siberia. Another example of new methods is a "Green Factor tool" to increase the

1731   share and effectiveness of green areas in urban environments and cities. An ambitious target set in this tool

1732   could encourage or force urban developers to aim higher with the planning of green areas and construction,

1733   however the existing regulations challenge the use of this approach (Juhola, 2018).

1734

1735   The energy production is of fundamental importance for the society functions, and new clean energy

1736   technologies are needed for hindering the climate change. The potential of hydropower production under

1737   probabilistic projections of annual runoff rate and future changes in the potential hydropower production

1738   need to be evaluated (Shevnina et al., 2019). All the Nordic countries are vulnerable to various degrees to

1739   potential cross-border impacts, due to their energy sectors being highly globalized and interconnected.

1740   However, cross-border impacts are not yet properly included in Nordic climate assessments or energy

1741   strategies. The EU's new Green Deal is pivotal in this respect, as for the first time emissions along the whole

1742   supply chain (oil, gas, coal, renewables) become under scrutiny and as part of a normative governance.

1743   Therefore, policy makers and energy planners should be assisted in making comprehensive vulnerability

1744   assessments that address both domestic and international climate risks (Groundstroem and Juhola, 2019).

1745

1746   2.4.2 Environmental impact (Q11)

1747

1748   *Reindeer (Rangifer tarandus L.) grazing and ground vegetation structure and biomass*

1749

Reindeer (*Rangifer tarandus L.*) grazing in the North affects the ground vegetation structure and biomass and cover of lichens. It seems that reindeers affect GHG fluxes from the forest field layer. Grazing changes affect the vegetation composition and thereby emissions (Köster et al., 2018). Köster et al. (2017) provided detailed information on soil CO_2 effluxes, which were mostly affected by the year of measurement, time of measurement, soil temperature and also by the management, resulting in higher CO_2 emissions on the grazed areas. Soil moisture content did not affect the soil CO_2 efflux. For example, in the Finnish Lapland the average soil CO_2 efflux values were significantly higher in 2014 compared with 2013, mainly due to differences in the soil temperature at the beginning of the season (Köster et al., 2017). Furthermore, grazing significantly decreased the biomass and cover of lichens and also the amount of tree regeneration. In a subarctic mature pine forest, grazing did not affect the soil temperature or soil moisture. No statistically significant effect of grazing on the soil CO_2 efflux, soil C stock or soil microbial C biomass was found. The soil microbial N biomass was significantly lower in the grazed areas compared to the non-grazed areas. It seems that in the boreal subarctic coniferous forests, grazing by reindeer can be considered as "C neutral" (Köster et al., 2015). There is also indication that reindeer grazing affects the boreal forest soils e.g. their fungal community structure and litter degradation (Santalahti et al., 2018).

2.4.3 Natural hazards (Q12)

Under this theme, the PEEX research has so far focused on environmental health issues. These include diseases, impact of UV radiation, and air pollution in urban environments. The spread of diseases caused by living pathogens is basically determined by environmental conditions. Medico-geographical assessments are usually based on identification of the links between the spread of diseases and factors of the geographical environment.

Naturally-determined diseases

Climatic factors are deemed among the main determinants for the spread of naturally-determined diseases (Malkhazova et al., 2018). Emerging zoonotic diseases are expected to be particularly vulnerable to climate and biodiversity disturbances. Anthrax is an archetypal zoonosis that manifests its most significant burden on vulnerable pastoralist communities. Ezhova et al. (2021) investigated the dynamics of environmental factors that led to an anthrax outbreak in Yamal Peninsula, Siberia, during 2016. They found that the local permafrost was thawing rapidly for the last 6 years before the outbreak, supporting the hypothesized role of permafrost thaw in triggering this outbreak, and concluded futher that the spread of antrax was likely intensified by the extremely dry summer of 2016 in the region. Overall, the recent findings highlight the significance of warming temperatures for anthrax ecology in northern latitudes, and suggest potential mitigating effects of interventions targeting megafauna biodiversity conservation in grassland ecosystems and animal health promotion among small to midsize livestock herds (Walsh, et al., 2018). Equally important is the monitoring of climatic factors, such warming and precipitation extremes, in Arctic regions previously contaminated by Anthrax (Ezhova et al., 2021).

1788

1789 *UV variations*

1790 Different geophysical parameters affecting the UV molecular number density show that especially at high

1791 altitudes, the increased surface albedo has a significant effect on the UV growth. The new parameterization

1792 of the on-line UV tool (*momsu.ru/uv/)* for Northern Eurasia allows us to determine the altitude dependence

1793 of UV and to estimate the possible effects of UV on human health considering different skin types and

1794 various open body fraction for January and April conditions in the Alpine region (Chubarova et al., 2016b).

1795 Using UV satellite retrievals, ERA-Interim data and the INM-RSHU chemistry-climate model, the changes

1796 in the UV irradiance and UV resources were estimated over Northern Eurasia for the 1979-2015 period,

1797 demonstrating significant UV increases over vast areas (Chubarova et al., 2020). Referring to long-term UV

1798 measurements and model simulations in Moscow, a statistically significant positive trend of more than 5%

1799 per decade since 1979 was evaluated (Chubarova et al., 2018). Related to the connection between UV

1800 variation and stratospheric O_3, see also the section 2.2.1 Atmospheric composition and chemistry.

1801

1802 *Examples of air pollution episodes*

1803

1804 Street-level urban air pollution is one of the key topics in urban environments. For example, in Norway,

1805 Bergen, the most extreme cases of repetitive wintertime air pollution episodes, followed by increased large-

1806 scale wind speeds above the valley, were transported by the local re-circulations to other less polluted areas

1807 with only slow dilution. This result underlines the need for better described assumptions on transport paths

1808 and weak dispersion in classical air pollution models, in order to improve the current air quality forecasts in

1809 urban areas (Wolf- Grosse et al., 2017b). A link between the persistence of the flow above the Bergen valley

1810 and the occurrence and severity of the local air pollution episodes was found. Analysis of the large-scale

1811 circulation over the North Atlantic-European region, with respect to air pollution in Bergen, revealed that the

1812 persistence in meteorological conditions connected with air pollution episodes is not necessarily caused by

1813 large-scale anomalies of the atmospheric circulation over the Norwegian west coast, but rather connected

1814 with anomalies as far away as Greenland (Wolf-Grosse et al., 2017a).

1815

1816 In Russia, especially intensive atmospheric pollution episodes have severe impacts on the environment and

1817 human health. Popovicheva et al (2019b) analyzed the Tver region, north of Moscow, which was

1818 considerably affected the secondary organic aerosol (SOA) formation originating from long-lasting peat bog

1819 fires. Spectral absorbance characteristics were similar to peat burning and traffic source emissions during fire

1820 and non-fire related days and confirmed the effect of transported peat smoke on air quality in a megacity

1821 environment (Popovicheva et al., 2019b). Popovicheva et al. (2019b) also showed that long-term transport

1822 from the North-West Russia and Scandinavia influence the local population.

1823

1824 Local Arctic air pollution alone can seriously affect public health and ecosystems locally, especially in

1825 wintertime when the pollution can accumulate under inversion layers (Schmale et al., 2018a). We need more

research on the contributing emission sources and the relevant atmospheric pollution mechanisms, and more detailed epidemiological or toxicological health impact studies in the Arctic. Socioeconomic changes (shipping, tourism, natural resources extraction, increasing number of population) are already taking place in the Arctic, and they will increase in the future. It is also expected that the emission types and magnitudes will increase the number of exposed individuals (Arnold et al., 2016). There is still a large variation in the amount of the location of emissions. Future predictions are even more difficult due to the yet unknown development of the Arctic economic activities and their emissions (Arnold et al., 2016, Schmale et al., 2018a, 2018b).

3. SYNTHESIS AND FUTURE PROSPECTS

3.1 Future research needs from the system perspectives

For the Land ecosystem, the recent progress towards understanding of the Northern Eurasian Arctic - boreal land ecosystems (section 3.1) are dealing with improved methodologies relevant to land processes (Q1), observations on permafrost thawing (Q2), and observed changes in the Northern ecosystems, especially soil conditions (Q3).

Improved satellite-based methods and (validation) data together with better quantification and, especially, the scaling of the gross primary production (GPP) are enabling a better identification and quantification of Earth surface characteristics and ecosystem carbon balance compared with the earlier capacity (Gurchenkov et al., 2017, Rautiainen et al., 2016, Nitzbon et al., 2019, Boike et al., 2019, Terentieva et al., 2016), Zhang et al, 2018, Pulliainen et al., 2017, Matkala et al., 2020; Bondur and Chimitdorzhiev, 2008 a,b). Intensive research has been carried out on the quantification of the GPP, a key variable for biological activity, in different conditions and at different scales (Pulliainen 2017, Kulmala et al., 2019, Matkala et al., 2020). Further investigations are called for a more detailed understanding of the seasonal dynamics of the biological activity.

The Northern Eurasian ecosystems' tipping points are related to multiple simultaneous stress factors. The key stress factors here are the permafrost thawing and factors important for ecosystems, such as the prolongation of the growing season, increase in the mean temperature of the growing season and forest fires (Kukkonen et al. 2020, Biskaborn et al. 2019, Payne et al., 2016. Köster et al. 2016, Miles and Esau 2016, Miles et al., 2019). New evidence on the progress of permafrost thawing in Siberia has been introduced by Kukkonen et al. (2020) and Biskaborn et al. (2019). The permafrost thawing is also triggering yet not clearly-known processes related to changing fluxes, ecosystem processes and dynamics of greenhouse gas sinks and sources (Schuur et al., 2008, Thomson et al., 2017, Commane et al., 2017, Euskirchen et al., 2017, Dean et al., 2018, Thonat et al., 2017). The progress affecting permafrost thawing has not yet been analyzed in detail. For example, we need more information on the dynamics of how the thawing processes vary between soil types due to differences in water movement and, in the winter time, how the snow cover affects

1864   ground surface temperatures (Bartsch et al. 2010). In addition to permafrost processes, the recent advances in

1865   observed changes in the Northern ecosystem reveal a significant role of soil processes in biogeochemical

1866   cycles, especially the nitrogen cycle (Voigt et al., 2016, Pärn et al., 2018). Knowledge of the soil

1867   microbiological composition and the effect of forest fires have been improved (Köster et al., 2015, 2016,

1868   Zhang-Turpeinen et al., 2020), but further research is called for vegetation changes influencing the below-

1869   ground microbiology, its composition and enzymatic activity (Payne et al., 2016. Köster et al. 2016). The

1870   NDVI methods have made it possible to detect vegetation changes (Miles and Esau 2016). A range of

1871   vegetation cover changes in Siberia have been reported, such as the Arctic greening and browning processes,

1872   but e.g. the greening of Siberian cities remains an issue of intensive research also in the future (Miles and

1873   Esau 2016, Miles et al., 2019).

1874   For the Atmospheric system, the recent progress in understanding the Northern Eurasian Arctic - boreal land

1875   atmospheric system and the aspects of the megacity air quality (section 3.2) are dealing with atmospheric

1876   composition changes (Q4), key feedbacks between climate and air quality (Q5), and synoptic scale weather

1877   (Q6). Recent results demonstrate improved quantification of the carbon balance and CO_2 fluxes and

1878   concentrations due to land use change, forest fires in Siberia, and new understanding of aerosol sources and

1879   properties in the Arctic environment and across the Northern Eurasia (Pulliainen et al., 2017, Karelin et al.,

1880   2017, Rakitin et al., 2018, Skorokhod et al., 2017, Alekseychik et al. 2017). However, most of the results

1881   deal with atmospheric aerosol chemistry and physics in boreal and Arctic environments originating from

1882   measurements in the few flagship stations in Finland and Russia (Kerminen et al., 2018, Wiedensohler et al.,

1883   2019, Freud et al., 2017, Paasonen et al., 2018, Östrom et al., 2017, Kalogridis et al., 2018, Bondur et al.,

1884   2016, Bondur and Ginzburg 2016, Bondur et al, 2019 c,d, Bondur and Gordo, 2018; Mikhailov et al., 2017,

1885   Breider et al., 2017), indicating the need for a comprehensive station network in the PEEX region. Black

1886   carbon emitted by the Siberian forest fires and some other sources, and its long range transport to the Arctic,

1887   are also widely discussed (Kalogridis et al., 2018, Bondur et al., 2016, Bondur and Ginzburg 2016,

1888   Mikhailov et al., 2017, Breider et al., 2017, Shevchenko et al., 2015, Konovalov et al., 2018, Marelle et al.,

1889   2018). In addition, measurements of ozone in the troposphere and stratosphere provide insight into

1890   atmospheric chemistry in urban environments (Skorohod et al., 2017), UV radiation and human health

1891   (Chubarova et al., 2019). Environmental health, including the impacts of air quality and UV radiation, is

1892   foreseen as a high momentum research topic in the PEEX domain, and further research is called for in this

1893   area.

1894

1895   Related to air pollution, we reported several new results on the dynamics between the haze pollution and

1896   boundary layer meteorology in enhancing air pollution in megacity environments (Zhao et al., 2017, Ding et

1897   al., 2016a, Wang et al., 2018b, Bai et al., 2018a, Ye et al., 2017). The long-term and comprehensive

1898   measurements carried out especially at the SORPES station in Nanjing provide valuable data pools for such

1899   studies (Ding et al., 2016a). However, the backbone of the recent progress has been the improved on-line

1900   atmospheric measurements and the use of machine learning methods combined with different methodologies,

1901   such as back trajectories together with the lidar and radiosonde data. In addition, improved models of

emission inventories together with the ECHAM-HAM and GAINS models have led to a better quantification of aerosol number emissions. New knowledge has enabled the introduction of new theoretical arguments on the feedbacks between high aerosol concentrations and the urban boundary layer (Petäjä et al. 2016). New measurements have also been obtained from Siberian cities (Elansky et al., 2016, Chubarova et al., 2016a, Mahura et al., 2018). However, we are still in the early phase of having a holistic picture on large-scale feedbacks due to the lack of long-term, comprehensive measurements in these regions.

Changes in the atmospheric dynamics in the North have potential impacts on short-term local/regional and sub-seasonal to seasonal large-scale weather predictions, and on long-term projections on biogeochemical systems. It is therefore crucial to understand changes in boundary-layer processes as well as synoptic- and large-scale circulation in the Arctic and Northern Eurasia. Recent results show potential, but causally arguable, connections between the alarming sea ice decline, evaporation, cloudiness, atmospheric circulation and moisture transport as well as Arctic and European winter temperatures (Nygård et al., 2019, Rinke et al., 2019, McCusker et al., 2016, Mori et al, 2014, Blackport et al., 2019; Cohen et al., 2020). Further investigations are called for atmosphere-ice-ocean interactions, coupling between small-scale processes (such as clouds and turbulence) and synoptic-scale weather, as well as for polar prediction and extreme events. Furthermore, more quantitative knowledge is needed on pan-Arctic energy budgets (Spengler et al., 2016). The urban heat island (UHI) phenomena taking place in Arctic cities has received an increasing attention, and there is a special need for improved forecasting services for Arctic cities (Miles and Esau 2017, Konstantinov et al., 2018, Varentsov et al., 2018b).

For the Water system, we discussed the Arctic sea ice dynamics and thermodynamics, snow depth and sea ice thickness, sea ice research supporting navigation, and rare elements in the snow and the ocean sediments, especially from the perspective of improvements in the observation and modelling methods (Q7, section 3.3.1.). New evidence on atmosphere–Arctic sea ice interactions have been provided by Lei et al. (2018), and Jakobson et al. (2019). Lei at al. (2018) analyzed how the climate warming would affect the winter growth rate of thin and thick ice, and Jakobson et al. (2019) gave new insight into the relation between sea ice concentration and the wind speed. Furthermore, advance has been made in understanding the thermodynamics and metamorphosis of the snowpack on sea ice and their interactions with surface albedo changes (Dou et al., 2019). Operational sea ice analysis is increasingly important for the Arctic shipping and navigation (Lei et al., 2015, Karvonen et al., 2017). New results on rare elements, mineral composition and CO_2 and methane fluxes associated with ocean sediments have been attained (Maslov, et al., 2018, Yasunaka et al., 2018). This serves as an important information for mitigation plans, as well as for new estimates on the river runoff and discharge in Russian rivers into the Arctic seas (Grigoriev and Frolova 2018, Agafonova et al., 2017).

The marine Arctic ecosystems are under a progressive increase of anthropogenic impacts, the main issues calling for better understanding being the integrated effect of Arctic warming, ice and snow melt, ocean

1940 freshening, air quality and acidification of the Arctic marine ecosystems, primary production and carbon

1941 cycle (Q8, section 3.3.2). Quantitative information about the CO_2 accumulation into the ocean is having a

1942 high momentum. Marine organisms, such as coccolithoprip algae, are influencing the CO_2 flux exchange

1943 (Kondrik, et al., 2018b, Pozdnyakov et al., 2017). In addition to changing marine environments, the Artic –

1944 boreal lakes and rivers may undergo changes in flooding, increasing the amount of fresh water and

1945 allochthonous materials (Q9, section 3.3.3). In addition to the Arctic Ocean, the ice and snow conditions of

1946 Northern lakes are under pressure. Lake Kilpisjärvi (Finland) (Arvola et al., 2017, Leppäranta et al., 2017)

1947 and Lake Ladoga (Russia) (Karetnikov et al., 2017) have been under an intensive research, and the recent

1948 results demonstrate changes in heat fluxes, ice cover periods and stratification. The browning of lakes and

1949 lake sediments were discussed, and new results were attained from the Selenga River of the Baikal Lake.

1950 Dramatic changes will be expected in the water runoff and in the amount of dissolved modes of metals, also

1951 having serious impact on the environmental health (Chalov et al., 2015, 2016, 2017 a, 2017b, Karthe et al.,

1952 2017 a, 2017b). As a comparison to the Northern high latitudes, we also discussed freezing lakes in Central

1953 Asia, where the climate is cold and arid. There the ice is typically snow-free, or possesses only a thin snow

1954 cover, allowing penetration of sunlight into the water body (Huang et al., 2019).

1955

1956 For the Societal system, the anthropogenic impact has been addressed as one of the main themes (Q10). The

1957 discussion on the mitigation and adaptation, including the urban infrastructure design (Juhola 2018) and risk

1958 assessment, were addressed in this context (section 3.4.1). In social transformations, a special attention was

1959 given to one of the most important local livelihoods in Lapland: reindeer grazing and how it interacts with

1960 the environment (Q11 section 3.4.2). The adaptive capacity of the Northern societies rest on their

1961 environment, demographic structure and economic activities (Q12). Referring to the earlier statement about

1962 the future research needs for the Atmospheric system with respect to environmental health, here again we

1963 would like to put an increasing attention to environmental health under changing climate, including the

1964 spread of diseases and air pollution and their combined effects (section 3.4.3.).

1965

1966 3.2 Feedback mechanisms under changing climate, cryosphere conditions and urbanization

1967

1968 During the recent years, Kulmala et al. (2004, 2020) have focused on the quantification of the COntinental

1969 Biosphere-Aerosol-Cloud-Climate (COBACC) feedback loop relevant to the boreal region in Northern

1970 Eurasia. Previous results on the COBACC feedback loop addressed the role of BVOC emission dynamics

1971 (Arneth et al., 2016). Both higher temperatures and increased CO_2 concentrations are (separately) expected

1972 to increase emissions of biogenic volatile organic compounds (BVOCs) to the atmosphere. It also seems that

1973 the GPP is controlled by the BVOC effects on the clouds. Sporre et al. (2019) used an Earth System model to

1974 estimate aerosol scattering due to enhanced BVOC emissions and estimated the associated negative direct

1975 radiative effect (-0.06 W m^{-2}). The total global radiative effect associated with this feedback was estimated to

1976 be -0.49 W m^{-2} (Sporre et al., 2019), indicating that it has the potential to offset about 13 % of the forcing

1977 associated with a doubling of CO_2. The direct effect of aerosol on GPP due to an increase in the fraction of

diffuse radiation was estimated between 6 and 14% increase in GPP at maximum observed aerosol loading compared to low aerosol loading in Northern Eurasia forests (Ezhova et al., 2018b).

The results from the Tibetan plateau demonstrate notable feedbacks between vegetation, BVOC emissions and aerosol particles. The historical wetting of the TP region has increased the vegetation cover, allowing for feedback processes via biogenic aerosol formation and aerosol-cloud-precipitation interactions. A significant wetting trend since the early 1980's in Tibetan Plateau is most conspicuous in central and eastern Asia. Fang et al. (2019) hypothesized that the current warming may enhance emissions of biogenic volatile organic compounds (BVOC), which can increase secondary organic aerosols concentrations, contributing to the precipitation increase. The wetting trend can increase the vegetation cover and has a positive feedback on the BVOC emissions. The simulations suggest a significant contribution of increased BVOC emissions to the regional organic aerosol mass, and the simulated increase in BVOC emissions is significantly correlated with the wetting trend in Tibetan Plateau.

To estimate the net effects of various feedback mechanisms on land cover changes, photosynthetic activity, GHG exchange, BVOC emissions, formation of aerosols and clouds, and radiative forcing (Q14) calls for intensive collaboration and integration between the Arctic Ocean sciences and terrestrial sciences across the Pan-Arctic domain and across the Arctic and high-latitude domain. The Arctic greening and browning (section 3.1.3.) call for a multi-disciplinary scientific approach, improved modelling tools and new data to deeply understand the biosphere-atmosphere-anthroposphere interactions and feedbacks. Petäjä et al. (2020a, 2020b) discussed the complexity of feedbacks, especially at the Arctic context, and the interplay between the temperature, GHG, permafrost, land cover and water bodies and between photosynthetic activity, aerosols, clouds and radiation budget. The current downturn of the arctic cryosphere (*section 3.1.2*), together with the changes in sea ice dynamics and glaciers and the permafrost thawing, affect bot marine and terrestrial carbon cycles in interconnected ways (section 3.3.1). Parmentier et al. (2017) discussed the changing arctic cryosphere and how the processes in the ocean and on land are too often studied as separate systems, although the sea ice decline connects the rapid warming of the Arctic, Arctic Ocean marine processes and air–sea exchange of CO_2. Thus, the future priorities would be on the development of our modelling tools towards an all-scale modelling approach to cover the feedbacks, processes and interactions at the land–ocean interface and also in urban environments in the Arctic region. We also need to support the further development of the ground-based observation networks.

3.3 Climate scenarios for the Arctic-boreal region

Climate scenarios set the urgency for the mitigation and adaptation actions for the Northern Eurasian region. The Arctic-boreal region combines an area of both amplified climate change (Arctic amplification) and large diversity in the model predictions (Collins et al., 2013; Hoegh-Guldberg et al., 2018). Under the "low-to-medium" RCP4.5 forcing scenario (van Vuuren et al., 2011), the CMIP5 multi-model mean temperature

2016 changes during the 21st century indicate the strongest winter-time warming of >5 ℃ in the Arctic Ocean,
2017 whereas the majority of the terrestrial region will warm by 2–4 ℃ (Fig. 12). Even during summertime, the
2018 continental warming over the region will generally exceed 2 ℃. It is important to note that the diversity of
2019 model projections is accentuated over the Arctic and Northern Eurasian domain: the mechanisms behind the
2020 Arctic amplification are implemented in varying details in the distinct models, and the associated interactions
2021 and feedback processes provide a diverse picture of the future in the Arctic-boreal regions.
2022
2023 In addition to considerable trends in atmospheric temperatures, the models further indicate prominent
2024 changes in precipitation (Collins et al., 2013, Hoegh-Guldberg et al., 2018). For the Arctic boreal region, this
2025 is largely depicted as an increasing rainfall during both winter and summer, extending to 15-25% over most
2026 of the terrestrial domain over the winter and somewhat less during summer (Fig. 9). Contemporary warm
2027 Arctic temperatures and large sea ice deficits (75% volume loss) demonstrate climate states outside our
2028 previous experience. The modeled changes in the Arctic cryosphere demonstrate that even limiting the global
2029 temperature increase to 2 ℃ will leave the Arctic a much different environment by mid-century, with less
2030 snow and sea ice, melted permafrost, altered ecosystems, and a projected annual mean Arctic temperature
2031 increase of +4 ℃. Even under ambitious emission reduction scenarios, high-latitude land ice melt, including
2032 Greenland, are foreseen to continue due to internal lags, leading to accelerating global sea level rise
2033 throughout the century (Overland et al., 2019).
2034
2035 **4.   CONCLUDING REMARKS**
2036
2037 Only the integration of different observing networks and programs into an inter-operable and integrated
2038 observation system can provide data needed for understanding the mechanisms of the Arctic-boreal system.
2039 There is a fundamental need for an integrated, comprehensive network of the-state-of-the art *in situ* stations
2040 measuring Earth surface – atmosphere interactions (Kulmala et al., 2016a, 2018; Uttal et al., 2016; Hari et
2041 al., 2016; Alekseychik et al., 2016; Vihma et al. 2019). The results obtained in the Pan Eurasian Experiment
2042 (PEEX) programme in Russian and China introduced in this paper are based on a combination of long-term
2043 observations and campaign data. In addition, the Arctic marine regions require comprehensive observations
2044 and subsequent synthesis, as these regions are under a lot of environmental stresses. Therefore, we need
2045 more *in situ* observations of the Artic system covering the marine atmosphere, sea ice and ocean. However,
2046 there are pronounced technological and logistical challenges to setup such continuous, marine *in situ*
2047 observations (e.g. Vihma et al. 2019). Furthermore, improved monitoring is needed for river discharge and
2048 associated fluxes of greenhouse gases and other key compounds and more research on the understanding of
2049 coastal processes and atmospheric transport and specific regional socioeconomic issues and their interactions
2050 with changing environments (Vihma et al., 2019; Petäjä et al., 2020a).
2051
2052 The international organizations and bodies like the Arctic Council (SAON's Roadmap for Arctic Observing
2053 and Data Systems, ROADS), EU Horizon2020 (Blue Growth INTAROS and APPLICATE projects), GEO-

CRI (high Mountains and cold regions), the Belmont Forum COPERNICUS and WMO are coordinating development of the Arctic data and services. New data products are expected from the large-scale MOSAiC campaign and projects like ERA-PLANET iCUPE (Petäjä et al. 2020b) or ArcticFLUX to monitor the interface between the marine Arctic and Eurasian continent. Also, national-based Arctic observations and research programs like AC[3] by German institutes play a significant role. Russia conducts extensive research in the Arctic region, notably on the manned drifting ice stations. These Arctic observation activities are coordinated and carried out by Roshydromet, universities and Russian Academy of Sciences' institutes.

Concerning global energy markets, the Artic region holds 25 % or more of the world's undiscovered oil and gas reservoirs (Arctic Oil & Gas, 2008). The plans of China and Russia to build 'Ice Silk Road' along Northern Sea linking the China and Russia to Europe is highlighting the growing economic and strategic importances of the polar regions, and the increasing pressure on the Arctic environment and local communities. In addition, wide areas of the high latitudes and Arctic regions are under the pressure of the changing economic activities of the Arctic, and also under high pressures of the changing environment and climate. A comprehensive observation network providing in-situ data in close coordination with satellite observations and ground-based remote sensing is required to monitor the environmental impacts of the envisioned operations.

Over the last few years, Earth system science is driven by the need to understand the scientific processes of climate change and air quality, their interrelations with the Earth system and their societal impacts. The interplay between science, politics and business, and the analysis of the existing policies and strategies, help us to recognize and analyze new and emerging trends of Arctic governance (e.g. protection and resilience vis-a-vis economic activities), geopolitics (e.g. state sovereignty vis-a-vis internationalization), geo-economics (e.g. tourism vis-à-vis reindeer herding), and science (e.g. climate change). The intensive work towards the new Arctic observations and data systems, together with the intensive observations on the land – atmosphere interactions taking place at the high latitudes, will provide the baseline for cross disciplinary research era. PEEX is aimed for these directions.

ACKNOWLEDGEMENTS

We thank the following funding agencies and projects: Academy of Finland contracts: No 280700, 294600, 296302 (Novel Assessment of Black Carbon in the Eurasian Arctic: From Historical Concentrations and Sources to Future Climate Impacts (NABCEA), 307331 (FCoE Atmospheric Sciences), 311932, 314798/99, 315203, 317999, 337549 (Atmosphere and Climate Competence Center (ACCC), Jane and Aatos Erkko Foundation, Russian Government megagrant project № 075-15-2021-574 "Megapolis - heat and pollution island: interdisciplinary hydroclimatic, geochemical and ecological analysis", Russian Foundation for Basic Research (RFBR) projects No. 17-29-05027 (Selenga-Baikal river system), 17-29-05102, 18-05-00306, 18-05-60037, 18-05-60219 (Arctic river), 18-35-20031, 18-44-860017, 18-45-700015, 18-05-60083 (Storm activity in the Barents Sea), 18-60084 (Dangerous impacts of large - scale industrial emissions on aerosol pollution and Arctic ecosystem), 19-05-50088, 19-05-00352, 19-55-80021 (MOST and DST studies), the IAO SB RAS supported by RFBR project No. 19-05-50024, Russian Science Foundation (RSF) projects;

RSF project 21-17-00181 (Monitoring at Lena River catchment)" No.17-17-01117, 18-17-00076 (Long-term measurement of aerosol chemical composition in Central Siberia, 19-77-20109 (Black carbon emissions from Siberian fires), 19-77-30004 (Moscow environment), 19-77-300-12 (Measurement networks and field sites in Kola Peninsula), Yugra State University grant No.13-01-20/39, Ministry of Science and Higher Education of Russia - Agreement No.13.1902.21.0003, State assignment No. 0148-2019-0006, Project N75295423 launched by St. Petersburg State University, European Research Council (ERC) projects No. 742206 (ATM-GTP), No. 850614 (CHAPAs), EU Horizon 2020 projects No. 727890 (Integrated Arctic Observing System, INTAROS), 689443 (Integrative and Comprehensive Understanding on Polar Environments, iCUPE), 654109 (Aerosol Clouds and Trace Gases Research Infrastructure, ACTRIS-2), EU7 FP MarcoPolo Grant No. 606953, Erasmus+ 561975-EPP-1-2015-1-FI-EPPKA2-CBHE-JP, Norwegian Research Council and the Belmont Forum project SERUS, No. 311986, National Natural Science Foundation of China Grant No. 41275137, ESA-MOST China Dragon Cooperation projects No. 10663 and 32771 (Dragon 3 and 4). We are also thankful for the support of the Russian Government project "Megapolis - heat and pollution island: interdisciplinary hydroclimatic, geochemical and ecological analysis" and Russian Science Foundation (RSF) 21-17-00181 (Monitoring at Lena River catchment)"

Our special thanks also to Mrs. Alla Borisova, INAR, University of Helsinki, for the technical editing of the manuscript.

REFERENCES

Andreae, M. O., Andreae, T. W., and Ditas, F.: How frequent is new particle formation in the boundary layer over the remote temperate/boreal forest?, AGU Fall Meeting, San Francisco, USA, doi:10.1002/essoar.10501148.1, 2019.

Aalto, J., Porcar-Castell, A., Atherton, J., Kolari, P., Pohja, T., Hari, P., Nikinmaa, E., Petäjä, T., and Bäck, J.: Onset of photosynthesis in spring speeds up monoterpene synthesis and leads to emission bursts, Plant, Cell and Environment., 38, 2299-2312, 2015.

Agafonova, S. A., Frolova, N. L., Surkova, G. V., and Koltermann, K., P.: Modern characteristics of the ice regime of Russian Arctic rivers and their possible changes in the 21st century, Geogr. Environ. Sustain., 10(4), 4-15, doi:10.24057/2071-9388-2017-10-4-4-15, 2017.

Alekseychik, P., Lappalainen, H.K., Petäjä, T., Zaitseva, N., Heimann, M., Laurila, T., Lihavainen, H., Asmi, E., Arshinov, M., Shevchenko, V., Makshtas, A., Dubtsov, S., Mikhailov, E., Lapshina, E., Kirpotin, S., Kurbatova, Y., Ding, A., Guo, H., Park, S., Lavric, J.V., Reum, F., Panov, A., Prokushkin, A., and Kulmala, M.: Ground-based station network in Arctic and Subarctic Eurasia: An overview, Geogr. Environ. Sustain., 9(2), 75-88, doi:10.24057/2071-9388-2016-9-2-19-35, 2016.

Alekseychik, P., Mammarella, I., Karpov, D., Dengel, S., Terentieva, I., Sabrekov, A., Glagolev, M., and Lapshina, E.: Net ecosystem exchange and energy fluxes measured with the eddy covariance technique in a western Siberian bog, Atmos. Chem. Phys., 17, 9333–9345, doi:10.5194/acp-17-9333-2017, 2017.

AMAP, 2017: Arctic Pollution 2017. Arctic Monitoring and Assessment Programme (AMAP), Oslo, Norway.

2133 Andreae, M. O.: Emission of trace gases and aerosols from biomass burning – an updated assessment,

2134 Atmos. Chem. Phys., 19, 8523-8546, doi:10.5194/acp-19-8523-2019, 2019.

2135 Arneth, A., Harrison, S., Zaehle, S., Tsigaridis, K., Menon, S., Bartlein, P. J., Feichter, J., Korhola, A.,

2136 Kulmala, M., O'Donnell, D., Schurgers, G., Sorvari, S., and Vesala, T.: Terrestrial biogeochemical feedbacks

2137 in the climate system. Nature Geosci, 3, 525–532, https://doi.org/10.1038/ngeo905, 2010.

2138 Arneth, A., Makkonen, R., Olin, S., Paasonen, P., Holst, T., Kajos, M. K., Kulmala, M., Maximov, T.,

2139 Miller, P. A., and Schurgers, G.: Future vegetation–climate interactions in Eastern Siberia: an assessment of

2140 the competing effects of CO2 and secondary organic aerosols, Atmos. Chem. Phys., 16, 5243–5262,

2141 doi:10.5194/acp-16-5243-2016, 2016.

2142 Arnold, S. R., Law, K. S., Brock, C. A., Thomas, J. L., Starkweather, S. M., von Salzen, K., Stohl, A.,

2143 Sharma S., Lund, M. T., Flanner, M. G., Petaja, T., Tanimoto, H., Gamble, J., Dibb J. E., Melamed M.,

2144 Johnson, N., Fidel, M., Tynkkynen, V.-P., Baklanov, A., Eckhardt, S., Monks, S. A., Browse, J., and Bozem,

2145 H.: Arctic air pollution: Challenges and opportunities for the next decade, Elementa: Science of the

2146 Anthropocene, 4:000104, https://dx.doi.org/10.12952/journal.elementa.00010. 2016.

2147 Arvola, L., Äijälä, C., and Leppäranta, M.: CDOM concentrations of large Finnish lakes relative to their

2148 landscape properties, Hydrobiologia, 780(1), 37-46, doi:10.1007/s10750-016-2906-4, 2016.

2149 Arvola, L., Leppäranta, M., and Äijälä, C.: CDOM variations in Finnish lakes and rivers between 1913 and

2150 2014, Sci. Total Environ., 601, 1638-1648, doi:10.1016/j.scitotenv.2017.06.034, 2017.

2151 Asmi, E., Kondratyev, V., Brus, D., Laurila, T., Lihavainen, H., Backman, J., Vakkari, V., Aurela, M.,

2152 Hatakka, J., Viisanen, Y., Uttal, T., Ivakhov, V., and Makshtas, A.: Aerosol size distribution seasonal

2153 characteristics measured in Tiksi, Russian Arctic, Atmos. Chem. Phys., 16, 1271–1287, doi:10.5194/acp-16-

2154 1271-2016, 2016.

2155 Backman, J., Schmeisser, L., Virkkula, A., Ogren, J. A., Asmi, E., Starkweather, S., Sharma, S.,

2156 Eleftheriadis, K., Uttal, T., Jefferson, A., Bergin, M., Makshtas, A., Tunved, P., and Fiebig, M.: On

2157 Aethalometer measurement uncertainties and an instrument correction factor for the Arctic, Atmos. Meas.

2158 Tech., 10, 5039–5062, doi:10.5194/amt-10-5039-2017, 2017.

2159 Badina, S. V.: Socio-economic potential of municipalities in the context of natural risk (case study –

2160 Southern Siberian regions), IOP Conference Series: Earth and Environmental Science, 190,

2161 doi:10.1088/1755-1315/190/1/012001, 2018.

2162 Bai, J.H.: Estimation of the isoprene emission from the Inner Mongolia grassland, Atmospheric Pollution

2163 Research, 6, 406-414, doi: 10.5094/APR.2015.045, 2015.

2164 Bai, J.H.: UV extinction in the atmosphere and its spatial variation in North China, Atmos. Environ., 154,

2165 318-330, doi:10.1016/j.atmosenv.2017.02.002, 2017a.

Bai, J.H., Guenther, A., Turnipseed, A., Duhl, T., Greenberg J.: Seasonal and interannual variations in whole-ecosystem BVOC emissions from a subtropical plantation in China. Atmospheric Environment, 161, 176-190. http://dx.doi.org/10.1016/j.atmosenv.2017.05.002, 2017b.

Bai, J.H., de Leeuw, G., van der Ronald, A., De Smedt, I., Theys, N., Van Roozendael, M., Sogacheva, L., and Chai, W. H.: Variations and photochemical transformations of atmospheric constituents in North China, Atmos. Environ., 189, 213-226, doi:10.1016/j.atmosenv.2018.07.004, 2018a.

Bai, Y., Zhang, J., Zhang, S., Yao, F., and Magliulo, V.: A remote sensing-based two-leaf canopy conductance model: Global optimization and applications in modeling gross primary productivity and evapotranspiration of crops, Remote Sensing of Environment, 215, 411-437, doi:10.1016/j.rse.2018.06.005, 2018b.

Bai, J. H.: A calibration method of solar radiometers, Atmos. Pollut. Res., 10(4), 1365-1373, doi:10.1016/j.apr.2019.03.011, 2019.

Bai, J. H.: O_3 Concentration and its relation with BVOC emissions in a subtropical plantation. Atmosphere, 12, 711. https://doi.org/10.3390/atmos12060711, 2021.

Baklanov, A., Mahura, A., Nazarenko, L., Tausnev, N., Kuchin, A., and Rigina, O.: Atmospheric Pollution and Climate Change in Northern Latitudes, Russ. Acad. Sci., Apatity, Russia, 2012.

Baklanov, A. A., Penenko, V. V., Mahura, A. G., Vinogradova, A. A., Elansky, N. F., Tsvetova, E. A., Rigina, O. Y., Maksimenkov, L. O., Nuterman, R. B., Pogarskii, F. A., and Zakey, A.: Aspects of Atmospheric Pollution in Siberia, in Regional Environmental Changes in Siberia and Their Global Consequences, edited by: Groismanm P. Y., and Gutman, G., 303–346, Springer, Dordrecht, Netherlands, 2013.

Baklanov, A., Molina, L.T., and Gauss, M.: Megacities, air quality and climate, Atmospheric Environment, 126, 235-249, https://doi.org/10.1016/j.atmosenv.2015.11.059, 2016.

Baklanov, A., Smith Korsholm, U., Nuterman, R., Mahura, A., Nielsen, K. P., Sass, B. H., Rasmussen, A., Zakey, A., Kaas, E., Kurganskiy, A., Sørensen, B., and González-Aparicio, I.: Enviro-HIRLAM online integrated meteorology–chemistry modelling system: strategy, methodology, developments and applications (v7.2), Geosci. Model Dev., 10, 2971–2999, https://doi.org/10.5194/gmd-10-2971-2017, 2017.

Baklanov, A., Brunner,, D., Carmichael, G., Flemming, J., Freitas, S., Gauss, M., Hov, O., R. Mathur, R., Schlünzen, K., Seigneur, C., and Vogel, B.: Key issues for seamless integrated chemistry-meteorology modeling, Bull. Amer. Meteor. Soc., doi:10.1175/BAMS-D-15-00166.1., 2018.

Balch, W. M., Bates, N. R., Lam, P. J., Twining, B. S., Rosengard, S. Z., Bowler, B. C., and Rauschenberg, S.: Factors regulating the Great Calcite Belt in the Southern Ocean, and its biogeochemical significance, Global Biogeochem. Cycles, 30(8), 1124-1144, doi:10.1002/2016GB005414, 2016.

2199   Balch, W. M.: The ecology, biogeochemistry, and optical properties of coccolithophores, Ann. Rev. Mar.
2200   Sci., 109, 71-98, doi:10.1146/annurev-marine-121916-063319, 2018.

2201   Bartsch, A., Kumpula, T., Forbes, B.C. and Stammler F.: Detection of snow surface thawing and refreezing
2202   in the Eurasian Arctic with QuikSCAT: implications for reindeer herding, Ecol Appl., 20, 2346-58., doi:
2203   10.1890/09-1927.1., 2010.

2204   Barreira, L. M. F., Duporté, G., Rönkkö, T., Parshintsev, J., Hartonen, K., Hyrsky, L., Heikkinen, E.,
2205   Kulmala, M., and Riekkola, M.-L.: Field measurements of biogenic volatile organic compounds in the
2206   atmosphere using solid-phase microextraction Arrow, Atmos. Meas. Tech., 11, 881–893, 2018.

2207   Bashmachnikov, I.L., Yurova, A.Y., Bobylev, L.P., and Vesman, A. V.: Seasonal and Interannual Variations
2208   of Heat Fluxes in the Barents Sea Region, Izv., Atmos. Ocean. Phys., 54, 213–222,
2209   doi:10.1134/S0001433818020032, 2018a.

2210   Bashmachnikov, I. L., Yurova, A.Y., Bobylev, L. P., Vesman, A.V.: Seasonal and interannual variations of
2211   the heat fluxes in the Barents Sea region, Izv. Atmos. Ocean. Phys., 54(2), 239-249,
2212   doi:10.7868/S0003351518020149, 2018b.

2213   Beer, C., Reichstein, M., Tomelleri, E., Ciais, P., Jung, M., Carvalhais, N., Rödenbeck, C., Altaf Arain,
2214   A., Baldocchi, D., Bonan, G.B., Bondeau, A.., Cescatti, A., Lasslop, G., Lindroth, A., Lomas, M.,
2215   Luyssaert, S., Margolis, H., Oleson, K.W., Roupsard, O., Veenendaal, E., Viovy, N., Williams, C., F Ian
2216   Woodward, F.,I., and Papale, D.:Terrestrial gross carbon dioxide uptake: global distribution and covariation
2217   with climate. Science, 329, 834–838, doi: 10.1126/science.1184984, 2010.

2218   Belikov, D., Arshinov, M., Belan, B., Davydov, D., Fofonov, A., Sasakawa, M., Machida, T.: Analysis of the
2219   Diurnal, Weekly, and Seasonal Cycles and Annual Trends in Atmospheric CO_2 and CH_4 at Tower Network
2220   in Siberia from 2005 to 2016, Atmosphere, 10 (11), 689, doi: 10.3390/atmos10110689, 2019.

2221   Berchet, A., Bousquet, P., Pison, I., Locatelli, R., Chevallier, F., Paris, J.-D., Dlugokencky, E. J., Laurila, T.,
2222   Hatakka, J., Viisanen, Y., Worthy, D. E. J., Nisbet, E., Fisher, R., France, J., Lowry, D., Ivakhov, V., and
2223   Hermansen, O.: Atmospheric constraints on the methane emissions from the East Siberian Shelf, Atmos.
2224   Chem. Phys., 16, 4147–4157, doi:10.5194/acp-16-4147-2016, 2016.

2225   Berezina, E., Moiseenko, K., Skorokhod, A., Elansky, N., Belikov, I., and Pankratova, N.: Isoprene and
2226   monoterpenes over Russia and their impacts in tropospheric ozone formation, Geogr., Environ., Sustain.,
2227   12(1), 63-74, doi:10.24057/2071-9388-2017-24, 2019.

2228   Bezuglaya, E. Y., Ed.: Air quality in largest cities of Russia for 10 years (1988-1997), Hydrometeoizdat, St.
2229   Petersburg, Russia, 1999.

2230   Biskaborn, B. K., Smith, S. L., Noetzli, J., Matthes, H., Vieira, G., Streletskiy, D. A., Schoeneich, P.,
2231   Romanovsky, V. E., Lewkowicz, A. G., Abramov, A., Allard, M., Boike, J., Cable, W. L., Christiansen, H.

2232   H., Delaloye, R., Diekmann, B., Drozdov, D., Etzelmüller, B., Grosse, G., … and Lantuit, H.: Permafrost is
2233   warming at a global scale, Nat. Commun., 10(1), 264, doi: 10.1038/s41467-018-08240-4, 2019.

2234   Blackport, R., Screen, J. A., van der Wiel, K., and Bintanja, R.: Minimal influence of reduced Arctic sea ice
2235   on coincident cold winters in mid-latitudes, Nat. Clim. Change, 9, 697–704, doi: 10.1038/s41558-019-0551-
2236   4, 2019.

2237   Bobylev, S.N., Chereshnya, O.Y., Kulmala, M., Lappalainen, H. K., Petäjä, T., Solov'eva, S.V., Tikunov,
2238   V.S., and Tynkkynen, V.-P.: Indicators for digitalization of sustainable development goals in PEEX
2239   program, J. Geogr. Sust., 11, 145-156, 2018.

2240   Boike, J., Nitzbon, J., Anders, K., Grigoriev, M., Bolshiyanov, D., Langer, M., Lange, S., Bornemann, N.,
2241   Morgenstern, A., Schreiber, P., Wille, C., Chadburn, S., Gouttevin, I, Burke, E., and Kutzbach, L.: A 16-
2242   year record (2002–2017) of permafrost, active-layer, and meteorological conditions at the Samoylov Island
2243   Arctic permafrost research site, Lena River delta, northern Siberia: an opportunity to validate remote-sensing
2244   data and land surface, snow, and permafrost models, Earth Syst. Sci. Data, 11, 261–299,
2245   https://doi.org/10.5194/essd-11-261-2019, 2019.
2246

2247   Bondur, G., and Vorobev, V. E.: Satellite Monitoring of Impact Arctic Regions, Izv. Atmos. Ocean. Phys.,
2248   51, 949–968, doi: 10.1134/S0001433815090054, 2015.

2249   Bondur, V. G., and Ginzburg, A. S.: Emission of carbon-bearing gases and aerosols from natural fires on the
2250   territory of Russia based on space monitoring, Dokl. Earth Sci., 466(2), 148-152,
2251   doi:10.1134/s1028334x16020045, 2016.

2252   Bondur, V. G.: Satellite monitoring of trace gas and aerosol emissions during wildfires in Russia. Izv.
2253   Atmos. Ocean. Phys., 52(9), 1078-1091, doi:10.1134/s0001433816090103, 2016.

2254   Bondur, V. G., Gordo, K. A., and Kladov, V. L.: Spacetime distributions of wildfire areas and emissions of
2255   carbon-containing gases and aerosols in northern eurasia according to satellite-Monitoring Data, Izv. Atmos.
2256   Ocean. Phys., 53(9), 859-874, doi:10.1134/s0001433817090055, 2017.

2257   Bondur, V. G. and Gordo, K. A.: Satellite Monitoring of Burned out Areas and Emissions of Harmful
2258   Contaminants due to Forest and other Wildfires in Russia, Izv., Atmos. Ocean. Phys., 54 (9),955–965, doi:
2259   10.1134/S0001433818090104, 2018.

2260   Bondur V. G., Chimitdorzhiev T. N., Dmitriev A. V., and Dagurov P. N.: Otsenka prostranstvennoy
2261   anizotropii neodnorodnostey lesnoy rastitelnosti pri razlichnykh azimutalnykh uglakh radarnogo
2262   polyarimetricheskogo zondirovaniya (Spatial anisotropy assessment of the forest vegetation heterogeneity at
2263   various azimuth angles of the radar polarimetric sensing), Issledovanie Zemli iz kosmosa, Russia, 3, 92-103,
2264   doi:10.31857/S0205-96142019392-103, 2019a.

Bondur, V. G., Chimitdorzhiev, T. N., Dmitriev, A. V., Dagurov, P. N., Zakharov, A. I., and Zakharova, L. N.: Metody radarnoj polyarimetrii dlya issledovaniya izmenenij mekhanizmov obratnogo rasseyaniya v zonah opolznej na primere obrusheniya sklona berega reki Bureya (Using radar polarimetry to monitor changes in backscattering mechanisms in landslide zones for the case study of the Bureya river bank collapse), Issledovanie Zemli iz kosmosa., Russia, 4, 3-17, doi:10.31857/S0205-9614201943-17, 2019b.

Bondur, V. G., Tsidilina, M. N., and Cherepanova, E.V.: Satellite Monitoring of Wildfire Impacts on The Conditions of Various Types of Vegetation Cover in The Federal Districts of the Russian Federation, Izv. Atmos. Ocean. Phys., 55 (9), 1238–1253, doi:10.1134/s000143381909010X, 2019 (c).

Bondur, V. G., Tsidilina, M. N., Kladov, V. L., and Gordo, K. A.: Irregular Variability of Spatiotemporal Distributions of Wildfires and Emissions of Harmful Trace Gases in Europe Based on Satellite Monitoring Data // Doklady Earth Sciences, Vol. 485, Part 2, pp. 461–464, doi: 10.1134/S1028334X19040202, 2019(d).

Bondur, V. G., Zakharova, L. N., and Zakharov, A. I.: Monitoring of the landslide area state on Bureya river in 2018-2019 according to radar and optical satellite images, Issledovanie Zemli iz kosmosa, Russia, No. 6, 26-35, doi:10.31857/S0205-96142019626-35, 2019(e).

Bondur, V. G., Zakharova, L. N., Zakharov, A. I., Chimitdorzhiev, T. N., Dmitriev, A. V., and Dagurov, P.N.: Monitoring of landslide processes by means of L-band radar interferometric observations: Bureya river bank caving case // Issledovanie Zemli iz kosmosa, Russia, No. 5, 3-14, DOI: https://doi.org/10.31857/S0205-9614201953-14. 2019 (f).

Bondur, V. G., Tsidilina, M. N., and Kladov, V. L.: Irregular Variability of Spatiotemporal Distributions of Wildfires and Emissions of Harmful Trace Gases in Europe Based on Satellite Monitoring Data, Dokl. Earth Sc., 485, 461–464, https://doi.org/10.1134/S1028334X19040202, 2019.

Bondur, V. G., Mokhov, I. I., Voronova, O. S., and Sitnov, S. A.: Satellite Monitoring of Siberian Wildfires and Their Effects: Features of 2019 Anomalies and Trends of 20-Year Changes, Doklady Earth Sciences, 492, 1, 370–375. doi: 10.1134/S1028334X20050049, 2020.

Bormann, K. J., Brown, R. D., Derksen, C., and Painter, T. H.: Estimating snow-cover trends from space, Nat. Clim. Chang., 8, 924-928, 2018.

Boy, M., Thomson, E. S., Acosta Navarro, J.-C., Arnalds, O., Batchvarova, E., Bäck, J., Berninger, F., Bilde, M., Brasseur, Z., Dagsson-Waldhauserova, P., Castarède, D., Dalirian, M., de Leeuw, G., Dragosics, M., Duplissy, E.-M., Duplissy, J., Ekman, A. M. L., Fang, K., Gallet, J.-C., Glasius, M., Gryning, S.-E., Grythe, H., Hansson, H.-C., Hansson, M., Isaksson, E., Iversen, T., Jonsdottir, I., Kasurinen, V., Kirkevåg, A., Korhola, A., Krejci, R., Kristjansson, J. E., Lappalainen, H. K., Lauri, A., Leppäranta, M., Lihavainen, H., Makkonen, R., Massling, A., Meinander, O., Nilsson, E. D., Olafsson, H., Pettersson, J. B. C., Prisle, N. L., Riipinen, I., Roldin, P., Ruppel, M., Salter, M., Sand, M., Seland, Ø., Seppä, H., Skov, H., Soares, J., Stohl, A., Ström, J., Svensson, J., Swietlicki, E., Tabakova, K., Thorsteinsson, T., Virkkula, A., Weyhenmeyer, G. A., Wu, Y., Zieger, P., and Kulmala, M.: Interactions between the atmosphere, cryosphere, and ecosystems

2300   at northern high latitudes, Atmos. Chem. Phys., 19, 2015–2061, https://doi.org/10.5194/acp-19-2015-2019,
2301   2019.

2302   Breider, T.J., Mickley, L.J., Jacob, D.J., Ge, C., Wang, J., Sulprizio, M.P., Croft, B., Ridley, D.A.,
2303   McConnell, J.R., Sharma, S., Husain, L., Dutkiewicz, V. A., Eleftheriadis, K., Skov, H., and Hopke, P. K.:
2304   Multidecadal trends in aerosol radiative forcing over the Arctic: Contribution of changes in anthropogenic
2305   aerosol to Arctic warming since 1980, J. Geophys. Res.: Atmos., 122, 3573-3594,
2306   https://doi.org/10.1002/2016JD025321, 2017.

2307   Burkhard, B., Kroll, F., Müller, F., and Windhorst, W. F., Landscapes' Capacities to Provide Ecosystem
2308   Services – a Concept for Land-Cover Based Assessments, Landscape Online 15(1), 1-12, DOI:
2309   10.3097/LO.200915, 2009.

2310   Chalov, S. R., Jarsjo, J., Kasimov, N. S., Romanchenko, A. O., Pietron, J., Thorslund, J., and Promakhova,
2311   E. V.: Spatio-temporal variation of sediment transport in the Selenga River Basin, Mongolia and Russia,
2312   Environ. Earth Sci., 73(2), 663-680, doi:10.1007/s12665-014-3106-z, 2015.

2313   Chalov, S. R., Bazilova, V. O., and Tarasov, M. K.: Modelling suspended sediment distribution in the
2314   Selenga River Delta using LandSat data, in Integrating Monitoring and Modelling for Understanding,
2315   Predicting and Managing Sediment Dynamics, edited by: Collins, A., Stone, M., Horowitz, A., and Foster, I.,
2316   Copernicus Gesellschaft, Gottingen, Germany, 375, 19-22, 2017a.

2317   Chalov, S., Thorslund, J., Kasimov, N., Aybullatov, D., Ilyicheva, E., Karthe, D., Kositsky, A., Lychagin,
2318   M., Nittrouer, J., Pavlov, M., Pietron, J., Shinkareva, G., Tarasov, M., Garmaev, E., Akhtman, Y., and Jarsjö,
2319   J.: The Selenga River delta: a geochemical barrier protecting Lake Baikal waters, Regional Environ. Change,
2320   17, 2039-2053, doi: 10.1007/s10113-016-0996-1, 2017b.

2321   Chalov, S. R., Millionshchikova, T. D., and Moreido, V. M.: Multi-Model Approach to Quantify Future
2322   Sediment and Pollutant Loads and Ecosystem Change in Selenga River System, Water Resour., 45, S22-S34,
2323   doi:10.1134/s0097807818060210, 2018.

2324   Che, Y., Xue, Y., Mei, L., Guang, J., She, L., Guo, J., Hu, Y., Xu, H., He, X., Di, A., and Fan, C.: Technical
2325   note: Intercomparison of three AATSR Level 2 (L2) AOD products over China, Atmos. Chem. Phys., 16,
2326   9655–9674, https://doi.org/10.5194/acp-16-9655-2016, 2016.

2327   Cheng, Y., Cheng, B., Zheng, F., Vihma, T., Kontu, A., Yang, Q. and Liao, Z.: Air/snow, snow/ice and
2328   ice/water interfaces detection from high-resolution vertical temperature profiles measured by ice mass-
2329   balance buoys on an Arctic lake. Annals of Glaciology, accepted (2020).

2330   Chernokulsky, A. V., Esau, I., Bulygina, O. N., Davy, R., Mokhov, II, Outten, S., and Semenov, V. A.:
2331   Climatology and interannual variability of cloudiness in the Atlantic Arctic from surface observations since
2332   the late nineteenth century, J. Clim., 30(6), 2103-2120, doi:10.1175/jcli-d-16-0329.1, 2017.

Chernokulsky, A., and Esau, I.: Cloud cover and cloud types in the Eurasian Arctic in 1936–2012. *Int. J. Climatol.*, **39**(15), 5771–5790, https://doi.org/10.1002/joc.6187, 2019

Chu, B., Kerminen, V.-M., Bianchi, F., Yan, C., Petäjä, T. and Kulmala, M.: Atmospheric new particle formation in China, Atmos. Chem. Phys., 19, 115-138, 2019.

Chubarova, N. Y., Poliukhov, A. A., and Gorlova, I. D.: Long-term variability of aerosol optical thickness in Eastern Europe over 2001–2014 according to the measurements at the Moscow MSU MO AERONET site with additional cloud and NO2 correction, Atmos. Meas. Tech., 9, 313–334, https://doi.org/10.5194/amt-9-313-2016, 2016a.

Chubarova, N., Zhdanova, Y., and Nezval, Y.: A new parameterization of the UV irradiance altitude dependence for clear-sky conditions and its application in the on-line UV tool over Northern Eurasia, Atmos. Chem. Phys., 16, 11867–11881, https://doi.org/10.5194/acp-16-11867-2016, 2016b.

Chubarova, N. E., Pastukhova, A. S., and Galin, V. Y.: Long-Term Variability of UV Irradiance in the Moscow Region according to Measurement and Modeling Data, Izv. Atmos. Ocean. Phys., 54, 139–146, https://doi.org/10.1134/S0001433818020056, 2018.

Chubarova, N. E., Androsova, E. E., Kirsanov, A. A., Vogel, B., Vogel, H., Popovicheva, O. B., and Rivin, G. S.: Aerosol and Its Radiative Effects during the Aeroradcity 2018 Moscow Experiment, Geography, Environment, Sustainability, 12, 114-131, https://doi.org/10.24057/2071-9388-2019-72 2019a.

Chubarova, N. E., Timofeev, Y. M., Virolainen, Y. A., and Polyakov, A. V.: Estimates of UV indices during the periods of reduced ozone content over Siberia in Winter-Spring 2016, Atmos. Oceanic Opt., 32, 177-179, doi:10.1134/s1024856019020040, 2019b.

Chubarova, N. E., Pastukhova, A.S., Zhdanova, E.Y., Volpert, E.V., Smyshlyaev and S.P., and Galin, V.Y.: Effects of Ozone and Clouds on Temporal Variability of Surface UV Radiation and UV Resources over Northern Eurasia Derived from Measurements and Modeling., Atmosphere, 11, 59, 2020.

Cohen, J., X. Zhang, T., Jung, R. Kwok, J., Overland, T., Ballinger, U.S., Bhatt, H. W., Chen, D., Coumou, S., Feldstein, H., Gu, D., Handorf, G., Henderson, M,. Ionita, M., Kretschmer, F., Laliberte, S., Lee, H. W., Linderholm, W., Maslowski, Y., Peings, K., Pfeiffer, I., Rigor, T., Semmler, J., Stroeve, P.C., Taylor, S., Vavrus, T., Vihma, S., Wang, M., Wendisch, Y., Wu, and Yoon, J.: Divergent consensuses on Arctic amplification influence on midlatitude severe winter weather. Nature Climate Change, 10, 20-29, doi:10.1038/s41558-019-0662-y, 2020.

Collins, M., Knutti, R., Arblaster, J., Dufresne, J.-L., Fichefet, T., Friedlingstein, P., Gao, X., Gutowski, W.J., Johns, T., Krinner, G., Shongwe, M., Tebaldi, C., Weaver, A.J., and Wehner, M.: Long-term climate change: Projections, commitments and irreversibility, in Climate Change 2013: The Physical Science Basis. Contribution of Working Group I to the Fifth Assessment Report of the Intergovernmental Panel on Climate Change, edited by: Stocker, T.F., Quin, D., Plattner, G.-K., Tignor, M., Allen, S.K., Doschung, J., Nauels,

2367 A., Xia, Y., Bex, V., and Midgley, P.M., Cambridge University Press, Cambridge, United-Kingdom, 1029-
2368 1136, doi:10.1017/CBO9781107415324.024, 2013.

2369 Commane, R., Lindaas, J., Benmergui, J., Luus K. A., Chang, R. Y.-W., Daube, B. C., Euskirchen, E. S.,
2370 Henderson, J. M., Karion, A., Miller, J. B., Miller, S. M., Parazoo, N. C., Randerson, J. T., Sweeney, C.,
2371 Tans, P., Thoning, K., Veraverbeke, S., Miller, C. E., and Wofsy, S. C.: Carbon dioxide sources from Alaska
2372 driven by increasing early winter respiration from Arctic tundra, PNAS, 114(21), 5361-5366, 2017.

2373 Coumou, C., Petoukhov, V., Rahmstorf, S., Petri, S., and Schellnhuber, H.-J.: Quasi-resonant circulation
2374 regimes and hemispheric synchronization of extreme weather in boreal summer, Proc. Natl. Acad. Sci., 111,
2375 12 331–12336, https://doi.org/10.1073/pnas.1412797111, 2014.

2376 Dada, L., Paasonen, P., Nieminen, T., Buenrostro Mazon, S., Kontkanen, J., Peräkylä, O., Lehtipalo, K.,
2377 Hussein, T., Petäjä, T., Kerminen, V.-M., Bäck, J. and Kulmala, M.: Long-term analysis of clear-sky new
2378 particle formation events and nonevents in Hyytiälä, Atmos. Chem. Phys., 17, 6227-6241, 2017.

2379 Dada, L., Chellapermal, R., Buenrostro Mazon, S., Paasonen, P., Lampilahti, J., Manninen, H. E., Junninen,
2380 H., Petäjä, T., Kerminen, V.-M., and Kulmala, M.: Refined classification and characterization of atmospheric
2381 new-particle formation events using air ions, Atmos. Chem. Phys., 18, 17883–17893,
2382 https://doi.org/10.5194/acp-18-17883-2018, 2018.

2383 Dagsson-Waldhauserova, P., Meinander, O.: Atmosphere-cryosphere interaction in the Arctic, at high
2384 latitudes and mountains with focus on transport, deposition and effects of dust, black carbon, and other
2385 aerosols., Front. Earth Sci., 7, 337, https://www.frontiersin.org/articles/10.3389/feart.2019.00337/full, 2019.

2386 Dave, B., and Kobayashi, Y.: China's silk road economic belt initiative in Central Asia: economic and
2387 security implications, Asia Europe Journal, 16. 1-15. doi:10.1007/s10308-018-0513-x, 2018.

2388 Davy, R., and Esau, I.: Differences in the efficacy of climate forcings explained by variations in atmospheric
2389 boundary layer depth, Nat. Commun., 7, 8, doi:10.1038/ncomms11690, 2016.

2390 Davy, R., Esau, I., Chernokulsky, A., Outten, S., and Zilitinkevich, S.: Diurnal asymmetry to the observed
2391 global warming, Int. J. Climatol., 37, 79-93, doi:10.1002/joc.4688, 2017.

2392 Dean, J. F., Middelburg, J. J., Röckmann, T., Aerts, R., Blauw, L. G., Egger, M., Jetten, M. S. M., de Jong,
2393 A. E. E., Meisel, O. H., Rasigraf, O., Slomp, C. P., in't Zandt, M. H., and Dolman, A. J.: Methane feedbacks
2394 to the global climate system in a warmer world, Rev. Geophys., 56(1), 207-250,
2395 https://doi.org/10.1002/2017RG00055, 2018.

2396 Derksen, C., and Brown, R.: Spring snow cover extent reductions in the 2008-2012 period exceeding climate
2397 model predictions, Geophys. Res. Lett., 39, L19504, 2012.

2398 Derome, J., and Lukina, N.: Interaction between environmental pollution and land-cover/land-use change in
2399 Arctic areas, in: Eurasian Arctic Land Cover and Land Use in a Changing Climate, edited by: Gutman, G.,
2400 and Reissell, A., 6, 269–290, Springer, Amsterdam, Netherlands, 2011.

2401 Ding, A. J., Huang, X., Nie, W., Sun, J. N., Kerminen, V.-M., Petäjä, T., Su, H., Chen, Y. F., Yang, X.-Q.,
2402 Wang, M. H., Chi, X. G., Wang, J. P., Virkkula, A., Guo, W. D., Yuan, J., Wang, S. Y., Zhang, R. J., Wu, Y.
2403 F., Song, Y. Zhu, T., Zilitinkevich, S., Kulmala, M., and Fu, C. B.: Enhanced haze pollution by black carbon
2404 in megacities in China, Geophys. Res. Lett., 43, 2873-2879, doi:10.1002/2016GL067745, 2016a.

2405 Ding, A. J., Nie, W., Huang, X., Chi, X., Sun, J., Kerminen, V.-M., Xu, Z., Guo, W., Petäjä, T., Yang, X.,
2406 Kulmala, M., and Fu, G.: Long-term observation of pollution-weather/climate interactions at the SORPES
2407 station: a review and outlook, Front. Environ. Sci. Eng., 10, doi:10.1007/s11783-016-0877-3, 2016b.

2408 Dou, T., Xiao, C., Liu, J., Han, W., Du, Z., Mahoney, A. R., Jones, J., and Eicken, H.: A key factor initiating
2409 surface ablation of Arctic sea ice: earlier and increasing liquid precipitation, The Cryosphere, 13, 1233–
2410 1246, https://doi.org/10.5194/tc-13-1233-2019, 2019.

2411 Dragosics, M., Meinander, O., Jonsdottir, T., Durig, T., De Leeuw, G., Palsson, F., Dagsson-Waldhauserová,
2412 P., and Thorsteinsson, T.: Insulation effects of Icelandic dust and volcanic ash on snow and ice, Arab. J.
2413 Geosci., 9, 126, DOI:10.1007/s12517-015-2224-6, 2016.

2414 Duporte, G., Parshintsev, J., Barreira, L. M. F., Hartonen, K., Kulmala, M., and Riekkola, M. L.: Nitrogen-
2415 containing low volatile compounds from pinonaldehyde-dimethylamine reaction in the atmosphere: a
2416 laboratory and field study, Environ. Sci. Technol., 50(9), 4693-4700, doi:10.1021/acs.est.6b00270, 2016.

2417 Durairaj, P., Sarangi., R., Ramalingam, S., Thirunavukarassu, T., and Chauhan, P.: Seasonal nitrate
2418 algorithms for nitrate retrieval using OCEANSAT-2 and MODIS-AQUA satellite data, Environ. Monit.
2419 Assess., 187, 176-189, doi: 10.1007/s10661-015-4340-x, 2015.

2420 Dyukarev, E.A., Godovnikov, E.A., Karpov, D.V., Kurakov, S.A., Lapshina, E.D., Filippov, I.V., Filippova,
2421 N.V., and Zarov, E.A.: Net ecosystem exchange, gross primary production and ecosystem respiration in
2422 ridge-hollow complex at Mukhrino Bog, Geography, Environment, Sustainability,12(2), 227-244,
2423 doi.10.24057/2071-9388-2018-77, 2019.

2424 Elansky, N. F., Lavrova, O. V., Skorokhod, A. I., and Belikov, I. B.: Trace gases in the atmophere over
2425 Russian cities, Atmos. Environ., 143, 108-119, doi:10.1016/j.atmosenv.2016.08.046, 2016.

2426 Esau, I., Miles, V. V., Davy, R., Miles, M. W., and Kurchatova, A.: Trends in normalized difference
2427 vegetation index (NDVI) associated with urban development in northern West Siberia, Atmos. Chem. Phys.,
2428 16, 9563–9577, https://doi.org/10.5194/acp-16-9563-2016, 2016.

2429 Esau, I., Varentsov, M., Laruelle, M., Miles, M. W., Konstantinov, P., Soromotin, A., Baklanov, A. A., and
2430 Miles, V. V.: Warmer Climate of Arctic Cities, Chapter 3 in the monography "The Arctic: Current Issues and
2431 Challenges", Edited by: Pokrovsky, O., NOVA Publishers, ISBN: 978-1-53617-306-2,
2432 https://novapublishers.com/shop/the-arctic-current-issues-and-challenges/, 2020.

2433 Euskirchen, E. S., Bret-Harte, M. S., Shaver, G. R., Edgar, C. W., and Romanovsky, V. E.: Long-term
2434 release of carbon dioxide from arctic tundra ecosystems in northern Alaska, Ecosystems, 1–15, 2017.

Evangeliou, N., Shevchenko, V. P., Yttri, K. E., Eckhardt, S., Sollum, E., Pokrovsky, O. S., Kobelev, V. O., Korobov, V. B., Lobanov, A. A., Starodymova, D. P., Vorobiev, S. N., Thompson, R. L., and Stohl, A.: Origin of elemental carbon in snow from western Siberia and northwestern European Russia during winter–spring 2014, 2015 and 2016, Atmos. Chem. Phys., 18, 963–977, https://doi.org/10.5194/acp-18-963-2018, 2018.

Ezhova, E., Orlov, D., Suhonen, E., Kaverin, D., Mahura, A., Gennadinik, V., Kukkonen, I., Drozdov, D., Lappalainen, H. K., Melnikov, V., Petäjä, T., Kerminen, V.-M., Zilitinkevich, S., Malkhazova, S. M, Christensen, T. R., and Kulmala, M.: Climatic Factors Influencing the Anthrax Outbreak of 2016 in Siberia, Russia. *EcoHealth*, https://doi.org/10.1007/s10393-021-01549-5, 2021.

Ezhova, E., Kerminen, V.-M., Lehtinen, K. E. J., and Kulmala, M.: A simple model for the time evolution of the condensation sink in the atmosphere for intermediate Knudsen numbers, Atmos. Chem. Phys., 18, 2431–2442, https://doi.org/10.5194/acp-18-2431-2018, 2018a.

Ezhova, E., Ylivinkka, I., Kuusk, J., Komsaare, K., Vana, M., Krasnova, A., Noe, S., Arshinov, M., Belan, B., Park, S.-B., Lavrič, J. V., Heimann, M., Petäjä, T., Vesala, T., Mammarella, I., Kolari, P., Bäck, J., Rannik, Ü., Kerminen, V.-M., and Kulmala, M.: Direct effect of aerosols on solar radiation and gross primary production in boreal and hemiboreal forests, Atmos. Chem. Phys., 18, 17863–17881, https://doi.org/10.5194/acp-18-17863-2018, 2018b.

Fang, K., Makkonen, R., Guo, Z., and Seppa, H.: An increase in the biogenic aerosol concentration as a contributing factor to the recent wetting trend in Tibetan Plateau. Sci Rep 5, 14628, https://doi.org/10.1038/srep14628, 2015.

Fang, Y., Changyou, L., Leppäranta, M., Xiaonghong, S., Shengnan, Z., and Chengfu, Z.: Notable increases in nutrient concentrations in a shallow lake during seasonal ice growth, Water Science and Technology, 74(12), 2773-2783, 2016.

Fang, K. , Makkonen, R. , Guo, Z , Zhao , Y., and Seppä, H.: An increase in the biogenic aerosol concentration as a contributing factor to the recent wetting trend in Tibetan Plateau, Scientific Reports , 5 , 14628, DOI: 10.1038/srep14628, 2015.

Fletcher, S. E. M., and Schaefer, H.: Rising methane: a new climate challenge, Science, 364, 932-933, 2019.

Franz, D., Mammarella, I., Boike, J., Kirillin, G., Vesala, T., Bornemann, N., Larmanou, E., Langer, M., and Sachs, T.: Lake-Atmosphere Heat Flux Dynamics of a Thermokarst Lake in Arctic Siberia, J. Geophys. Res.: Atmos., 123(10), 5222-5239, doi:10.1029/2017jd027751, 2018.

Freud, E., Krejci, R., Tunved, P., Leaitch, R., Nguyen, Q. T., Massling, A., Skov, H., and Barrie, L.: Pan-Arctic aerosol number size distributions: seasonality and transport patterns, Atmos. Chem. Phys., 17, 8101–8128, https://doi.org/10.5194/acp-17-8101-2017, 2017.

2468 Frolova, N.L., Belyakova, P.A., Grigoriev, V.Y. *et al.* : Runoff fluctuations in the Selenga River Basin, Reg
2469 Environ Change, 17**,** 1965–1976, doi.org/10.1007/s10113-017-1199-0, 2017.

2470

2471 Fu, B. J., and Forsius, M.: Ecosystem services modeling in contrasting landscapes, Landscape Ecol., 30(3),
2472 375-379, doi:10.1007/s10980-015-0176-6, 2015.

2473 Garmaev, E. Z., Kulikov, A. I., Tsydypov, B. Z., Sodnomov, B. V., and Ayurzhanaev, A. A.: Environmental
2474 Conditions Of Zakamensk Town (Dzhida River Basin Hotspot), Geography, Environment,
2475 Sustainability,12(3), 224-239, https://doi.org/10.24057/2071-9388-2019-32, 2019.

2476 Georgiadi, A. G., Koronkevich, N. I., Milyukova, I. P., and Barabanova, E. A.: Integrated projection for
2477 runoff changes in large Russian river basins in the XXI Century, Geography, Environment, Sustainability,
2478 9(2), 38-46, 2016.

2479 GGO: Air quality in cities of Russia during the year 2015, St. Petersburg, Voeikov Main Geophysical
2480 Observatory, RosHydroMet, 2016.

2481 Giamarelou, M., Eleftheriadis, K., Nyeki, S., Tunved, P., Torseth, K., and Biskos, G.: Indirect evidence of
2482 the composition of nucleation mode atmospheric particles in the high Arctic, J. Geophys. Res.: Atmos.,
2483 121(2), 965-975, doi:10.1002/2015jd023646, 2016.

2484 Gil, J., Pérez, T., Boering, K., Martikainen, P. J., and Biasi, C.: Mechanisms responsible for high N2O
2485 emissions from subarctic permafrost peatlands studied via stable isotope techniques, Global Biogeochem.
2486 Cycles, 31(1), 172, doi:10.1002/2015GB005370, 2017.

2487 Glagolev, M.V., Ilyasov, D. V. I., Terentieva, E., Sabrekov, A. F., Yu Mochenov, S., and Maksutov, S. S.:
2488 Methane and carbon dioxide fluxes in the waterlogged forests of south and middle taiga of Western Siberia,
2489 IOP Conf. Ser.: Earth Environ. Sci., 138 012005, 2018.

2490 Gnatiuk, N., Radchenko, I., Davy, R., Morozov E., and Bobylev, L.: Simulation of factors affecting
2491 Emiliania huxleyi blooms in Arctic and sub-Arctic seas by CMIP5 climate models: model validation and
2492 selection, Biogeosciences, 17, 1199–1212. doi: 10.5194/bg-17-1199-2020, 2020.

2493 Godrijan, J., Drapeau, D., and Balch, W. M.: Mixotrophic uptake of organic compounds by coccolithphores,
2494 Limnol. Ocean., Early bird publication, https://doi.org/10.1002/lno.11396, 2020.

2495 Gordov, E.P., Okladnikov, I.G., Titov, A.G., Voropay N.N., Ryazanova A.A., and Lykosov V.N.:
2496 Development of Information-computational Infrastructure for Modern Climatology, Russ. Meteorol. Hydrol.,
2497 43, 722–728, https://doi.org/10.3103/S106837391811002X, 2018.

2498 Granath, G., Rydin, H., Baltzer, J. L., Bengtsson, F., Boncek, N., Bragazza, L., Bu, Z.-J., Caporn, S. J. M.,
2499 Dorrepaal, E., Galanina, O., Gałka, M., Ganeva, A., Gillikin, D. P., Goia, I., Goncharova, N., Hájek, M.,
2500 Haraguchi, A., Harris, L. I., Humphreys, E., Jiroušek, M., Kajukało, K., Karofeld, E., Koronatova, N. G.,

Kosykh, N. P., Lamentowicz, M., Lapshina, E., Limpens, J., Linkosalmi, M., Ma, J.-Z., Mauritz, M., Munir, T. M., Natali, S. M., Natcheva, R., Noskova, M., Payne, R. J., Pilkington, K., Robinson, S., Robroek, B. J. M., Rochefort, L., Singer, D., Stenøien, H. K., Tuittila, E.-S., Vellak, K., Verheyden, A., Waddington, J. M., and Rice, S. K.: Environmental and taxonomic controls of carbon and oxygen stable isotope composition in Sphagnum across broad climatic and geographic ranges, Biogeosciences, 15, 5189–5202, https://doi.org/10.5194/bg-15-5189-2018, 2018.

Grigoriev, V.Y., and Frolova, N.L.: Terrestrial water storage change of European Russia and its impact on water balance, Geography, Environment, Sustainability, 11(1), 38-50. https://doi.org/10.24057/2071-9388-2018-11-1-38-50, 2018.

Groundstroem, F., and Juhola, S.: A framework for identifying cross-border impacts of climate change on the energy sector, Environment Systems and Decisions, 39(1), 3-15, doi:10.1007/s10669-018-9697-2, 2019.

Gunchin, G., Manousakas, M., Osan, J., Karydas, A. G., Eleftheriadis, K., Lodoysamba, S., Shagjjamba, D., Migliori, A., Padilla-Alvarez, R., Streli, C., and Darby, I.: Three-year long source apportionment study of airborne particles in Ulaanbaatar using x-ray fluorescence and positive matrix factorization, Aerosol and Air Quality Research, 19(5), 1056-1067, doi:10.4209/aaqr.2018.09.0351, 2019.

Guo, Y., Yan, C., Li, C., Feng, Z., Zhou, Y., Lin, Z., Dada, L., Stolzenburg, D., Yin, R., Kontkanen, J., Daellenbach, K. R., Kangasluoma, J., Yao, L., Chu, B., Wang, Y., Cai, R., Bianchi, F., Liu, Y., and Kulmala, M.: Formation of Nighttime Sulfuric Acid from the Ozonolysis of Alkenes in Beijing, Atmos. Chem. Phys. Discuss., https://doi.org/10.5194/acp-2019-1111, in review, 2020.

Gurchenkov, A. A., Murynin, A. B., Trekin, A. N., and Ignatyev, V. Y.: Object-oriented classification of substrate surface objects in Arctic impact regions aerospace monitoring, Herald of the Bauman Moscow State Technical University, 135-146. doi:10.18698/1812-3368-2017-3-135-146, 2017.

Göckede, M., Kittler, F., Kwon, M. J., Burjack, I., Heimann, M., Kolle, O., Zimov, N., and Zimov, S.: Shifted energy fluxes, increased Bowen ratios, and reduced thaw depths linked with drainage-induced changes in permafrost ecosystem structure, The Cryosphere, 11, 2975–2996, https://doi.org/10.5194/tc-11-2975-2017, 2017.

Göckede, M., Kwon, M. J., Kittler, F., Heimann, M., Zimov, N., and Zimov, S.: Negative feedback processes following drainage slow down permafrost degradation, Glob. Change Biol., 25, 3254– 3266, https://doi.org/10.1111/gcb.14744, 2019.

Hao, L., Garmash, O., Ehn, M., Miettinen, P., Massoli, P., Mikkonen, S., Jokinen, T., Roldin, P., Aalto, P., Yli-Juuti, T., Joutsensaari, J., Petäjä, T., Kulmala, M., Lehtinen, K. E. J., Worsnop, D. R., and Virtanen, A.: Combined effects of boundary layer dynamics and atmospheric chemistry on aerosol composition during new particle formation periods, Atmospheric Chemistry and Physics, 18(23), 17705-17716. doi:10.5194/acp-18-17705-2018, 2018.

Hari, P. & Kulmala, M.: Station for Measuring Ecosystem–Atmosphere Relations (SMEAR II). Boreal Env. Res. 10: 315–322, 2005.

Hari, P., Andreae M., Kabat P., and Kulmala M.: A comprehensive network of measuring stations to monitor climate change. Boreal Env. Res. 14: 442-446, 2009.

Hari, P., Petäjä, T., Bäck, J., Kerminen, V.-M., Lappalainen, H. K., Vihma, T., Laurila, T., Viisanen, Y., Vesala, T., and Kulmala, M..: Conceptual design of a measurement network of the global change, Atmos. Chem. Phys., 16, 1017-1028, doi:10.5194/acp-16-1017-2016, 2016.

Hari, P., Kerminen, V.-M., Kulmala, L., Kulmala, M., Noe, S., Petäjä, T., Vanhatalo, A., and Bäck, J.: Annual cycle of Scots pine photosynthesis, Atmos. Chem. Phys., 17, 15045–15053, doi:10.5194/acp-17-15045-2017, 2017.

Heikkilä, A., Makelä, J. S., Lakkala, K., Meinander, O., Kaurola, J., Koskela, T., Karhu, J. M., Karppinen, T., Kyro, E., and De Leeuw, G.: In search of traceability: two decades of calibrated Brewer UV measurements in Sodankyla and Jokioinen, Geoscientific Instrumentation, Methods and Data Systems, 5(2), 531-540, doi:10.5194/gi-5-531-2016, 2016.

Heintzenberg, J., Tunved, P., Galí, M., and Leck, C.: New particle formation in the Svalbard region 2006–2015, Atmos. Chem. Phys., 17, 6153–6175, doi:10.5194/acp-17-6153-2017, 2017.

Helin, A., Sietiö, O.-M., Heinonsalo, J., Bäck, J., Riekkola, M.-L., and Parshintsev, J.: Characterization of free amino acids, bacteria and fungi in size-segregated atmospheric aerosols in boreal forest: seasonal patterns, abundances and size distributions, Atmos. Chem. Phys., 17, 13089–13101, doi.org/10.5194/acp-17-13089-2017, 2017.

Hellén, H., Praplan, A. P., Tykkä, T., Ylivinkka, I., Vakkari, V., Bäck, J., Petäjä, T., Kulmala, M., and Hakola, H.: Long-term measurements of volatile organic compounds highlight the importance of sesquiterpenes for the atmospheric chemistry of a boreal forest, Atmos. Chem. Phys., 18, 13839–13863, https://doi.org/10.5194/acp-18-13839-2018, 2018.

Hinzman, L.D., Bettez, N.D., Bolton, W.R. et al. :Evidence and Implications of Recent Climate Change in Northern Alaska and Other Arctic Regions, Climatic Change, 72, 251–298, doi.org/10.1007/s10584-005-5352-2, 2005.

Hoegh-Guldberg, O., Jacob, D., Taylor, M., Bindi, M., Brown, S., Camilloni, I., Diedhiou, A., Djalante, R., Ebi, K. L., Engelbrecht, F., Guiot, J., Hijioka, Y., Mehrotra, S., Payne, A., Seneviratne, S. I., Thomas, A., Warren, R., and Zhou, G.: Impacts of 1.5ºC Global Warming on Natural and Human Systems, in: Global Warming of 1.5°C: An IPCC Special Report on the impacts of global warming of 1.5°C above pre-industrial levels and related global greenhouse gas emission pathways, in the context of strengthening the global response to the threat of climate change, sustainable development, and efforts to

2570   eradicate poverty, edited by: Masson-Delmotte, V., Zhai, P., Pörtner, H.-O., Roberts, D., Skea, J., Shukla, P.

2571   R., Pirani, A., Moufouma-Okia, W., Péan, C., Pidcock, R., Connors, S., Matthews, J. B. R., Chen, Y., Zhou,

2572   X., Gomis, M. I., Lonnoy, E., Maycock, T., Tignor, M., and Waterfield, T., WMO, Geneva, Switzerland,

2573   2018.

2574   Hong, J., Kim, J., Nieminen, T., Duplissy, J., Ehn, M., Äijälä, M., Hao, L. Q., Nie, W., Sarnela, N., Prisle, N.

2575   L., Kulmala, M., Virtanen, A., Petäjä, T., and Kerminen, V.-M.: Relating the hygroscopic properties of

2576   submicron aerosol to both gas- and particle-phase chemical composition in a boreal forest environment,

2577   Atmos. Chem. Phys., 15, 11999–12009, https://doi.org/10.5194/acp-15-11999-2015, 2015.

2578   Huang, W., Cheng, B., Zhang, J., Zhang, Z., Vihma, T., Li, Z., and Niu, F.: Modeling experiments on

2579   seasonal lake ice mass and energy balance in the Qinghai–Tibet Plateau: a case study, Hydrol. Earth Syst.

2580   Sci., 23, 2173-2186, 2019a.

2581   Huang, W., Zhang, J., Leppäranta, M., Li, Z., Cheng, B. and Lin, Z. 2019b. Thermal structure and water-ice

2582   heat transfer in a shallow ice–covered thermokarst lake in central Qinghai-Tibet Plateau, Journal of

2583   Hydrology, 578, [124122], 2019b.

2584   Hölttä, T., Lintunen, A., Chan, T., Mäkelä, A., and Nikinmaa, E.: A steady state stomatal model of balanced

2585   leaf gas exchange, hydraulics and maximal source-sink flux, Tree Physiology, 37, 851-868, doi:

2586   10.1093/treephys/tpx011, 2017.

2587   IPCC: Special Report on the Ocean and Cryosphere in a Changing Climate, edited by Pörtner, H.-O.,

2588   Roberts, D.C., Masson-Delmotte, V., Zhai, P., Tignor, M., Poloczanska, E., Mintenbeck, K., Alegría, A.,

2589   Nicolai, M., Okem, A., Petzold, J., Rama, B., and Weyer, N. M., 2019.

2590   IPCC, 2021: Climate Change 2021: The Physical Science Basis. Contribution of Working Group I to the

2591   Sixth Assessment Report of the Intergovernmental Panel on Climate Change[Masson-Delmotte, V., P. Zhai,

2592   A. Pirani, S. L. Connors, C. Péan, S. Berger, N. Caud, Y. Chen, L. Goldfarb, M. I. Gomis, M. Huang, K.

2593   Leitzell, E. Lonnoy, J.B.R. Matthews, T. K. Maycock, T. Waterfield, O. Yelekçi, R. Yu and B. Zhou (eds.)].

2594   Cambridge University Press.In Press.Summary for PolicymakersIPCC, 2021: Summary for Policymakers.

2595   In: Climate Change 2021: The Physical Science Basis. Contribution of Working Group I to the Sixth

2596   Assessment Report of the Intergovernmental Panel on Climate Change[Masson-Delmotte, V., P. Zhai, A.

2597   Pirani, S. L. Connors, C. Péan, S. Berger, N. Caud, Y. Chen, L. Goldfarb, M. I. Gomis, M. Huang, K.

2598   Leitzell, E. Lonnoy, J.B.R. Matthews, T. K. Maycock, T. Waterfield, O. Yelekçi, R. Yu and B. Zhou (eds.)].

2599   Cambridge University Press. In Press.

2600   Ivakhov, V. M., Paramonova, N. N., Privalov, V. I., Zinchenko, A. V., Loskutova, M. A., Makshtas, A. P.,

2601   Kustov, V. Y., Laurila, T., Aurela, M., and Asmi, E.: Atmospheric Concentration of Carbon Dioxide at Tiksi

2602   and Cape Baranov Stations in 2010-2017, Russ. Meteorol. Hydrol., 44, 291–299,

2603   doi:10.3103/s1068373919040095, 2019.

Jaffe, D., Bertschi, I., Jaegle, L., Novelli, P., Reid, J. S., Tanimoto, H., Vingarzan, R. and Westphal, D. L.: Long-range transport of Siberian biomass burning emissions and impact on surface ozone in western North America, Geophys. Res. Lett., 31(16), L16106, doi:10.1029/2004GL020093, 2004.

Jakobson, L., T. Vihma, and E. Jakobson,: Relationships between Sea Ice Concentration and Wind Speed over the Arctic Ocean during 1979–2015., J. Climate, 32, 7783–7796, https://doi.org/10.1175/JCLI-D-19-0271.1, 2019.

Juhola, S.: Planning for a green city: The Green Factor tool, Urban Forestry and Urban Greening, 34, 254-258, doi:10.1016/j.ufug.2018.07.019, 2018.

Juutinen, S., Virtanen, T., Kondratyev, V., Laurila, T., Linkosalmi, M., Mikola, J., Nyman, J., Räsänen, A., Tuovinen, J.-P., and Aurela, M.: Spatial variation and seasonal dynamics of leaf-area index in the arctic tundra-implications for linking ground observations and satellite images, Environ. Res. Lett., 12(9), 10, doi:10.1088/1748-9326/aa7f85, 2017.

Kalogridis, A.C., Popovicheva, O.B., Engling, G., Diapouli, E., Kawamura, K., Tachibana, E., Ono, K., Kozlov, V.S., and Eleftheriadis, K.: Smoke aerosol chemistry and aging of Siberian biomass burning emissions in a large aerosol chamber, Atmos. Environ., 185,15-28, 2018.

Kangasluoma, J., Ahonen, L. R., Laurila, T., Cai, R., Enroth, J., Mazon, S., Korhonen, F., Aalto, P., Kulmala, M., Attoui, M. and Petäjä, T.: Laboratory verification of a new high flow differential mobility particle sizer, and field measurements in Hyytiälä, J Aerosol Sci, 124, 1-9, 2018.

Karelin, D. V., Goryachkin, S. V., Zamolodchikov, D. G., Dolgikh, A. V., Zazovskaya, E. P., Shishkov, V. A., and Kraev, G. N.: Human footprints on greenhouse gas fluxes in cryogenic ecosystems, Dokl. Earth Sc., 477, 1467–1469, doi:10.1134/S1028334X17120133, 2017.

Karetnikov, S., Leppäranta, M., and Montonen, A.: A time series of over 100 years of ice seasons on Lake Ladoga, Journal of Great Lakes Research, 43(6), 979-988, doi:10.1016/j.jglr.2017.08.010, 2017.

Karthe, D., Abdullaev, I., Boldgiv, B., Borchardt, D., Chalov, S., Jarsjö, J., Li, L., and Nittrouer, J.A.: Water in Central Asia: an integrated assessment for science-based management, Environmental Earth Sciences, 76(20), 15, doi:10.1007/s12665-017-6994-x, 2017a.

Karthe, D., Chalov, S., Moreido, V., Pashkina, M., Romanchenko, A., Batbayar, G., Kalugin, A., Westphal, K., Malsy, M., and Flörke, M.: Assessment of runoff, water and sediment quality in the Selenga River basin aided by a web-based geoservice, Water Resources, 44(3), 399-416, 2017b.

Karthe D., Chalov S., Gradel A., and Kusbach A.: Special issue: Environment change on the Mongolian plateau: atmosphere, forests, soils and water, Geography, Environment, Sustainability, 12(3), 60-65, doi:10.24057/2071-9388-2019-1411, 2019.

Karvonen, J., Shi, L., Cheng, B., Similä, M., Mäkynen, M., and Vihma, T.: Bohai Sea ice parameter estimation based on thermodynamic ice model and Earth observation data, Remote Sensing, 9, 234, doi:10.3390/rs9030234, 2017.

Kasimov, N., Karthe, D., and Chalov, S.: Environmental change in the Selenga River—Lake Baikal Basin, Reg. Environ. Chang., 17, 1945–1949, 2017a.

Kasimov, N. S., Kosheleva, N. E., Nikiforova, E. M., and Vlasov, D. V.: Benzo a pyrene in urban environments of eastern Moscow: pollution levels and critical loads, Atmos. Chem. Phys., 17(3), 2217-2227, doi:10.5194/acp-17-2217-2017, 2017b.

Kasimov, N., Shinkareva, G., Lychagin, M., Kosheleva, N., Chalov, S., Pashkina, M., Thorslund, J., and Jarsjö, J.:River water quality of the selenga-baikal basin: Part i—spatio-temporal patterns of dissolved and suspended metals, Water, 12(8), 2137, 2020a.

Kasimov, N., Shinkareva, G., Lychagin, M., Chalov, S., Pashkina, M., Thorslund, J., and Jarsjö, J.: River water quality of the selenga-baikal basin: part ii — metal partitioning under different hydroclimatic conditions, Water, 12(9), 2392, 2020b.

Kaus, A., Schäffer, M., Karthe, D., Büttner, O., von Tümpling, W., and Borchardt, D.: Regional patterns of heavy metal exposure and contamination in the fish fauna of the Kharaa River basin, Mongolia, Reg. Environ. Change, 17, 2023–2037, doi: 10.1007/s10113-016-0969-4, 2017.

Kazakov, E., Kondrik, D., and Pozdnyakov, D.: A synthetic satellite dataset of the spatio-temporal distributions of Emiliania huxleyi blooms and their impacts on Arctic and sub-Arctic marine environments (1998–2016), Earth Systems Science Data, 11, 119–128, doi: 10.5194/essd-11-119-2019, 2019.

Kecorius, S., Vogl, T., Paasonen, P., Lampilahti, J., Rothenberg, D., Wex, H., Zeppenfeld, S., van Pinxteren, M., Hartmann, M., Henning, S., Gong, X., Welti, A., Kulmala, M., Stratmann, F., Herrmann, H., and Wiedensohler, A.: New particle formation and its effect on cloud condensation nuclei abundance in the summer Arctic: a case study in the Fram Strait and Barents Sea, Atmos. Chem. Phys., 19, 14339–14364, doi: 10.5194/acp-19-14339-2019, 2019.

Kerminen, V.-M., Chen, X., Vakkari, V., Petäjä, T., Kulmala, M., and Bianchi, F.: Atmospheric new particle formation and growth: review of field observations, Environ. Res. Lett., 13, 103003, doi: 10.1088/1748-9326/aadf3c, 2018.

Kim, J., Kim, H. M., Cho, C.-H., Boo, K.-O., Jacobson, A. R., Sasakawa, M., Machida, T., Arshinov, M., and Fedoseev, N.: Impact of Siberian observations on the optimization of surface CO2 flux, Atmos. Chem. Phys., 17, 2881–2899, https://doi.org/10.5194/acp-17-2881-2017, 2017.

Kirillin, G., Leppäranta, M., Terzhevik, A., Bernhardt, J., Engelhardt, C., Granin, N., Golosov, S., Efremova, T., Palshin, N., Sherstyankin, P., Zdorovennova, G., and Zdorovennov, R.: Physics of seasonally ice-covered lakes: major drivers and temporal/spatial scales, Aquatic Ecol., 74, 659–682, 2012.

Kirillin, G., Aslamov, I., Leppäranta, M., and Lindgren, E.: Turbulent mixing and heat fluxes under lake ice: the role of seiche oscillations, Hydrology of Earth System Sciences, 22(12), 6493-6504, doi:10.5194/hess-22-6493-2018, 2018.

Kirschke, S., Bousquet, P., Ciais, P., Saunois, M., Canadell, J. G., Dlugokencky, E. J., Bergamaschi, P. Bergmann, D, Blake, D. R., Bruhwiler, L., Cameron-Smith, P., Castaldi, S., Chevallier, F., Feng, L., Fraser, A., Heimann, M., Hodson, E. L., Houweling, S., Josse, B., Fraser, P. J., Krummel, P. B., Lamarque, J.-F., Langenfelds, R. L., Le Quere, C., Naik, V., O'Doherty, S., Palmer, P. I., Pison, I., Plummer, D., Poulter, B., Prinn, R. G., Rigby, M., Ringeval, B., Santini, M., Schmidt, M., Shindell, D. T., Simpson, I. J., Spahni, R., Steele, L. P., Strode, S. A., Sudo, K., Szopa, S., van der Werf, G.R., Voulgarakis, A., van Weele, M., Weiss, R. F., Williams, J. E., and Zeng, G.: Three decades of global methane sources and sinks, Nature Geoscience, 6(10), 813-823, doi: 10.1038/ngeo1955, 2013.

Kiselev, M. V., Voropay, N. N., and Cherkashina, A. A.: influence of anthropogenic activities on the temperature regime of soils of the South-Western Baikal region, IOP Conf. Ser.: Earth Environ. Sci., 381, 012043, doi: 10.1088/1755-1315/381/1/012043, 2019.

Kittler, F., Heimann, M., Kolle, O., Zimov, N., Zimov, S., and Göckede, M.: Long-term drainage reduces CO2 uptake and CH4 emissions in a Siberian permafrost ecosystem, Global Biogeochemical Cycles, 31, 1704– 1717. doi: 10.1002/2017GB005774, 2017.

Kiuru, P., Ojala, A., Mammarella, I., Heiskanen, J., Kämäräinen, M., Vesala, T. and Huttula, T.: Effects of Climate Change on CO2 Concentration and Efflux in a Humic Boreal Lake: A Modeling Study, Journal of Geophysical Research, Biogeosciences, 123, 7, 2212-2233, 2018.

Kondrik, D., Pozdnyakov, D., and Pettersson, L.: Particulate inorganic carbon production within E. huxleyi blooms in subpolar and polar seas: a satellite time series study (1998–2013), International Journal of Remote Sensing, 38:22, 6179-6205, doi: 10.1080/01431161.2017.1350304, 2017.

Kondrik, D. V., Pozdnyakov, D. V., and Johannessen, O. M.: Satellite evidence that E. huxleyi phytoplankton blooms weaken marine carbon sinks, Geophys. Res. Lett., 5, 846–854. doi: 10.1002/2017GL076240, 2018a.

Kondrik, D. V., Pozdnyakov, D. V., and Pettersson, L. H.: Tendencies in Coccolithophorid Blooms in Some Marine Environments of the Northern Hemisphere according to the Data of Satellite Observations in 1998– 2013. Izv. Atmos. Ocean. Phys., 53, 955-964, doi: 10.1134/S000143381709016X, 2018b.

Kondrik, D. V., Kazakov, E. E., Pozdnyakov, D. V., and Johannessen, O. M.: Satellite evidence for enhancement of the column mixing ratio of atmospheric CO2 over E. huxleyi blooms, Transactions of the

Karelian Research Centre of the Russian Academy of Sciences, Limnologoia i Oceanologia series, 9, 1-11, doi: 10/17076/lim1107, 2019.

Konovalov, I. B., Lvova, D. A., Beekmann, M., Jethva, H., Mikhailov, E. F., Paris, J.-D., Belan, B. D., Kozlov, V. S., Ciais, P., and Andreae, M. O.: Estimation of black carbon emissions from Siberian fires using satellite observations of absorption and extinction optical depths, Atmos. Chem. Phys., 18, 14889–14924, doi: 10.5194/acp-18-14889-2018, 2018.

Konovalov V., Rets E., and Pimankina N.: Interrelation between glacier summer mass balance and runoff in mountain river basins, Geography, Environment, Sustainability, 12(1), 23-33, doi: 10.24057/2071-9388-2018-26, 2019.

Konstantinov, P. I., Grishchenko, M. Y., and Varentsov, M. I.: Mapping urban heat islands of arctic cities using combined data on field measurements and satellite images based on the example of the city of Apatity (Murmansk Oblast), Izv. Atmos. Ocean. Phys., 51(9), 992-998, doi:10.1134/s000143381509011x, 2015.

Konstantinov, P., Varentsov, M., and Esau, I.: A high density urban temperature network deployed in several cities of Eurasian Arctic, Environ. Res. Lett., 13(7), 12, doi:10.1088/1748-9326/aacb84, 2018.

Kontkanen, J., Paasonen, P., Aalto, J., Back, J., Rantala, P., Petäjä, T., and Kulmala, M.: Simple proxies for estimating the concentrations of monoterpenes and their oxidation products at a boreal forest site, Atmos. Chem. Phy., 16(20), 13291-13307, doi:10.5194/acp-16-13291-2016, 2016.

Kontkanen, J., Deng, C., Fu, Y., Dada, L., Zhou, Y., Cai, J., Daellenbach, K.R., Hakala, S., Kokkonen, T.V., Lin, Z., Liu, Y., Wang, Y., Yan, C., Petäjä, T., Jiang, J., Kulmala, M. and Paasonen, P. : Size-resolved particle number emissions in Beijing determined from measured particle size distributions, Atmos. Chem. Phys. 20, 11329-11348, 2020.

Kooijmans, L. M. J., Sun, W., Aalto, J., Erkkilä, K.M., Maseyk, K., Seibt, U., Vesala, T., Mammarella, I., and Chen, H.: Influences of light and humidity on carbonyl sulfide-based estimates of photosynthesis, Proceedings of the National Academy of Sciences, 116 (7), 2470-2475, doi:10.1073/pnas.1807600116, 2019.

Korneykova, M. V., and Evdokimova, G. A.: Microbiota of the ground air layers in natural and industrial zones of the Kola Arctic, J Environ. Sci. Health A, 53(3), 271-277, doi:10.1080/10934529.2017.1397444, 2018a.

Korneikova, M. V., Redkina, V. V., and Shalygina, R. R.: Algological and mycological characterization of soils under pine and birch forests in the Pasvik Reserve, Eurasian Soil Science, 51(2), 211-220, doi:10.1134/s1064229318020047, 2018b.

Koronatova, N. G., & Milyaeva, E. V.:Plant community succession in post-mined quarries in the northern-taiga zone of West Siberia. Contemporary Problems of Ecology, 4(5), 513–518, 2011.

Kukkonen, I., Ezhova, E., Suhonen, E. A. J., Lappalainen, H. K., Gennadinik, V., Ponomareva, O., Gravis, A., Miles, V., Kulmala, M., Melnikov, V., and Drozdov, D.: Observations and modelling of ground temperature evolution in the discontinuous permafrost zone in Nadym, North-West Siberia, Permafrost and Periglacial Processes, 1– 17, doi:10.1002/ppp.2040, 2020.

Kulmala, M., Vehkamäki, H., Petäjä, T., .Dal Maso, M., Lauri, A., Kerminen, V-M., Birmili, W., and McMurry, P.H.: Formation and growth rates of ultrafine atmospheric particles: a review of observations, Journal of Aerosol Science, 35, 143-176, doi:10.1134/S1995425511050, 2004.

Kulmala, M.: Atmospheric chemistry: China's choking cocktail, Nature, 526, 497-499, doi:10.1038/526497a, 2015a.

Kulmala, M., Lappalainen, H. K., Petäjä, T., Kurten, T., Kerminen, V.-M., Viisanen, Y., Hari, P., Sorvari, S., Bäck, J., Bondur, V., Kasimov, N., Kotlyakov, V., Matvienko, G., Baklanov, A., Guo, H. D., Ding, A., Hansson, H.-C., and Zilitinkevich, S.: Introduction: The Pan-Eurasian Experiment (PEEX) – multidisciplinary, multiscale and multicomponent research and capacity-building initiative, Atmos. Chem. Phys., 15, 13085-13096, doi:10.5194/acp-15-13085-2015, 2015b.

Kulmala, M., Lappalainen, H. K., Petäjä, T., Kerminen, V.-M., Viisanen, Y., Matvienko, G., Melnikov, V., Baklanov, A., Bondur, V., Kasimov, N., and Zilitinkevich, S.: Pan-Eurasian Experiment (PEEX) Program: Grant Challenges in the Arctic-boreal context, J. Geography Environment Sustainability, 2, 5–18, 2016a.

Kulmala, M., Petäjä, T., Kerminen, V. M., Kujansuu, J., Ruuskanen, T., Ding, A., Nie, W., Hu, M., Wang, Z., Wu, Z., and Wang, L.: On secondary new particle formation in China, Front. Environ. Sci. Eng., 10, 8, doi:10.1007/s11783-016-0850-1, 2016b.

Kulmala, M., Kerminen, V.-M., Petäjä, T., Ding, A. J., and Wang L.: Atmospheric gas-to-particle conversion: why NPF events are observed in megacities?, Faraday Discuss., 200, 271-288, doi:10.1039/c6fd00257a, 2017.

Kulmala, M.: Build a global Earth observatory, Nature, 553, 21-23, doi: 10.1038/d41586-017-08967-y, 2018.

Kulmala, L., Pumpanen, J., Kolari, P., Dengel, S., Berninger, F., Köster, K., Matkala, L., Vanhatalo, A., Vesala, T., and Bäck, J.: Inter- and intra-annual dynamics of photosynthesis differ between forest floor vegetation and tree canopy in a subarctic Scots pine stand, Agricultural and Forest Meteorology, 271, 1-11, doi: 10.1016/j.agrformet.2019.02.029, 2019.

Kulmala, M., Dada, L., Daellenbach, K. R., Yan, C., Stolzenburg, D., Kontkanen, J., Ezhova, E., Hakala, S., Tuovinen, S., Kokkonen, T. V., Kurppa, M., Cai, R., Zhou, Y., Yin, R., Baalbaki, R., Chan, T., Chu, B., Deng, C., Fu, Y., Ge, M., He, H., Heikkinen, L., Junninen, H., Liu, Y., Lu, Y., Nie, W., Rusanen, A., Vakkari, V., Wang, V., Yang, G., Yao, L., Zheng, J., Kujansuu, J., Kangasluoma, J., Petäjä, T., Paasonen, P., Järvi, L., Worsnop, D., Ding, A., Liu, Y., Wang, L., Jiang, J., Bianchi, F., and Kerminen, V.-M.: Is reducing

2768   new particle formation a plausible solution to mitigate particulate air pollution in Beijing and other Chinese
2769   megacities?, Faraday Discussions, doi: 10.1039/D0FD00078G.2021.

2770   Kwon, M. J., Beulig, F., Ilie, I., Wildner, M., Küsel, K., Merbold, L., Mahecha, M. D., Zimov, N., Zimov, S.
2771   A., Heimann, M., Schuur, E. A. G., Kostka, J. E., Kolle, O., Hilke, I. and Göckede, M.: Plants,
2772   microorganisms, and soil temperatures contribute to a decrease in methane fluxes on a drained Arctic
2773   floodplain, Glob. Change Biol., 23, 2396-2412, doi:10.1111/gcb.13558, 2017.

2774   Kwon, M. J., Natali, S. M., Hicks Pries, C. E., Schuur, E. A., Steinhof, A., Crummer, K .G., Zimov, N.,
2775   Zimov, S. A., Heimann, M., Kolle, O., and Göckede, M.: Drainage enhances modern soil carbon contribution
2776   but reduces old soil carbon contribution to ecosystem respiration in tundra ecosystems, Glob. Change Biol.,
2777   25, 1315– 1325, doi: 10.1111/gcb.14578, 2019.

2778   Kühn, T., Kupiainen, K., Miinalainen, T., Kokkola, H., Paunu, V.-V., Laakso, A., Tonttila, J., Van
2779   Dingenen, R., Kulovesi, K., Karvosenoja, N., and Lehtinen, K. E. J.: Effects of black carbon mitigation on
2780   Arctic climate, Atmos. Chem. Phys., 20, 5527–5546, doi: 10.5194/acp-20-5527-2020, 2020.

2781   Köster, E., Köster, K., Berninger, F., and Pumpanen, J.: Carbon dioxide, methane and nitrous oxide fluxes
2782   from podzols of a fire chronosequence in the boreal forests in Värriö, Finnish Lapland, Geoderma Regional,
2783   5, 181-187, doi:10.1016/j.geodrs.2015.07.001, 2015.

2784   Köster, E., Köster, K., Berninger, F., Prokushkin, A., Aaltonen, H., Zhou, X., and Pumpanen, J.: Changes in
2785   fluxes of carbon dioxide and methane caused by fire in Siberian boreal forest with continuous permafrost,
2786   Journal of Environmental Management, 228, 405-415, doi:10.1016/j.jenvman.2018.09.051, 2018.

2787   Köster, K., Berninger, F., Koster, E., and Pumpanen, J.: Influences of reindeer grazing on above- and
2788   belowground biomass and soil carbon dynamics, Arctic Antarctic and Alpine Res., 47(3), 495-503,
2789   doi:10.1657/aaar0014-062, 2015.

2790   Köster, K., Berninger, F., Heinonsalo, J., Lindén, A., Köster, E., Ilvesniemi, H., and Pumpanen J.: The long-
2791   term impact of low-intensity surface fires on litter decomposition and enzyme activities in boreal coniferous
2792   forests, Int. J Wildland Fire, 25(2), 213-223, doi:10.1071/wf14217_co, 2016.

2793   Köster, K., Koster, E., Berninger, F., Heinonsalo, J., and Pumpanen, J.: Contrasting effects of reindeer
2794   grazing on CO2, CH4, and N2O fluxes originating from the northern boreal forest floor. Land Degradation
2795   and Development, 29(2), 374-381, doi:10.1002/ldr.2868, 2018.

2796   Köster, K., Koster, E., Kulmala, L., Berninger, F., and Pumpanen, J.: Are the climatic factors combined with
2797   reindeer grazing affecting the soil CO2 emissions in subarctic boreal pine forest? Catena, 149, 616-622,
2798   doi:10.1016/j.catena.2016.06.011, 2017.

2799   Lan, H., Holopainen, J., Hartonen, K., Jussila, M., Ritala, M. and Riekkola, M.-L.: Fully automated online
2800   dynamic in-tube extraction for continuous sampling of volatile organic compounds in air, Anal. Chem., 91,
2801   8507, 2019.

2802 Lappalainen, H.K., Kulmala, M. and Zilitinkevich, S. (Eds.): Pan Eurasian Experiment (PEEX) Science Plan,
2803 web: www.atm.helsinki.fi/peex, ISBN 978-951-51-0587-5 (printed), ISBN 978-951-51-0588-2 (online),
2804 2015.

2805 Lappalainen H.K., Petäjä T., Kujansuu J., Kerminen V., Shvidenko A., Bäck J., Vesala T., Vihma T., De
2806 Leeuw G., Lauri A., Ruuskanen T., Lapshin V.B., Zaitseva N., Glezer O., Arshinov M., Spracklen D.V.,
2807 Arnold S.R., Juhola S., Lihavainen H., Viisanen Y., Chubarova N., Chalov S., Filatov N., Skorokhod A.,
2808 Elansky N., Dyukarev E., Esau I., Hari P., Kotlyakov V., Kasimov N., Bondur V., Matvienko G., Baklanov
2809 A., Mareev E., Troitskaya Y., Ding A., Guo H., Zilitinkevich S., and Kulmala M.: Pan-Eurasian Experiment
2810 (PEEX) –a research initiative meeting the grand challenges of the changing environment of the northern Pan-
2811 Eurasian arctic-boreal areas, J. Geography Environment Sustainability, 2(7), 13-48, doi:10.24057/2071-
2812 9388-2014-7-2-13-48, 2014.

2813 Lappalainen, H. K., Kerminen, V.-M., Petäjä, T., Kurten, T., Baklanov, A., Shvidenko, A., Bäck, J., Vihma,
2814 T., Alekseychik, P., Andreae, M. O., Arnold, S. R., Arshinov, M., Asmi, E., Belan, B., Bobylev, L., Chalov,
2815 S., Cheng, Y., Chubarova, N., de Leeuw, G., Ding, A., Dobrolyubov, S., Dubtsov, S., Dyukarev, E., Elansky,
2816 N., Eleftheriadis, K., Esau, I., Filatov, N., Flint, M., Fu, C., Glezer, O., Gliko, A., Heimann, M., Holtslag, A.
2817 A. M., Hõrrak, U., Janhunen, J., Juhola, S., Järvi, L., Järvinen, H., Kanukhina, A., Konstantinov, P.,
2818 Kotlyakov, V., Kieloaho, A.-J., Komarov, A. S., Kujansuu, J., Kukkonen, I., Duplissy, E.-M., Laaksonen, A.,
2819 Laurila, T., Lihavainen, H., Lisitzin, A., Mahura, A., Makshtas, A., Mareev, E., Mazon, S., Matishov, D.,
2820 Melnikov, V., Mikhailov, E., Moisseev, D., Nigmatulin, R., Noe, S. M., Ojala, A., Pihlatie, M., Popovicheva,
2821 O., Pumpanen, J., Regerand, T., Repina, I., Shcherbinin, A., Shevchenko, V., Sipilä, M., Skorokhod, A.,
2822 Spracklen, D. V., Su, H., Subetto, D. A., Sun, J., Terzhevik, A. Y., Timofeyev, Y., Troitskaya, Y.,
2823 Tynkkynen, V.-P., Kharuk, V. I., Zaytseva, N., Zhang, J., Viisanen, Y., Vesala, T., Hari, P., Hansson, H. C.,
2824 Matvienko, G. G., Kasimov, N. S., Guo, H., Bondur, V., Zilitinkevich, S., and Kulmala, M.: Pan-Eurasian
2825 Experiment (PEEX): towards a holistic understanding of the feedbacks and interactions in the land–
2826 atmosphere–ocean–society continuum in the northern Eurasian region, Atmos. Chem. Phys., 16, 14421–
2827 14461, https://doi.org/10.5194/acp-16-14421-2016, 2016.

2828 Lappalainen, H.K., Kulmala, M., Kujansuu, J., Petäjä, T., Mahura, A., de Leeuw, G., Zilitinkevich, S.,
2829 Juustila, M., Kerminen, V.M., Bornstein, B. and Jiahua, Z.: The Silk Road agenda of the Pan-Eurasian
2830 Experiment (PEEX) program, Big Earth Data, 2(1), 8-35, doi:10.1080/20964471.2018.1437704, 2018.

2831 Lei, R. B., Xie, H. J., Wang, J., Leppäranta, M., Jonsdottir, I., and Zhang, Z. H.: Changes in sea ice
2832 conditions along the Arctic Northeast Passage from 1979 to 2012, Cold Regions Science and Technology,
2833 119, 132-144. doi:10.1016/j.coldregions.2015.08.004, 2015.

2834 Lei, R., Tian-Kunze, X., Leppäranta, M., Wang, J., Kaleschke, L., and Zhang, Z.: Changes in summer sea
2835 ice, albedo, and portioning of surface solar radiation in the Pacific sector of Arctic Ocean during 1982-2009,
2836 J. Geophys. Res.: Oceans, 121(8), 5470-5486, doi:10.1002/2016jc011831, 2016.

2837   Lei, R. B., Cheng, B., Heil, P., Vihma, T., Wang, J., Ji, Q., and Zhang, Z. H.: Seasonal and interannual
2838   variations of sea ice mass balance from the Central Arctic to the Greenland Sea, J. Geophys. Res.: Oceans,
2839   123(4), 2422-2439, doi:10.1002/2017jc013548, 2018.

2840   Leino, K., Nieminen, T., Manninen, H. E., Petäjä, T., Kerminen, V.-M., and Kulmala, M.: Intermediate ions
2841   as a strong indicator of new particle formation bursts in a boreal forest, Boreal Environ. Res., 21(3-4), 274-
2842   286, 2016.

2843   Leppäranta, M.: Structure and properties of lake ice. Freezing of Lakes and the Evolution of their Ice Cover,
2844   Springer, Berlin/Heidelberg, Germany, 51–90. doi: 10.1007/978-3-642-29081-7_3, 2015.

2845   Leppäranta, M., Lindgren, E., and Shirasawa, K.: The heat budget of Lake Kilpisjarvi in the Arctic tundra,
2846   Hydrol. Res., 48(4), 969-980, doi:10.2166/nh.2016.171, 2017.

2847   Leppäranta, M., Lewis, J. E., Heini, A., and Arvola, L.: Spatial statistics of hydrography and water chemistry
2848   in a eutrophic boreal lake based on sounding and water samples, Environ. Monit. Assess., 190(7), 378,
2849   doi:10.1007/s10661-018-6742-z, 2018.

2850   Leppäranta, M., Lindgren, E., Wen, L. and Kirillin, G.: Ice cover decay and heat balance in Lake Kilpisjärvi
2851   in Arctic tundra, Journal of Limnology, 78(2). doi: 10.4081/jlimnol.2019.1879, 2019.

2852   Leppäranta, M., Meleshko, V., Uotila, P., and Pavlova, T.: Sea ice modelling, 315-387, Sea Ice in the Arctic
2853   (Springer, Cham), 2020.

2854   Li, H., Väliranta, M., Mäki, M., Kohl, L., Sannel, B., Pumpanen, J., Koskinen, M., Bäck, J. and Bianchi, F.:
2855   Overlooked organic vapor emissions from thawing Arctic permafrost, Environmental Research Letters 15,
2856   Issue 10, id.104097, 12 pp., 2020a.

2857   Li, M., Wang, L., Liu, J., Gao, W., Song, T., Sun, Y., Li, L., Li, X., Wang, Y., Liu, L. and Daellenbach,
2858   K.R., Paasonen, P.J., Kerminen, V.-M., Kulmala, M., and Wang Y.: Exploring the regional pollution
2859   characteristics and meteorological formation mechanism of PM2. 5 in North China during 2013–2017,
2860   Environment international, 134, 105283, 2020b.

2861   Liao, Z., Cheng, B., Zhao, J., Vihma, T., Jackson, K., Yang, Q., Yang, Y., Zhang, L., Li, Z., Qiu, Y., and
2862   Cheng, X.: Snow depth and ice thickness derived from SIMBA ice mass balance buoy data using an
2863   automated algorithm, Int. J. Digital Earth, 12(8), 962-979, doi:10.1080/17538947.2018.1545877, 2018.

2864   Lin, X., Rogers, B. M., Sweeney, C., Chevallier, F., Arshinov, M., Dlugokencky, E., Machida, T., Motoki
2865   Sasakawa, Tans, P., Keppel-Aleks, G.: Siberian and temperate ecosystems shape Northern Hemisphere
2866   atmospheric CO_2 seasonal amplification, PNAS, 117 (35), 21079-21087, doi:10.1073/pnas.1914135117 ,
2867   2020.

2868   Lintunen, A., Paljakka, T., Salmon, Y., Dewar, R., Riikonen, A, and Hölttä, T.: The influence of soil
2869   temperature and water content on belowground hydraulic conductance and leaf gas exchange in mature trees
2870   of three boreal species, Plant, Cell and Environment, 43, 532-547, doi: 10.1111/pce.13709, 2020.

Liu, Y.C., Yan, C., Feng, Z., Zheng, F., Fan, X., Zhang, Y., Li, C., Zhou, Y., Lin, Z., Guo, Y., Zhang, Y., Ma, L., Zhou, W., Liu, Z., Dada, L., Dällenbach, K., Kontkanen, J., Cai, R., Chan, T., Chu, B., Du, W., Yao, L., Wang, Y., Cai, J., Kangasluoma, J., Kokkonen, T., Kujansuu, J., Rusanen, A., Deng, C., Fu, Y., Yin, R., Li, X., Lu, Y., Liu, Y., Lian, C., Yang, D., Wang, W., Ge, M., Wang, Y., Worsnop, D.R., Junninen, H., He, H., Kerminen, V.-M., Zheng, J., Wang, L., Jiang, J., Petäjä, T., Bianchi, F. and Kulmala, M. : Continuous and comprehensive atmospheric observation in Beijing: a station to understand the complex urban atmospheric environment, Big Earth Data, 4, 295-321, 2020.

Liu, J., Wang, L., Li, M., Liao, Z., Sun, Y., Song, T., Gao, W., Wang, Y., Li, Y., Ji, D., Hu, B., Kerminen, V.-M., Wang, Y., and Kulmala, M.: Quantifying the impact of synoptic circulation patterns on ozone variability in northern China from April to October 2013–2017, Atmos. Chem. Phys., 19, 14477–14492, doi:10.5194/acp-19-14477-2019, 2019 a.

Liu, W., Atherton, J., Mõttus, M., Gastellu-Etchegorry, J.P., Malenovský, Z., Raumonen, P., Åkerblom, M., Mäkipää, R. and Porcar-Castell, A.: Simulating solar-induced chlorophyll fluorescence in a boreal forest stand reconstructed from terrestrial laser scanning measurements, Remote Sensing of Environment, 232, 111274, 2019b.

Liu, Y., de Leeuw, G., Kerminen, V.-M., Zhang, J., Zhou, P., Nie, W., Qi, X., Hong, J., Wang, Y., Ding, A., Guo, H., Krüger, O., Kulmala, M., and Petäjä, T.: Analysis of aerosol effects on warm clouds over the Yangtze River Delta from multi-sensor satellite observations, Atmos. Chem. Phys., 17, 5623–5641, doi:10.5194/acp-17-5623-2017, 2017.

Liu, Y., Zhang, J., Zhou, P., Lin, T., Hong, J., Shi, L., Yao, F., Wu, J., Guo, H., and de Leeuw, G.: Satellite-based estimate of the variability of warm cloud properties associated with aerosol and meteorological conditions, Atmos. Chem. Phys., 18, 18187–18202, doi:10.5194/acp-18-18187-2018, 2018.

López-Blanco, E., Exbrayat, J.-F., Lund, M., Christensen, T. R., Tamstorf, M. P., Slevin, D., Hugelius, G., Bloom, A. A., and Williams, M.: Evaluation of terrestrial pan-Arctic carbon cycling using a data-assimilation system, Earth Syst. Dynam., 10, 233–255, doi:10.5194/esd-10-233-2019, 2019.

Lu, P., Leppäranta, M., Cheng, B., and Li, Z.: Influence of melt-pond depth and ice thickness on Arctic sea-ice albedo and light transmittance, Cold Regions Science and Technology, 124, 1-10, doi:10.1016/j.coldregions.2015.12.010, 2016.

Lu, P., Cheng, B., Leppäranta, M., and Li, Z. J.: Partitioning of solar radiation in Arctic sea ice during melt season, Oceanologia, 60(4), 464-477, doi:10.1016/j.oceano.2018.03.002, 2018a.

Lu, P., Leppäranta, M., Cheng, B., Li, Z., Istomina, L., and Heygster, G.: The color of melt ponds on Arctic sea ice, The Cryosphere, 12, 1331–1345, doi:10.5194/tc-12-1331-2018, 2018b.

Lu, Y., Yan, C., Fu, Y., Chen, Y., Liu, Y., Yang, G., Wang, Y., Bianchi, F., Chu, B., Zhou, Y., Yin, R., Baalbaki, R., Garmash, O., Deng, C., Wang, W., Liu, Y.C., Petäjä, T., Kerminen, V.-M., Jiang, J., Kulmala,

M. and Wang, L. : A proxy for atmospheric daytime gaseous sulfuric acid concentration in urban Beijing, Atmos. Chem. Phys. 19, 1971-1983, 2019.

Luoma, K., Virkkula, A., Aalto, P.P, Petäjä, T., and Kulmala, M.: Over a 10-year record of aerosol optical properties at SMEAR II, Atmos. Chem. Phys., 19, 11363–11382, doi:10.5194/acp-19-11363-2019, 2019.

Lychagin, M., Chalov, S., Kasimov, N., Shinkareva, G., Jarsjo, J., and Thorslund, J.: Surface water pathways and fluxes of metals under changing environmental conditions and human interventions in the Selenga River system, Environ. Earth Sci., 76(1), 14, doi:10.1007/s12665-016-6304-z, 2017.

Ma,J., Yan, X., Dong, W. et al.: Gross primary production of global forest ecosystems has been overestimated, Sci Rep 5, 10820, doi:10.1038/srep10820, 2015.

Magritsky, D. V., Frolova, N. L. , Evstigneev, V. M. , Povalishnikova, E. S. , Kireeva, M. B., and Pakhomova, O. M.: Long-term changes of river water inflow into the seas of the Russian Arctic sector, Polarforschung, 87(2),177-194, doi: 10.2312/polarforschung.87.2.177, 2018.

Mahura A., Baklanov A., Sørensen, J. H., Svetlov, A., and Koshkin, V.: Assessment of Long-Range Transport and Deposition from Cu-Ni Smelters of Russian North. In ”Air, Water and Soil Quality Modelling for Risk and Impact Assessment", Security Through Science, Series C - Environmental Security. Eds. A. Ebel, T. Davitashvili, Springer Elsevier Publishers, pp. 115-124, 2007.

Mahura, A., Gonzalez-Aparacio, I., Nuterman, R., and Baklanov, A.: Seasonal Impact Analysis on Population due to Continuous Sulphur Emissions from Severonikel Smelters of the Kola Peninsula. Geography, Environment, Sustainability, 11(1), 130-144, doi:10.24057/2071-9388-2018-11-1-130-144, 2018.

Malkhazova, S. M., Mironova, V. A., Orlov, D. S., and Adishcheva, O. S.: Influence of climatic factor on naturally determined diseases in a regional context, Geography, Environment, Sustainability, 11(1), 157-170, doi:10.24057/2071-9388-2018-11-1-157-170, 2018.

Malsy, M., Flörke, M., and Borchardt, D.:What drives the water quality changes in the Selenga basin: climate change or socio-economic development?, Reg Environ Chang., 17, 1977–1989 doi:10.1007/s10113-016-1005-4, 2017.

Mammarella, I., Nordbo, A., Rannik, Ü., Haapanala, S., Levula, J., Laakso, H., Ojala, A., Peltola, O., Heiskanen, J., Pumpanen, J. and Vesala, T.: Carbon dioxide and energy fluxes over a small boreal lake in Southern Finland, J. Geophys. Res.: Biogeosciences, 120(7), 1296-1314, doi:10.1002/2014jg002873, 2015.

Manasypov, R. M., Vorobyev, S. N., Loiko, S. V., Krivtzov, I. V., Shirokova, L. S., Shevchenko, V. P., Kirpotin, S. N., Kulizhsky, S. P., Kolesnichenko, L. G., Zemtsov, V. A. and Sinkinov, V. V.: Seasonal dynamics of thermokarst lake chemical composition in discontinuous permafrost zone of Western Siberia, Biogeosciences, 12, 3009-3028, 2015.

2938 Marelle, L., Raut, J. C., Law, K. S., and Duclaux, O.: Current and future arctic aerosols and ozone from
2939 remote emissions and emerging local sources-modeled source contributions and radiative effects, J.
2940 Geophys. Res.: Atmos., 123(22), 12942-12963, doi:10.1029/2018jd028863, 2018.

2941 Maslov, A. V., Shevchenko, V. P., Bobrov, V. A., Belogub, E. V., Ershova, V. B., Vereshchagin, O. S., and
2942 Khvorov, P. V.: Mineralogical-geochemical features of ice-rafted sediments in some arctic regions,
2943 Lithology and Mineral Resources, 53(2), 110-129, doi:10.1134/s0024490218020037, 2018a.

2944 Maslov, A. V., Shevchenko, V. P., Kuznetsov, A. B., and Stein, R.: Geochemical and Sr-Nd-Pb-isotope
2945 characteristics of ice-rafted sediments of the Arctic Ocean, Geochem. Int., 56(8), 751-765,
2946 doi:10.1134/s0016702918080050, 2018b.

2947 Matkala, L., Kulmala, L., Kolari, P., Aurela, M., and Bäck, J.: Resilience of carbon dioxide and water
2948 exchange to extreme weather events in subarctic Scots pine and Norway spruce stands, Agricultural and
2949 Forest Meteorology, 296, 108239, 2020.

2950 McCusker, K., Fyfe, J., and Sigmond, M.: Twenty-five winters of unexpected Eurasian cooling unlikely due
2951 to Arctic sea-ice loss, Nature Geoscience 9, 838–842, doi:10.1038/ngeo2820, 2016.

2952 Meinander, O., Heikkinen, E., Aurela, M., and Hyvärinen, A.: Sampling, Filtering, and Analysis Protocols to
2953 Detect Black Carbon, Organic Carbon, and Total Carbon in Seasonal Surface Snow in an Urban Background
2954 and Arctic Finland (>60° N), Atmosphere, 11, 923. doi:10.3390/atmos11090923, 2020a.

2955 Meinander, O., Kontu, A., Kouznetsov, R., Sofiev, M.: Snow Samples Combined with Long-Range
2956 Transport Modeling to Reveal the Origin and Temporal Variability of Black Carbon in Seasonal Snow in
2957 Sodankylä (67° N), Front. Earth Sci., 8, 13,
2958 https://www.frontiersin.org/articles/10.3389/feart.2020.00153/full, 2020b.

2959 Merkouriadi, I., Cheng, B., Graham, R. M., Rösel, A., and Granskog, M. A.: Critical role of snow on sea ice
2960 growth in the Atlantic sector of the Arctic Ocean. Geophysical Research Letters, 44.
2961 doi:10.1002/2017GL075494, 2017

2962 Merkouriadi, I., Cheng, B., Graham, R. M., Rösel, A., and Granskog, M. A.: Critical role of snow on sea ice
2963 growth in the Atlantic sector of the Arctic Ocean, Geophys. Res. Lett., 44, doi: 10.1002/2017GL075494,
2964 2018.

2965 Mikhailov, E. F., Mironova, S. Y., Makarova, M. V., Vlasenko, S. S., Ryshkevich, T. I., Panov, A. V., and
2966 Andreae, M. O.: Studying seasonal variations in carbonaceous aerosol particles in the atmosphere over
2967 central Siberia, Izv. Atmos. Oceanic Phys., 51(4), 423-430, doi:10.1134/s000143381504009x, 2015a.

2968 Mikhailov, E. F., Mironov, G. N., Pöhlker, C., Chi, X., Krüger, M. L., Shiraiwa, M., Förster, J.-D., Pöschl,
2969 U., Vlasenko, S. S., Ryshkevich, T. I., Weigand, M., Kilcoyne, A. L. D., and Andreae, M. O.: Chemical
2970 composition, microstructure, and hygroscopic properties of aerosol particles at the Zotino Tall Tower

2971 Observatory (ZOTTO), Siberia, during a summer campaign, Atmos. Chem. Phys., 15, 8847–8869,

2972 doi:10.5194/acp-15-8847-2015, 2015b.

2973 Mikhailov, E. F., Mironova, S., Mironov, G., Vlasenko, S., Panov, A., Chi, X., Walter, D., Carbone, S.,

2974 Artaxo, P., Heimann, M., Lavric, J., Pöschl, U., and Andreae, M. O.: Long-term measurements (2010–2014)

2975 of carbonaceous aerosol and carbon monoxide at the Zotino Tall Tower Observatory (ZOTTO) in central

2976 Siberia, Atmos. Chem. Phys., 17, 14365–14392, doi:10.5194/acp-17-14365-2017, 2017.

2977 Mikola, J., Virtanen, T., Linkosalmi, M., Vähä, E., Nyman, J., Postanogova, O., Räsänen, A., Kotze, D. J.,

2978 Laurila, T., Juutinen, S., Kondratyev, V., and Aurela, M.: Spatial variation and linkages of soil and

2979 vegetation in the Siberian Arctic tundra – coupling field observations with remote sensing data,

2980 Biogeosciences, 15, 2781–2801, doi:10.5194/bg-15-2781-2018, 2018.

2981 Miles, V. V., and Esau, I.: Spatial heterogeneity of greening and browning between and within bioclimatic

2982 zones in northern West Siberia, Environ. Res. Lett., 11(11), 12, doi:10.1088/1748-9326/11/11/115002, 2016.

2983 Miles, V., and Esau, I.: Seasonal and Spatial Characteristics of Urban Heat Islands (UHIs) in Northern West

2984 Siberian Cities., Remote Sens., 9, 989, 2017.

2985 Miles, M. W., Miles, V, and Esau, I.: Varying climate response across the tundra, forest–tundra and boreal

2986 forest biomes in northern West Siberia, Environ. Res. Lett., 14, 075008, doi:10.1088/1748-9326/ab2364,

2987 2019.

2988 Miles, V., and Esau, I.: Surface urban heat islands in 57 cities across different climates in northern

2989 Fennoscandia, Urban Climate, 31, 10.1016/j.uclim.2019.100575, 2020.

2990 Miles, V.: Arctic surface Urban Heat Island (UHI), MODIS Land Surface Temperature (LST) data, 2000-

2991 2016. Arctic Data Center. doi:10.18739/A2TB0XW4T, 2020.

2992 MNRE (2019): Methods for calculating emissions of pollutants into the atmosphe from stationary sources.

2993 Ministry of Natural Resources and Ecology. In Russian

2994 (www.mnr.gov.ru/docs/metodiki_rascheta_vybrosov_vrednykh_zagryaznyayushchikh_veshchestv_v_atmosf

2995 ernyy_vozdukh_statsionarn/perechen), 2019.

2996

2997 Mori, M., Watanabe, M., Shiogama, H., Inoue, J., and Kimoton, M.: Robust Arctic sea-ice influence on the

2998 frequent Eurasian cold winters in past decades, Nat. Geosci., 7, 869–873, doi:10.1038/ngeo2277, 2014.

2999 Mori, M., Kosaka, Y., Watanabe, M., Nakamura, H., and Kimoto, M.: A reconciled estimate of the influence

3000 of Arctic sea-ice loss on recent Eurasian cooling, Nat. Clim. Change, 9, 123–129, doi: 10.1038/s41558-018-

3001 0379-3, 2019.

3002 Morozov, E. A., Kondrik, D. V., Chepikova, S. S., and Pozdnyakov, D. V.: Atmospheric columnar CO_2

3003 enhancement over E. huxleyi blooms: case studies in the North Atlantic and Arctic waters. Transactions of

3004 the Karelian Research Centre of the Russian Academy of Sciences, Limnologoia i Oceanologia series, 3, 1-6.
3005 doi:10.17076/lim989, 2019.

3006 Myslenkov S., Medvedeva A., Arkhipkin V., Markina M., Surkova G., Krylov A., Dobrolyubov S.,
3007 Zilitinkevich S., and Koltermann P.: Long-term statistics of storms in the Baltic, Barents and White Seas and
3008 their future climate projections,. Geography, environment, sustainability, 11, 93-112, doi:10.24057/2071-
3009 9388-2018-11-1-93-112, 2018.

3010 Mäki, M., Krasnov, D., Hellén, H., Noe, S. M., and Bäck, J.: Stand type affects fluxes of volatile organic
3011 compounds from the forest floor in hemiboreal and boreal climates, Plant Soil, 441, 363–381,
3012 doi:10.1007/s11104-019-04129-3, 2019.

3013 Naakka, T., Nygård, T., Vihma, T., Graversen, R., and Sedlar, J.: Atmospheric moisture transport between
3014 mid-latitudes and the Arctic: regional, seasonal and vertical distributions, Int. J. Climatol., 32, 1–18,
3015 doi:10.1002/joc.5988, 2019.

3016 Natali, S.M., Watts, J.D., Rogers, B.M., Potter, S., Ludwig, S. M., Selbmann, A. K., Sullivan, P.F. Abbott, B.
3017 W., Arndt, K. A., Birch, L., Björkman, M.P., Bloom, A., Celis, G., Christensen, T. R., Christiansen, C. T.,
3018 Commane, R., Cooper, E. J., Crill, P., Czimczik, C., Davydov, S., Du, J., Egan, J.E., Elberling, B.,
3019 Euskirchen, B.S., Friborg, T., Genet, H., Göckede, M., Goodrich, J.P., Grogan, P., Helbig, M., Jafarov, E.E.,
3020 Jastrow, J. D., Kalhori, A.A.M., Kim, Y Kimball, J. S., Kutzbach, L., Lara, M. J, Larsen, K., S., Lee, B.-Y.,
3021 Liu, Z., Loranty, M. M., Lund, M., Lupascu, M., Madani, N., Malhotra, A., Matamala, R., McFarland, J.,
3022 McGuire, A. D., Michelsen, A., Minions, C., Oechel, W., Olefeldt, D., Parmentier, F.-J., Pirk, N., Poulter,
3023 B., Quinton, W., Rezanezhad, F., Risk, D., Sachs, T., Schaefer, K., Schmidt, N. M., Schuur, E., Semenchuk,
3024 P. R., Shaver, G., Sonnentag, O., Starr, G., Treat, C. C., Waldrop, M. P., Wang, Y., Welker, J., Wille, C., Xu,
3025 X., Zhang, Z., Zhuang, Q., and Zona, D.: Large loss of CO2 in winter observed across the northern
3026 permafrost region, Nat. Clim. Chang., 9, 852–857, doi:10.1038/s41558-019-0592-8, 2019.

3027 Nikandrova, A., Tabakova, K., Manninen, A., Väänänen, R., Petäjä, T., Kulmala, M., Kerminen, V.-M., and
3028 O'Connor, E.: Combining airborne in situ and ground-based lidar measurements for attribution of aerosol
3029 layers, Atmos. Chem. Phys., 18, 10575–10591, doi:10.5194/acp-18-10575-2018, 2018.

3030 NILU, 2013: Sandanger, T.M., Anda, E., Berglen, T.F., Evenset, A., Christensen, G., and Heimstad, E.S.:
3031 Health and environmental impacts in the Norwegian border area related to local Russian industrial emissions.
3032 Knowledge status, 40/2013, 2013.

3033 Nissen, C., Munnich, M., Grube, M., and Haumann, N.: Factors controlling coccolithophore biogeography in
3034 the Southern Ocean, Biogeosciences, 15(22), 6997-7024, doi:10.5194/bg-15-6997-2018, 2018.

3035 Nitzbon, J., Langer, M., Westermann, S., Martina, L., Aas, K. S., and Boike, J.: Pathways of ice-wedge
3036 degradation in polygonal tundra under different hydrological conditions, Cryosphere, 13(4), 1089-1123,
3037 doi:10.5194/tc-13-1089-2019, 2019.

3038 Nygård, T., Graversen, R. G., Uotila, P., Naakka, T., and Vihma, T.: Strong dependence of wintertime Arctic
3039 moisture and cloud distributions on atmospheric large-scale circulation, J. Climate, 32, 8771-8790, doi:
3040 10.1175/JCLI-D-19-0242.1, 2019.

3041 Overland, J., Dunlea, E., Box, J. E., Corell, R., Forsius, M., Kattsov, V., Olsen, M. S., Pawlak, J., Reiersen,
3042 L. O., and Wang, M.: The urgency of Arctic change, Polar Science, 21, 6-13,
3043 doi:10.1016/j.polar.2018.11.008, 2019.

3044 Paasonen, P., Peltola, M., Kontkanen, J., Junninen, H., Kerminen, V.-M., and Kulmala, M.: Comprehensive
3045 analysis of particle growth rates from nucleation mode to cloud condensation nuclei in boreal forest, Atmos.
3046 Chem. Phys., 18, 12085–12103, doi:10.5194/acp-18-12085-2018, 2018.

3047 Palo, T., Vihma, T., Jaagus, J., and Jakobson, E.: Observations on temperature inversion over central Arctic
3048 sea ice in summer, Q. J. R. Meteorol. Soc., 143(708), 2741-2754, doi:10.1002/qj.3123, 2017.

3049 Panov, A. V., Prokushkin, A. S., Bryukhanov, A. V., Korets, M. A., Ponomarev, E. I., Sidenko, N. V.,
3050 Zrazhevskaya, G. K., Timokhina, A. V., and Andreae, M. O.: A complex approach for the estimation of
3051 carbonaceous emissions from wildfires in Siberia, Russian Meteorol, Hydrol., 43(5), 295-301, 2018.

3052 Parmentier, F. W., Christensen, T. R., Rysgaard, S. Bendtsen, J., Glud, R. N., Else, B., van Huissteden, J.,
3053 Sachs, T., Vonk, J. E., and Sejr, M. K.: A synthesis of the arctic terrestrial and marine carbon cycles under
3054 pressure from a dwindling cryosphere, Ambio, 46, 53–69, doi:10.1007/s13280-016-0872-8, 2017.

3055 Parshintsev, J., Vaikkinen, A., Lipponen, K., Vrkoslav, V., Cvačka, J., et al. : Desorption atmospheric
3056 pressure photoionization high-resolution mass spectrometry: a complementary approach for the chemical
3057 analysis of atmospheric aerosols, Rapid Commun. Mass Spectrom., 29, 1233–1241, 2015.

3058 Passananti, M., Zapadinsky, E., Zanca, T., Kangasluoma, J., Myllys, N., Rissanen, M.P., Kurtén, T., Ehn,
3059 M., Attoui, M., and Vehkamäki, H.: How well can we predict cluster fragmentation inside a mass
3060 spectrometer? Chem. Commun., 55, 5946-5949, 2019.

3061 Payne, R. J., Creevy, A., Malysheva, E., Ratcliffe, J., Andersen, R., Tsyganov, A. N., Rowson, J., Marcisz,
3062 K., Zielinska, M., Lamentowicz, M., Lapshina, E. D., and Mazei, Y.: Tree encroachment may lead to
3063 functionally-significant changes in peatland testate amoeba communities. Soil Biology & Biochemistry, 98,
3064 18-21. doi:10.1016/j.soilbio.2016.04.002, 2016.

3065 Peltola, O., Vesala,T., Gao, Y.; Räty, O. et al. : Monthly gridded data product of northern wetland methane
3066 emissions based on upscaling eddy covariance observations, Earth System Science Data, 11, 1263-1289,
3067 doi:10.5194/essd-11-1263-2019, 2019.

3068 Peltoniemi, J. I., Gritsevich, M., Hakala, T., Dagsson-Waldhauserová, P., Arnalds, Ó., Anttila, K., Hannula,
3069 H.-R., Kivekäs, N., Lihavainen, H., Meinander, O., Svensson, J., Virkkula, A., and de Leeuw, G.: Soot on

Snow experiment: bidirectional reflectance factor measurements of contaminated snow, The Cryosphere, 9, 2323–2337, doi:10.5194/tc-9-2323-2015, 2015.

Peterson, B. J., Holmes, R. M., McClelland, J. W., Vörösmarty, C. J., Lammers, R. B., Shiklomanov, A. I., Shiklomanov, I. A., and Rahmstorf, S.: Increasing river discharge to the Arctic Ocean, Science, 80, 298, 2171–2173, doi: 10.1126/science.1077445, 2002.

Petäjä, T., Järvi, L., Kerminen, V.-M., Ding, A. J., Sun, J. N., Nie, W., Kujansuu, J., Virkkula, A., Yang, X.-Q., Fu, C. B., Zilitinkevich, S., and Kulmala M.: Enhanced air pollution via aerosol-boundary layer feedback in China, Scientific Reports, 6, 18998, doi:10.1038/srep18998, 2016.

Petäjä, T., Duplissy, E.-M., Tabakova, K., Schmale, J., Altstädter, B., Ancellet, G., Arshinov, M., Balin, Y., Baltensperger, U., Bange, J., Beamish, A., Belan, B., Berchet, A., Bossi, R., Cairns, W. R. L., Ebinghaus, R., El Haddad, I., Ferreira-Araujo, B., Franck, A., Huang, L., Hyvärinen, A., Humbert, A., Kalogridis, A.-C., Konstantinov, P., Lampert, A., MacLeod, M., Magand, O., Mahura, A., Marelle, L., Masloboev, V., Moisseev, D., Moschos, V., Neckel, N., Onishi, T., Osterwalder, S., Ovaska, A., Paasonen, P., Panchenko, M., Pankratov, F., Pernov, J. B., Platis, A., Popovicheva, O., Raut, J.-C., Riandet, A., Sachs, T., Salvatori, R., Salzano, R., Schröder, L., Schön, M., Shevchenko, V., Skov, H., Sonke, J. E., Spolaor, A., Stathopoulos, V., K., Strahlendorff, M., Thomas, J. L., Vitale, V., Vratolis, S., Barbante, C., Chabrillat, S., Dommergue, A., Eleftheriadis, K., Heilimo, J., Law, K. S., Massling, A., Noe, S. M., Paris, J.-D., Prévôt, A. S. H., Riipinen, I., Wehner, B., Xie, Z., and Lappalainen, H. K.: Overview: Integrative and Comprehensive Understanding on Polar Environments (iCUPE) – concept and initial results, Atmos. Chem. Phys., 20, 8551–8592, doi:10.5194/acp-20-8551-2020, 2020a.

Petäjä, T., Ganzei, K. S., Lappalainen, H. K., Tabakova, K., Makkonen, R., Räisänen, J., Chalov, S., Kulmala, M., Zilitinkevich, S. S., Baklanov, P., Shakirov, R. B., Mishina, N.V., Egidarev, E.G., and Kondrat'ev, I. I.: Research agenda for the Russian Far East and utilization of multi-platform compherensive environmental observations, J. Big Data, 5:3, 277-305, doi:10.1080/17538947.2020.1826589 , 2020b.

Pietron, J., Jarsjo, J., Romanchenko, A. O., and Chalov, S. R.: Model analyses of the contribution of in-channel processes to sediment concentration hysteresis loops, Journal of Hydrology, 527, 576-589. doi:10.1016/j.jhydrol.2015.05.009, 2015.

Pietroń, J., Nittrouer, J. A., Chalov, S. R., Dong, T. Y., Kasimov, N., Shinkareva, G., and Jarsjö, J.: Sedimentation patterns in the Selenga River delta under changing hydroclimatic conditions, Hydrological Processes, 32(2), 278-292, doi:10.1002/hyp.11414, 2018.

Pirazzini, R., Leppanen, L., Picard, G., Lopez-Moreno, J. I., Marty, C., Macelloni, G., Kontu, A., Von Lerber, A., Tanis, C.M., Schneebeli, M., De Rosnay, P., Arslan, A. N.: European in-situ snow measurements: practices and purposes, Sensors, 18(7), 51, doi:10.3390/s18072016, 2018.

Pisso, I., Myhre, C. L., Platt, S. M., Eckhardt, S., Hermansen, O., Schmidbauer, N., Mienert, J., Vadakkepuliyambatta, S., Bauguitte, S., Pitt, J., Allen, G., Bower, K. N., O'Shea, S., Gallagher, M. W.,

3105 Percival, C. J., Pyle, J., Cain, M., and Stohl, A.: Constraints on oceanic methane emissions west of Svalbard
3106 from atmospheric in situ measurements and Lagrangian transport modeling, J. Geophys. Res. Atmos.,
3107 121(23), 14188-14200, doi:10.1002/2016jd025590, 2016.

3108 Platt, S. M., Eckhardt, S., Ferré, B., Fisher, R. E., Hermansen, O., Jansson, P., Lowry, D., Nisbet, E. G.,
3109 Pisso, I., Schmidbauer, N., Silyakova, A., Stohl, A., Svendby, T. M., Vadakkepuliyambatta, S., Mienert, J.,
3110 and Lund Myhre, C.: Methane at Svalbard and over the European Arctic Ocean, Atmos. Chem. Phys., 18,
3111 17207–17224, doi:10.5194/acp-18-17207-2018, 2018.

3112 Ponomarev, Evgenii I., Kharuk, Viacheslav I., and Ranson, Kenneth J.:Wildfires Dynamics in Siberian Larch
3113 Forests, Forests, 7(6), 125, 2016.

3114 Popovicheva O., Evangeliou N., Eleftheriadis K., Kalogridis A. C., Sitnikov V. N., Eckhardt S., Stohl A.:
3115 Black carbon sources constrained by observations and modeling in the Russian high Arctic, Environmental
3116 Science Technology, 51(7), 3871-3879, 2017.

3117 Popovicheva, O., Diapouli, E., Makshtas, A., Shonija, N., Manousakas, M., Saraga, D., Uttal, T., and
3118 Eleftheriadis, K.: East Siberian Arctic background and black carbon polluted aerosols at HMO Tiksi, Science
3119 of the Total Environment, 655, 924-938, doi:10.1016/j.scitotenv.2018.11.165, 2019a.

3120 Popovicheva, O. B., Engling, G., Ku, I. T., Timofeev, M. A., and Shonija, N. K.: Aerosol emissions from
3121 long-lasting smoldering of boreal peatlands: chemical composition, markers, and microstructure, Aerosol
3122 and Air Quality Research, 19(3), 484-503, doi:10.4209/aaqr.2018.08.0302, 2019b.

3123 Popovicheva, O. B., Padoan, S., Schnelle- Kreis, J., Nguyen, D. L., Adam, T.W., Kistler, M., Steinkogler, T.,
3124 Kasper-Giebl, A., Zimmermann, R., and Chubarova, N. E.: Spring aerosol in urban atmosphere of megacity:
3125 analytical and statistical assessment for source impacts, Aerosol and Air Quality Research, 20, 702–719,
3126 2020a.

3127 Popovicheva O., Ivanov A., and Vojtisek M.: Functional Factors of Biomass Burning Contribution to Spring
3128 Aerosol Composition in a Megacity: Combined FTIR-PCA Analyses, Atmosphere, 11, 319-339, 2019b.

3129 Popovicheva, O., Volpert, E., Sitnikov, N., Chichaeva, M., and Padoan, S.: Black carbon in spring aerosols
3130 of Moscow urban background, Geography, Environment, Sustainability, 13, 1, 233-243, 2020c

3131 Pozdnyakov D. V., Pettersson L. H., and Korosov A. A.: Exploring the Marine Ecology from Space.
3132 Springer, Switzerland, 2017.

3133 Pozdnyakov, D. V., Kondrik, D.V., Kazakov, E. E., and Chepikova, S.: Environmental conditions favoring
3134 coccolithophore blooms in subarctic and arctic seas: a 20-year satellite and multi-dimensional statistical
3135 study, Proc. SPIE 11150, Remote Sensing of the Ocean, Sea Ice, Coastal Waters, and Large Water Regions,
3136 111501W, 14 October 2019, doi: 10.1117/12.2547868, 2019.

3137 Pozdnyakov D., Kondrik D., and Chepikova S.: Origination of E. huxleyi extraordinary bloom outbursts in
3138 the Bering Sea between the late 1990s and early 2000s, and in 2018-2019: A hypothesis, Fisheries
3139 Oceanography, submitted, 2020.

3140 Preis, Y. I., Simonova, G. V., Voropay, N. N., and Dyukarev, E. A.: Estimation of the influence of
3141 hydrothermal conditions on the carbon isotope composition in Sphagnum mosses of bogs of Western Siberia,
3142 IOP Conf. Series: Earth Environ. Sci., 211, doi:10.1088/1755-1315/211/1/012031, 2018.

3143 Pugac,h S. P., Pipko I. I., Shakhova, N. E., Shirshin, E. A., Perminova, I. V., Gustafsson, O., Bondur, V. G.,
3144 Ruban, A. S., and Semiletov, I. P.: Dissolved organic matter and its optical characteristics in the Laptev and
3145 East Siberian seas: spatial distribution and interannual variability (2003–2011), Ocean Sci., 14, 87–103,
3146 doi:10.5194/os-14-87-2018, 2018.

3147 Pulliainen, J., Aurela, M., Laurila, T., Aalto, T., Takala, M., Salminen, M., Kulmala, M., Barr, A., Heimann,
3148 M., Lindroth, A., Laaksonen, A., Derksen, C., Mäkelä, A., Markkanen, T., Lemmetyinen, J., Susiluoto, J.,
3149 Dengel, S., Mammarella, I., Tuovinen, J.-P., and Vesala, T.: Early snowmelt significantly enhances boreal
3150 springtime carbon uptake, PNAS, 114(42), 11081-11086, doi:10.1073/pnas.1707889114, 2017.

3151 Pulliainen, J., Luojus, K., Derksen, C., Mudryk, L., Lemmetyinen, J., Salminen, M., Ikonen, J., Takala, M.,
3152 Cohen, J., Smolander, T., and Norberg, J.: Patterns and trends of Northern Hemisphere snow mass from
3153 1980 to 2018, Nature 581, 294–298, doi:10.1038/s41586-020-2258-0, 2020.

3154 Pärn, J., Verhoeven, J.T., Butterbach-Bahl, K., Dise, N.B., Ullah, S., Aasa, A., Egorov, S., Espenberg, M.,
3155 Järveoja, J., Jauhiainen, J. and Kasak, K.: Nitrogen-rich organic soils under warm well-drained conditions
3156 are global nitrous oxide emission hotspots, Nat. Commun., 9, 1135, doi:10.1038/s41467-018-03540-1, 2018.

3157 Qi, X. M., Ding, A. J., Nie, W., Petäjä, T., Kerminen, V.-M., Herrmann, E., Xie, Y. N., Zheng, L. F.,
3158 Manninen, H., Aalto, P., Sun, J. N., Xu, Z. N., Chi, X. G., Huang, X., Boy, M., Virkkula, A., Yang, X.-Q.,
3159 Fu, C. B., and Kulmala, M.: Aerosol size distribution and new particle formation in the western Yangtze
3160 River Delta of China: 2 years of measurements at the SORPES station, Atmos. Chem. Phys., 15, 12445–
3161 12464, doi:10.5194/acp-15-12445-2015, 2015.

3162 Rakitin, V. S., Elansky, N. F., Wang, P., Wang, G., Pankratova, N. V., Shtabkin, Y. A., Skorokhod A.I.,
3163 Safronov A.N., Makarova M.V., and Grechko E.I.: Changes in trends of atmospheric composition over urban
3164 and background regions of Eurasia: estimates based on spectroscopic observations, Geography,
3165 Environment, Sustainability, 11(2), 84-96, doi:10.24057/2071-9388-2018-11-2-84-96, 2018.

3166 Rautiainen, K., Parkkinen, T., Lemmetyinen, J., Schwank, M., Wiesmann, A., Ikonen, J., Derksen, C.,
3167 Davydov, S., Davydova, A., Boike, J., Langer, M., Druschg, M., and Pulliainen, J.: SMOS prototype
3168 algorithm for detecting autumn soil freezing, Remote Sensing of Environment, 180, 346-360,
3169 doi:10.1016/j.rse.2016.01.012, 2016.

Rinke, A., Segger, B., Crewell, S., Maturilli, M., Naakka, T., Nygård, T., Vihma, T., Alshawaf, F., Dick, G., Wickert, J., and Keller, J.: Trends of vertically integrated water vapor over the Arctic during 1979-2016: Consistent moistening all over?, J. Climate, 32, 6097–6116, doi:10.1175/JCLI-D-19-0092.1, 2019.

Ripple, W. J., Wolf, C., Newsome, T. M., Galetti, M., Alamgir, M., Crist, E., Mahmoud, M. I., Laurance, W. F., and 15,364 scientist signatories from 184 countries. World scientists' warning to humanity: A second notice, BioScience, 67(12), 1026-1028, 2017.

Rivero-Calle, S., Gnanadesikan, A., Del Castilo, C., Balch, W., and Guikema, S.: Multidecadal increase in North Atlantic coccolithophores and the potential role of rising CO_2, Science, 350 (6267), 1533-1537, doi: 10.1126/science.aaa8026, 2015.

Romanowsky, E., Handorf, D., Jaiser, R., Wohltmann, I., Dorn, W., Ukita, J., Cohen, J., Dethloff, K., and Rex, M.: The role of stratospheric ozone for Arctic-midlatitude linkages, Sci. Rep. 9, 7962, doi:10.1038/s41598-019-43823-1, 2019.

Romanovsky, V. E., and Osterkamp, T. E.: Effects of unfrozen water on heat and mass transport processes in the active layer and permafrost, Permafrost Periglac. Process, 11, 219–39, 2000.

Roshydromet & GGO (2019): The State of Atmospheric Pollution in Cities on the Territory of Russia for 2018. Yearbook. Federal Service on Hydrometeorology and Monitoring Environment, Roshydromet & A.I. Voeikov Main Geophisical Observatory, ISBN 978-5-9500883-8-4, St.Petersburg, 250 p., In Russian (http://voeikovmgo.ru/images/stories/publications/2019/ejegodnik_zagr_atm_2018+.pdf)

Rost, B., and Riebesell, U.: Coccolithophores and the biological pump: responses to environmental changes, in: Coccolithophores, from molecular processes to global impact, edited by: Thierstein, H. R., Young, J. R., 99–125, Springer, Heidelberg, Germany, 2004.

Ryazanova, A., and Voropay, N. N.: Droughts and Excessive Moisture Events in Southern Siberia in the Late XXth - Early XXIst Centuries, IOP Conf. Ser.: Earth Environ. Sci., 96, 012015, 2017.

Räisänen, J.: Effect of atmospheric circulation on recent temperature changes in Finland, Clim. Dyn., 53, 5675–5687, doi:10.1007/s00382-019-04890-2, 2019.

Räisänen, J.: Effect of atmospheric circulation on surface air temperature trends in years 1979–2018. Clim. Dyn., 56, 2303–2320, doi:10.1007/s00382-020-05590-y, 2021.

Saarela, T., Rissanen, A. J., Ojala, A. et al.: CH_4 oxidation in a boreal lake during the development of hypolimnetic hypoxia, Aquat Sci, 82, 19, /doi.org/10.1007/s00027-019-0690-8, 2020.

Salmon, Y., Lintunen, A., Dayet, A., Chan, T., Dewar, R., Vesala, T. and Hölttä, T.: Leaf carbon and water status control stomatal and non-stomatal limitations of photosynthesis in trees, New Phytologist 226, 690-703. doi: 10.1111/nph.16436, 2020.

3203 Santalahti, M., Sun, H., Sietiö, O.M., Köster, K., Berninger, F., Laurila, T., Pumpanen, J., and Heinonsalo,

3204 J.: Reindeer grazing alter soil fungal community structure and litter decomposition related enzyme activities

3205 in boreal coniferous forests in Finnish Lapland, App. Soil Ecol., 132, 74-82,

3206 doi:10.1016/j.apsoil.2018.08.013, 2018.

3207 Schallhart, S., Rantala, P., Kajos, M. K., Aalto, J., Mammarella, I., Ruuskanen, T. M., and Kulmala, M.:

3208 Temporal variation of VOC fluxes measured with PTR-TOF above a boreal forest, Atmospheric Chemistry

3209 and Physics, 18(2), 815-832. doi:10.5194/acp-18-815-2018, 2018.

3210 Schmale, J., Arnold, S. R., Law, K. S., Thorp, T., Anenberg, S., Simpson, W. R., Mao, J. and Pratt, K. A.:

3211 Local Arctic air pollution: a neglected but serious problem, Earths Future, 6(10), 1385-1412,

3212 doi:10.1029/2018ef000952, 2018a.

3213 Schmale, J., Henning, S., Decesari, S., Henzing, B., Keskinen, H., Sellegri, K., Ovadnevaite, J., Pöhlker, M.

3214 L., Brito, J., Bougiatioti, A., Kristensson, A., Kalivitis, N., Stavroulas, I., Carbone, S., Jefferson, A., Park,

3215 M., Schlag, P., Iwamoto, Y., Aalto, P., Äijälä, M., Bukowiecki, N., Ehn, M., Frank, G., Fröhlich, R.,

3216 Frumau, A., Herrmann, E., Herrmann, H., Holzinger, R., Kos, G., Kulmala, M., Mihalopoulos, N., Nenes,

3217 A., O'Dowd, C., Petäjä, T., Picard, D., Pöhlker, C., Pöschl, U., Poulain, L., Prévôt, A. S. H., Swietlicki, E.,

3218 Andreae, M. O., Artaxo, P., Wiedensohler, A., Ogren, J., Matsuki, A., Yum, S. S., Stratmann, F.,

3219 Baltensperger, U., and Gysel, M.: Long-term cloud condensation nuclei number concentration, particle

3220 number size distribution and chemical composition measurements at regionally representative observatories,

3221 Atmos. Chem. Phys., 18, 2853–2881, doi:10.5194/acp-18-2853-2018, 2018b.

3222 Schmeisser, L., Backman, J., Ogren, J. A., Andrews, E., Asmi, E., Starkweather, S., Uttal, T., Fiebig, M.,

3223 Sharma, S., Eleftheriadis, K., Vratolis, S., Bergin, M., Tunved, P., and Jefferson, A.: Seasonality of aerosol

3224 optical properties in the Arctic, Atmos. Chem. Phys., 18, 11599–11622, doi:10.5194/acp-18-11599-2018,

3225 2018.

3226 Schuur, E. A. G., Bockheim, J., Canadell, J. G., Euskirchen, E., Field, C. B., Goryachkin, S. V., Hagemann,

3227 S., Kuhry, P., Lafleur, P.M., Lee, H., Mazhitova, G., Nelson, F. E., Rinke, A.,. Romanovsky, V. E.,

3228 Shiklomanov, N., Tarnocai, C., Venevsky, S., Vogel, J. G., and Zimov, S. A.: Vulnerability of permafrost

3229 carbon to climate change: implications for the global carbon cycle, BioScience, 58(8), 701–714,

3230 doi:10.1641/B580807, 2008.

3231 Schuur, E. A. G., McGuire, A. D., Romanovsky, V., Schädel, C., and Mack, M.: Chapter 11: Arctic and

3232 boreal carbon, in: Second State of the Carbon Cycle Report (SOCCR2): A Sustained Assessment Report,

3233 edited by: Cavallaro, N., Shrestha, G., Birdsey, R., Mayes, M. A., Najjar, R. G., Reed, S. C., Romero-

3234 Lankao, P., and Zhu, Z., U.S. Global Change Research Program, Washington, DC, USA, 428-468,

3235 doi:10.7930/SOCCR2.2018.Ch11, 2018.

3236 Scott, C. E., Monks, S. A., Spracklen, D. V., Arnold, S. R., Forster, P. M., Rap, A., Äijälä, M., Artaxo, P.,

3237 Carslaw, K. S., Chipperfield, M. P., Ehn, M., Gilardoni, S., Heikkinen, L., Kulmala, M., Petäjä, T.,

Reddington, C. L. S., Rizzo, L. V., Swietlicki, E., Vignati, E., and Wilson, C.: Impact on short-lived climate forcers increases projected warming due to deforestation, Nat. Commun., 9, 9, doi:10.1038/s41467-017-02412-4, 2018.

Shakhova, N., Semiletov, I., and Belcheva, N.: The great Siberian rivers as a source of methane on the Russian Arctic shelf, Dokl. Earth Sci., 415, 734–736, doi: 10.1134/S1028334X07050169, 2007.

Shalina, E. V., and Sandven, S.: Snow depth on Arctic sea ice from historical in situ data, Cryosphere, 12(6), 1867-1886, doi:10.5194/tc-12-1867-2018, 2018.

Shen, Y., Virkkula, A., Ding, A., Wang, J., Chi, X., Nie, W., Qi, X., Huang, X., Liu, Q., Zheng, L., Xu, Z., Petäjä, T., Aalto, P. P., Fu, C., and Kulmala, M.: Aerosol optical properties at SORPES in Nanjing, east China, Atmos. Chem. Phys., 18, 5265–5292, doi: 10.5194/acp-18-5265-2018, 2018.

Shen, Y., Virkkula, A., Ding, A., Luoma, K., Keskinen, H., Aalto, P. P., Chi, X., Qi, X., Nie, W., Huang, X., Petäjä, T., Kulmala, M., and Kerminen, V.-M.: Estimating cloud condensation nuclei number concentrations using aerosol optical properties: role of particle number size distribution and parameterization, Atmos. Chem. Phys., 19, 15483–15502, doi:10.5194/acp-19-15483-2019, 2019.

Shestakova, T. A., Gutierrez, E., Valeriano, C., Lapshina, E., and Voltas, J.: Recent loss of sensitivity to summer temperature constrains tree growth synchrony among boreal Eurasian forests, Agr. Forest Meteorol., 268, 318-330, doi:10.1016/j.agrformet.2019.01.039, 2019.

Shevchenko, V. P., Starodymova, D. P., Vinogradova, A. A., Lisitzin, A. P., Makarov, V. I., Popova, S. A., Sivonen, V. V., and Sivonen, V. P.: Elemental and organic carbon in atmospheric aerosols over the northwestern coast of Kandalaksha Bay of the White Sea, Dokl. Earth Sci., 461(1), 242-246, doi:10.1134/s1028334x1503006x, 2015.

Shevchenko, V. P., Maslov, A. V., and Stein, R.: Distribution of some rare and trace elements in ice-rafted sediments in the Yermak Plateau area, the Arctic Ocean, Oceanol., 57(6), 855-863, doi:10.1134/s0001437017060157, 2017a.

Shevchenko, V. P., Pokrovsky, O. S., Vorobyev, S. N., Krickov, I. V., Manasypov, R. M., Politova, N. V., Kopysov, S. G., Dara, O. M., Auda, Y., Shirokova, L. S., Kolesnichenko, L. G., Zemtsov, V. A., and Kirpotin, S. N.: Impact of snow deposition on major and trace element concentrations and elementary fluxes in surface waters of the Western Siberian Lowland across a 1700 km latitudinal gradient, Hydrol. Earth Syst. Sci., 21, 5725–5746, doi:10.5194/hess-21-5725-2017, 2017b.

Shevchenko, V. P., Kopeikin, V. M., Novigatsky, A. N., and Malafeev, G. V.: Black carbon in the atmospheric boundary layer over the North Atlantic and the Russian Arctic seas in June–September 2017, Oceanol., 59(5), doi:10.1134/S0001437019050199, 692–696, 2019.

3270 Shevnina, E., Kourzeneva, E., Kovalenko, V., and Vihma, T.: Assessment of extreme flood events in a
3271 changing climate for a long-term planning of socio-economic infrastructure in the Russian Arctic, Hydrol.
3272 Earth Syst. Sci., 21(5), 2559-2578, doi:10.5194/hess-21-2559-2017, 2017.

3273 Shevnina, E., Silaev, A., and Vihma, T.: Probabilistic projections of annual runoff and potential hydropower
3274 production in Finland, Universal Journal of Geoscience, 7(2), 43-55, doi:10.13189/ujg.2019.070201, 2019.

3275 Shiklomanov, A.I., and Lammers, R.B.: Record Russian river discharge in 2007 and the limits of analysis,
3276 Environ. Res. Lett., 4, doi: 10.1088/1748-9326/4/4/045015, 2009.

3277 Shinkareva G. L., Lychagin M. Y., Tarasov M. K., Pietroń J., Chichaeva M. A., and Chalov S. R.:
3278 Biogeochemical specialization of macrophytes and their role as a biofilter in the Selenga delta, Geography,
3279 Environment, Sustainability,12(3), 240-263, 2019.

3280 Silkin, V. A., Pautova, L., Giordano, M., Chasovnikov, V., Vostokov, S., Podymov, O., Parkhomova, S., and
3281 Moskalenko, L.: Drivers of phytoplankton blooms in the northeastern Black Sea, Mar. Pollution Bull., 138,
3282 274-284, doi:10.1016/j.marpolbul.2018.11.042, 2018.

3283 Sizov O. S., and Lobotrosova S. A.: Features of revegetation of drift sand sites in the northern taiga subzone
3284 of Western Siberia. Earth Cryosphere, (3), 3–13, doi:10.21782/kz1560-7496-2016-3(3-13), 2016.

3285 Skorokhod, A. I., Berezina, E. V., Moiseenko, K. B., Elansky, N. F., and Belikov, I. B.: Benzene and toluene
3286 in the surface air of northern Eurasia from TROICA-12 campaign along the Trans-Siberian Railway, Atmos.
3287 Chem. Phys., 17(8), 5501-5514, doi:10.5194/acp-17-5501-2017, 2017.

3288 Slukovskaya, M. V., Vasenev, V. I., Ivashchenko, K. V., Morev, D. V., Drogobuzhskaya, S. V., Ivanova, L.
3289 A., and Kremenetskaya, I. P.: Technosols on mining wastes in the subarctic: Efficiency of remediation under
3290 Cu-Ni atmospheric pollution, Int. Soil Water Conserv. Res., 7(3), 297-307, doi:10.1016/j.iswcr.2019.04.002,
3291 2019.

3292 Smith, L.: The new north: The world in 2050, Profile Books, London, UK, 2011.

3293 Song, S., Li, C., Shi , X., Zhao, S., Li, Z., Bai, Y., Cao, X., Wang, Q., Huotari, J., Tulonen, T., Uusheimo, S.,
3294 Leppäranta, M., and Arvola, L.: Under-ice metabolism in a shallow lake (Wuliangsuhai) in Inner Mongolia,
3295 in cold and arid climate zone, Freshw. Biol., 1–11, 2019.

3296 Spengler, T., Renfrew, I. A., Terpstra, A., Tjernström, M., Screen, J., Brooks, I. M., Andrew Carleton, A.,
3297 Chechin, D., Chen, L., Doyle, J., Esau, I., Hezel, P. J., Jung, T., Kohyama, T., Lüpkes, C., McCusker, C. E.,
3298 Nygård, T., Sergeev, D., Shupe, M. D., Sodemann, H., and Vihma, T.: High-latitude dynamics of
3299 atmosphere–ice–ocean interactions, Bull. Am. Meteorol. Soc., 97(9), ES179-ES182, doi:10.1175/bams-d-15-
3300 00302.1, 2016.

3301 Sporre, M. K., Blichner, S. M., Karset, I. H. H., Makkonen, R., and Berntsen, T. K.: BVOC–aerosol–climate
3302 feedbacks investigated using NorESM, Atmos. Chem. Phys., 19, 4763–4782, doi:10.5194/acp-19-4763-
3303 2019, 2019.

3304 Starodymova, D. P., Shevchenko, V. P., Sivonen, V. P., and Sivonen, V. V.: Material and elemental

3305 composition of surface aerosols on the north-western coast of the Kandalaksha Bay of the White Sea, Atmos.

3306 Oceanic Opt., 29(6), 507-511, doi:10.1134/s1024856016060154, 2016.

3307 Sun, H., Santalahti, M., Pumpanen, J., Koster, K., Berninger, F., Raffaello, T., Asiegbu, F. O., and

3308 Heinonsalo, J.: Bacterial community structure and function shift across a northern boreal forest fire

3309 chronosequence, Scientific Rep., 6, 12, doi:10.1038/srep32411, 2016.

3310 Sun, Y., Frankenberg C., Wood JD, Schimel DS., Jung, M., Guanter L., Drewry, DT., Verma, M., Porcar-

3311 Castell, A., Griffis, TJ., Gu, L., Magney, S., Köhler P., Evans B., and Yuen, K.: OCO-2 advances

3312 photosynthesis observation from space via solar-induced chlorophyll fluorescence, Science 358, 189,

3313 doi:10.1126/science.aam5747, 2017.

3314 Suomi, I.,, Gryning, S-E. , O'Connor E.J., and Vihma, T.:, Methodology for obtaining wind gusts

3315 using Doppler lidar, Quarterly Journal of the Royal Meteorological Society, 143, 2061-2072,

3316 doi.org/10.1002/qj.3059, 2016.

3317 Svensson, J., Virkkula, A., Meinander, O., Kivekäs, N., Hannula, H.-R., Järvinen, O., Peltoniemi, J.I.,

3318 Gritsevich, M., Heikkilä, A., Kontu, A., Neitola, K., Brus, D., DagssonWaldhauserova, P., Anttila, K.,

3319 Vehkamäki, M., Hienola, A., de Leeuw, G., and Lihavainen, H.: Soot-doped natural snow and its albedo —

3320 results from field experiments, Boreal Environment Research, 21, 481-503, 2016.

3321 Svensson, J., Ström, J., Kivekäs, N., Dkhar, N. B., Tayal, S., Sharma, V. P., Jutila, A., Backman, J.,

3322 Virkkula, A., Ruppel, M., Hyvärinen, A., Kontu, A., Hannula, H.-R., Leppäranta, M., Hooda, R. K., Korhola,

3323 A., Asmi, E., and Lihavainen, H.: Light absorption of dust and elemental carbon in snow in the Indian

3324 Himalayas and the Finnish Arctic, Atmos. Meas. Tech., 11, 1403-1416, doi:10.5194/amt-11-1403-2018,

3325 2018.

3326 Svensson, J., Ström, J., and Virkkula, A.: Multiple-scattering correction factor of quartz filters and the effect

3327 of filtering particles mixed in water: implications for analyses of light absorption in snow samples, Atmos.

3328 Meas. Tech., 12, 5913-5925, doi:10.5194/amt-12-5913-2019, 2019.

3329 Taylor, K. E., Stouffer, R. J., and Meehl, G. A.: An overview of CMIP5 and the experiment design, Bull.

3330 Am. Meteorol. Soc., 93, 485-498, doi: 10.1175/BAMS-D-11-00094.1, 2012.

3331 Taylor., A., Brownlee., C., and Wheeler., G.: Coccolithophore cell biology: chalking up progress, Ann. Rev.

3332 Mar. Sci., 9, 283-310, doi:10.1146/annurev-marine-122414-034032, 2017.

3333 Terentieva, I. E., Glagolev, M. V., Lapshina, E. D., Sabrekov, A. F., and Maksyutov, S.: Mapping of West

3334 Siberian taiga wetland complexes using Landsat imagery: implications for methane emissions,

3335 Biogeosciences, 13, 4615–4626, doi:10.5194/bg-13-4615-2016, 2016.

3336   Thompson, R. L., Sasakawa, M., Machida, T., Aalto, T., Worthy, D., Lavric, J. V., Lund Myhre, C., and
3337   Stohl, A.: Methane fluxes in the high northern latitudes for 2005–2013 estimated using a Bayesian
3338   atmospheric inversion, Atmos. Chem. Phys., 17, 3553–3572, doi:10.5194/acp-17-3553-2017, 2017.

3339   Thonat, T., Saunois, M., Bousquet, P., Pison, I., Tan, Z., Zhuang, Q., Crill, P. M., Thornton, B. F., Bastviken,
3340   D., Dlugokencky, E. J., Zimov, N., Laurila, T., Hatakka, J., Hermansen, O., and Worthy, D. E. J.:
3341   Detectability of Arctic methane sources at six sites performing continuous atmospheric measurements,
3342   Atmos. Chem. Phys., 17, 8371–8394, doi:10.5194/acp-17-8371-2017, 2017.

3343   Thorslund, J., Jarsjo, J., Wallstedt, T., Morth, C. M., Lychagin, M. Y., and Chalov, S. R.: Speciation and
3344   hydrological transport of metals in non-acidic river systems of the Lake Baikal basin: Field data and model
3345   predictions, Reg. Environ. Chang., 17(7), 2007-2021, doi:10.1007/s10113-016-0982-7, 2017.

3346   Tian, Z. X., Cheng, B., Zhao, J. C., Vihma, T., Zhang, W. L., Li, Z. J., and Zhang, Z. H.: Observed and
3347   modelled snow and ice thickness in the Arctic Ocean with CHINARE buoy data, Acta Oceanologica Sinica,
3348   36(8), 66-75, doi:10.1007/s13131-017-1020-4, 2017.

3349   Tillman, H., Yang, J. and Nielsson, E.: The Polar Silk Road: China's New Frontier of International
3350   Cooperation, China Quarterly of International Strategic Studies, 4. 10.1142/S2377740018500215, 2018.

3351   Timokhina, A. V., Prokushkin, A. S., Onuchin, A. A., Panov, A. V., Kofman, G. B., and Heimann, M.:
3352   Variability of ground CO_2 concentration in the middle taiga subzone of the Yenisei region of Siberia, Russ.
3353   J. Ecol., 46, 143-151, doi:10.1134/s1067413615020125, 2015a.

3354   Timokhina, A. V., Prokushkin, A. S., Onuchin, A. A., Panov, A. V., Kofman, G. B., Verkhovets, S. V., and
3355   Heimann, M., Long-term trend in CO_2 concentration in the surface atmosphere over Central Siberia, Russ.
3356   Meteorol. Hydrol., 40, 186-190, 2015b.

3357   Tsuruta, A., Aalto, T., Backman, L., Hakkarainen, J., … and Peters, W.: Global methane emission estimates
3358   for 2000–2012 from CarbonTracker Europe-CH4 v1.0. Geosci. Model Dev., 10, 1261–1289, 2017.

3359   Tuovinen, J-P., Aurela, M., Hatakka, J., Räsänen, A., … Laurila, T.: Interpreting eddy covariance data from
3360   heterogeneous Siberian tundra: land-cover-specific methane fluxes and spatial representativeness,
3361   Biogeosciences, 16, 255–274, 2019.

3362   Uotila, P., Vihma, T., and Haapala, J.: Atmospheric and oceanic conditions and the extremely low Bothnian
3363   Bay sea ice extent in 2014/2015, 42, 7740-7749, Geophysical Research and Letters, 2015.

3364   Uotila, P., Iovino, D., Vancoppenolle, M., Lensu, M., and Rousset, C., Comparing sea ice, hydrography and
3365   circulation between NEMO3.6 LIM3 and LIM2, Geosci. Model Dev., 10, 1009–1031, doi:10.5194/gmd-10-
3366   1009-2017, 2017.

3367   Uotila, P., Goosse, H., Haines, K., Chevallier, M., Barthélemy, A., Bricaud, C., Carton, J., Fučkar, N.,
3368   Garric, G., Iovino, D., Kauker, F., Korhonen, M., Lien, V. S., Marnela, M., Massonnet, F., Mignac, D.,

3369   Peterson, K. A., Sadikni, R., Shi, L., Tietsche, S., Toyoda, T., Xie, J., and Zhang, A.: An assessment of ten

3370   ocean reanalyses in the polar regions, Clim Dyn 52, 1613–1650, doi:10.1007/s00382-018-4242-z, 2019.

3371   Uttal, T., Starkweather, S., Drummond, J. R., Vihma, T., Makshtas, A. P., Darby, L. S., Burkhart, J. F., Cox,

3372   C. J., Schmeisser, L. N., Haiden, T., Maturilli, M., Shupe, M. D., De Boer, G., Saha, A., Grachev, A. A.,

3373   Crepinsek, S. M., Bruhwiler, L., Goodison, B., McArthur, B., Walden, V. P., Dlugokencky, E. J., P. Persson,

3374   O., Lesins, G., Laurila, T., Ogren, J. A., Stone, R., Long, C. N., Sharma, S., Massling, A., Turner, D. D.,

3375   Stanitski, D. M., Asmi, E., Aurela, M., Skov, H., Eleftheriadis, K., Virkkula, A., Platt, A., Førland, E. J.,

3376   Iijima, Y., Nielsen, I. E., Bergin, M. H., Candlish, L., Zimov, N. S., Zimov, S. A., O'Neill, N. T., Fogal, P.

3377   F., Kivi, R., Konopleva-Akish, E. A., Verlinde, J., Kustov, V. Y., Vasel, B., Ivakhov, V. M., Viisanen Y.,

3378   and Intrieri, J. M.: International Arctic Systems for Observing the Atmosphere: An International Polar Year

3379   Legacy Consortium, Bull. Amer. Meteor. Soc., 97, 1033–1056, doi:10.1175/BAMS-D-14-00145.1, 2016.

3380   Vanhatalo, A., Ghirardo, A., Juurola, E., Schnitzler, J.-P., Zimmer, I., Hellén, H., Hakola, H., and Bäck, J.:

3381   Long-term dynamics of monoterpene synthase activities, monoterpene storage pools and emissions in boreal

3382   Scots pine, Biogeosciences, 15, 5047–5060, doi:10.5194/bg-15-5047-2018, 2018.

3383   Varentsov, M., Konstantinov, P., Baklanov, A., Esau, I., Miles, V., and Davy, R.: Anthropogenic and natural

3384   drivers of a strong winter urban heat island in a typical Arctic city, Atmos. Chem. Phys., 18(23), 17573-

3385   17587, doi:10.5194/acp-18-17573-2018, 2018a.

3386   Varentsov, M., Wouters, H., Platonov, V., and Konstantinov, P.: Megacity-induced mesoclimatic effects in

3387   the lower atmosphere: a modeling study for multiple summers over Moscow, Russia, Atmos., 9(2), 24,

3388   doi:10.3390/atmos9020050, 2018b.

3389   Vasileva, A., Moiseenko, K., Skorokhod, A., Belikov, I., Kopeikin, V., and Lavrova, O.: Emission ratios of

3390   trace gases and particles for Siberian forest fires on the basis of mobile ground observations, Atmos. Chem.

3391   Phys., 17(20), 12303-12325, doi:10.5194/acp-17-12303-2017, 2017.

3392   Vestenius, M., Hellén, H., Levula, J., Kuronen, P., Helminen, K. J., Nieminen, T., Kulmala, M., and Hakola,

3393   H.: Acidic reaction products of monoterpenes and sesquiterpenes in atmospheric fine particles in a boreal

3394   forest, Atmos. Chem. Phys., 14, 7883–7893, doi:10.5194/acp-14-7883-2014, 2014.

3395   Vihma, T., Uotila, P., Sandven, S., Pozdnyakov, D., Makshtas, A., Pelyasov, A., Pirazzini, R., Danielsen, F.,

3396   Chalov, S., Lappalainen, H. K., Ivanov, V., Frolov, I., Albin, A., Cheng, B., Dobrolyubov, S., Arkhipkin, V.,

3397   Myslenkov, S., Petäjä, T., and Kulmala, M.: Towards an advanced observation system for the marine Arctic

3398   in the framework of the Pan-Eurasian Experiment (PEEX), Atmos. Chem. Phys., 19, 1941-1970,

3399   doi:10.5194/acp-19-1941-2019, 2019.

3400   Vihma, T., Graversen, R., Chen, L., Dörthe H., Skific, N., Francis, J.A., Tyrrell, N., Hall, R., Hanna, E.,

3401   Uotila, P., Dethloff, K., Karpechko, A. Y., Björnsson, H. and Overland, J. E.: Effects of the tropospheric

3402   large-scale circulation on European winter temperatures during the period of amplified Arctic warming, Int J

3403   Climatol., 40, 509– 529, doi:10.1002/joc.6225, 2020

3404 Virkkula, A., Chi, X., Ding, A., Shen, Y., Nie, W., Qi, X., Zheng, L., Huang, X., Xie, Y., Wang, J., Petäjä,
3405 T., and Kulmala, M.: On the interpretation of the loading correction of the aethalometer, Atmos. Meas.
3406 Tech., 8, 4415-4427, doi:10.5194/amt-8-4415-2015, 2015.

3407 Voigt, C., Marushchak, M.E., Lamprecht, R.E., et al.: Nitrous oxide emissions from thawing permafrost,
3408 PNAS May 2017, 201702902; DOI: 10.1073/pnas.1702902114.

3409 Voigt, C., Lamprecht, R. E., Marushchak, M. E., Lind, S. E., Novakovskiy, A., Aurela, M., Martikainen, P. J.
3410 and Biasi, C.: Warming of subarctic tundra increases emissions of all three important greenhouse gases -
3411 carbon dioxide, methane, and nitrous oxide, Glob. Change Biol., 23(8), 3121-3138, doi:10.1111/gcb.13563,
3412 2016.

3413 Voropay, N. N., Kichigina, N. V.: Long-term changes in the hydroclimatic characteristics in the Baikal
3414 region, IOP Conf. Ser.: Earth Environ. Sci., 107, 012042, 2018.

3415 Voropay N.N., Ryazanova A.A., Dyukarev E.A. Variability of vegetation index NDVI during periods of
3416 drought in the Tomsk Region, IOP Conf. Series: Earth Environ. Sci., 381, 012096, doi:10.1088/1755-
3417 1315/381/1/012096, 2019.

3418 Walker, X. J., Baltzer, J. L., Cumming, S. G., Day, N. J., Ebert, C., Goetz, S., Johnstone, J. F., Potter, S.,
3419 Rogers, B. M., Schuur, E. A. G., Turetsky, M. R., and Mack, M. C., Increasing wildfires threaten historic
3420 carbon sink of boreal forest soils, Nature, 572, 520-523, doi:10.1038/s41586-019-1474-y, 2019.

3421 Walsh, M. G., de Smalen, A. W., and Mor, S. M.: Climatic influence on anthrax suitability in warming
3422 northern latitudes, Sci Rep, 8(1), 9269, doi:10.1038/s41598-018-27604-w, 2018.

3423 van Vuuren, D. P., Edmonds, J., Kainuma, M., Riahi, K., Thomson, A., Hibbard, K., Hurtt, G. C., Kram, T.,
3424 Krey, V., Lamarque, J. F., Masui, T., Meinshausen, M., Nakicenovic, N., Smith, S. J., and Rose, S. K.: The
3425 representative concentration pathways: an overview, Clim. Chang., 109, 5-31, doi:10.1007/s10584-011-
3426 0148-z, 2011.

3427 Wang, J., Ge, X., Chen, Y., Shen, Y., Zhang, Q., Sun, Y., Xu, J., Ge, S., Yu, H., and Chen, M.: Highly time-
3428 resolved urban aerosol characteristics during springtime in Yangtze River Delta, China: insights from soot
3429 particle aerosol mass spectrometry, Atmos. Chem. Phys., 16, 9109–9127, doi:10.5194/acp-16-9109-2016,
3430 2016.

3431 Wang, J., Zhao, B., Wang, S., Yang, F., Xing, J., Morawska, L., Ding, A., Kulmala, M., Kerminen, V.-M.,
3432 Kujansuu, J., Wang, Z., Ding, D., Zhang, X., Wang, H., Tian, M., Petäjä, T., Jiang, J., and Hao J.: Particulate
3433 matter pollution over China and the effects of control policies, Sci. Total Environ., 584-585, 426-447, 2017a.

3434 Wang, Z. B., Wu, Z. J., Yue, D. L., Shang, D. J., Guo, S., Sun, J. Y., Ding, A. J., Wang, L., Jiang, J. K., Guo,
3435 H., Gao, J., Cheung, H. C., Morawska, L., Keywood, M., and Hu, M.: New particle formation in China:
3436 Current knowledge and further directions, Sci. Total Environ., 577, 258–266,
3437 doi:10.1016/j.scitotenv.2016.10.177, 2017b.

Wang, Z., Huang, X., and Ding, A.: Dome effect of black carbon and its key influencing factors, Atmos. Chem. Phys., 18, 2821-2834, 2018b.

Wang, P. C., Elansky, N. F., Timofeev, Y. M., Wang, G. C., Golitsyn, G. S., Makarova, M. V., Rakitin, V. S., Shtabkin, Yu., Skorokhod, A. I., Grechko, E. I., Fokeeva, E. V., Safronov, A. N., Ran, L., and Wang, T.: Long-term trends of carbon monoxide total columnar amount in urban areas and background regions: ground- and satellite-based spectroscopic measurements, Adv. Atmos. Sci., 35(7), 785-795, doi:10.1007/s00376-017-6327-8, 2018a.

Wang, Y., Wang, Y., Wang, L., Petäjä, T., Zha, Q., Gong, C., Li, S., Pan, Y., Hu, B., Xin, J., and Kulmala, M.: Increased inorganic aerosol fraction contributes to air pollution and haze in China, Atmos. Chem. Phys., 19, 5881–5888, doi:10.5194/acp-19-5881-2019, 2019.

Wang, Y.H., Yu, M., Wang, Y., Tang, G., Song, T., Zhou, P., Liu, Z., Hu, B., Ji, D.S., Wang, L., Zhu, X., Yan, C., Ehn, M., Gao, W.K., Pan, Y.P., Xin, J.Y., Sung, Y., Kerminen, V.-M., Kulmala, M. and Petäjä, T.: Rapid formation of intense haze episode via aerosol-boundary layer feedback in Beijing, Atmos. Chem. Phys., 10, 45-53, 2020.

Wei, L. X., Deng, X. H., Cheng, B., Vihma, T., Hannula, H. R., Qin, T., and Pulliainen, J.: The impact of meteorological conditions on snow and ice thickness in an Arctic lake, Tellus A: Dyn. Meteorol. Oceanogr., 68, 12, doi:10.3402/tellusa.v68.31590, 2016.

Wickström, S., Jonassen, M., Vihma, T., and Uotila, P.: Trends in cyclones in the high latitude North Atlantic during 1979-2016, Q. J. R. Meteorol. Soc., 146, 762– 779, doi:10.1002/qj.3707, 2020.

Wiedensohler, A., Ma, N., Birmili, W., Heintzenberg, J., Ditas, F., Andreae, M. O., and Panov, A.: Infrequent new particle formation over the remote boreal forest of Siberia, Atmos. Environ., 200, 167-169, doi:10.1016/j.atmosenv.2018.12.013, 2019.

Wild, B., Andersson, A., Bröder, L., Vonk, J., Hugelius, G., McClelland, J.W., Song, W., Raymond, P.A., and Gustafsson, Ö.: Rivers across the Siberian Arctic unearth the patterns of carbon release from thawing permafrost Proceedings of the National Academy of Sciences, 116 (21) 10280-10285., 2019.

Williams, P. J., and Smith, M. W.: The Frozen Earth: Fundamentals of Geocryology, Cambridge University Press, Cambridge, UK, 1989.

WMO, 2019 Guidance on Integrated Urban Hydrometeorological, Climate and Environmental Services. Volume 1: Concept and Methodology, Grimmond, S., Bouchet, S., Molina, L., Baklanov, A., Joe, P. et al., WMO-No. 1234, https://library.wmo.int/doc_num.php?explnum_id=9903, 2019.

Wolf-Grosse, T., Esau, I., and Reuder, J.: The large-scale circulation during air quality hazards in Bergen, Norway, Tellus A: Dyn. Meteorol. Oceanogr., 69, 16, doi:10.1080/16000870.2017.1406265, 2017a.

3470 Wolf-Grosse, T., Esau, I., and Reuder, J.: Sensitivity of local air quality to the interplay between small- and

3471 large-scale circulations: a large-eddy simulation study, Atmos. Chem. Phys., 17(11), 7261-7276,

3472 doi:10.5194/acp-17-7261-2017, 2017b.

3473 Xausa, F., Paasonen, P., Makkonen, R., Arshinov, M., Ding, A., Denier Van Der Gon, H., Kerminen, V.-M.,

3474 and Kulmala, M.: Advancing global aerosol simulations with size-segregated anthropogenic particle number

3475 emissions, Atmos. Chem. Phys., 18, 10039–10054, doi:10.5194/acp-18-10039-2018, 2018.

3476 Xiao., S., Wang, M. Y., Yao, L., Zhou, B., Yang, X., Chen, J. M., Wang, D. F., Fu, Q. Y., Worsnop, D. R.

3477 and Wang, L.: Strong atmospheric new particle formation in winter in urban Shanghai, China, Atmos. Chem.

3478 Phys., 15, 1769-1781, 2015.

3479 Xie, Y. N., Ding, A. J., Nie, W., Mao, H. T., Qi, X. M., Huang, X., Xu, Z., Kerminen, V. K., Petäjä, T., Chi,

3480 X., Virkkula, A., Boy, M., Xue, L., Guo, J., Sun, J., Yang, X., Kulmala, M., and Fu, C. B.: Enhanced sulfate

3481 formation by nitrogen dioxide: Implications from in situ observations at the SORPES station, J Geophys.

3482 Res.: Atmos., 120(24), 12679-12694, doi:10.1002/2015jd023607, 2015.

3483 Yan, C., Yin, R., Lu, Y., Dada, L., Yang, D., Fu, Y., Kontkanen, J., Deng, C., Garmash, O., Ruan, J.,

3484 Baalbaki, R., Schervish, M., Cai, R., Bloss, M., Chan, T., Chen, T., Chen, Q., Chen, X., Chen, Y., Chu, B.,

3485 Dällenbach, K., Foreback, B., He, X., Heikkinen, L., Jokinen, T., Junninen, H., Kangasluoma, J., Kokkonen,

3486 T., Kurppa, M., Lehtipalo, K., Li, H., Li, H., Li, X., Liu, Y. Ma, Q., Paasonen, P., Rantala, P., Pileci, R. E.,

3487 Rusanen, A., Sarnela, N., Simonen, P., Wang, S., Wang , W., Wang, Y. Xue, M., Yang, G., Yao, L., Zhou,

3488 Y., Kujansuu, J., Petäjä, T., Nie, W., Ma, N., Ge, M., He, H., Donahue, N. M.,Worsnop, D. R., Kerminen,

3489 V.-M., Wang, L., Liu, Y., Zheng, J., Kulmala, M., Jiang, J. and Bianchi, F. (2021) The synergistic role of

3490 sulfuric acid, bases, and oxidized organics governing new-particle formation in Beijing. *Geophys. Res. Lett.*

3491 (in press).

3492 Yang, F., Li, C., Leppäranta, M., Shi, X., Zhao, S. and Zhang, C.: Notable increases in nutrient

3493 concentrations in a shallow lake during seasonal ice growth, Water Sci. Technol., 74(12), 2773–2883, 2016.

3494 Yang, Y., Leppäranta, M. J., Ki, Z., Cheng, B., Zhai, M., and Demchev, D.: Model simulations of the annual

3495 cycle of the landfast ice thickness in the East Siberian Sea, Advances in Polar Sciences, 26(2), 168-178,

3496 doi:10.13679/j.advps.2015.2.00168, 2015.

3497 Yao, L., Garmash, O., Bianchi, F., Zheng, J., Yan, C., Kontkanen, J., Junninen, H., Mazon, S.B., Ehn, M.,

3498 Paasonen, P., Sipilä, M., Wang, M.Y., Wang, X.K., Xiao, S., Chen, H.F., Lu, Y.Q., Zhang, B.W., Wang,

3499 D.F., Fu, Q.Y., Geng, F.H., Li, L., Wang, H.L., Qiao, L.P., Yang, X., Chen, J.M., Kerminen, V.-M., Petäjä,

3500 T., Worsnop, D.R., Kulmala, M. and Wang, L.: Atmospheric new particle formation from sulfuric acid and

3501 amines in a Chinese megacity, Science, 361, 278-281, 2018.

3502 Yasunaka, S., Siswanto, E., Olsen, A., Hoppema, M., Watanabe, E., Fransson, A., Chierici, M., Murata, A.,

3503 Lauvset, S. K., Wanninkhof, R., Takahashi, T., Kosugi, N., Omar, A. M., van Heuven, S., and Mathis, J. T.:

Arctic Ocean CO2 uptake: an improved multiyear estimate of the air–sea CO2 flux incorporating chlorophyll a concentrations, Biogeosciences, 15, 1643–1661, doi:10.5194/bg-15-1643-2018, 2018.

Ye, Z., Liu, J., Gu, A., Feng, F., Liu, Y., Bi, C., Xu, J., Li, L., Chen, H., Chen, Y., Dai, L., Zhou, Q., and Ge, X.: Chemical characterization of fine particulate matter in Changzhou, China, and source apportionment with offline aerosol mass spectrometry, Atmos. Chem. Phys., 17, 2573–2592, doi:10.5194/acp-17-2573-2017, 2017.

Ylivinkka, I., Kaupinmäki, S., Virman, M., Peltola, M., Taipale, D., Petäjä, T., Kerminen, V.-M., Kulmala, M., and Ezhova, E.: Clouds over Hyytiälä, Finland: an algorithm to classify clouds based on solar radiation and cloud base height measurements, Atmos. Meas. Tech., 13, 5595–5619, 2020.

He, Y., Chen, F., Jia, H., and Valery, G.: Bondur: Different Drought Legacies between Rain-fed and Irrigated Croplands in a Typical Russian Agricultural Region, Remote Sens., 12(11), 1700, doi:10.3390/rs12111700, 2020

Zaidan, M. A., Haapasilta, V., Relan, R., Junninen, H., Aalto, P. P., Kulmala, M., Laurson, L., and Foster, A. S.: Predicting atmospheric particle formation days by Bayesian classification of the time series features, Tellus B: Chem. Phys. Meteorol., 70, 10, doi:10.1080/16000889.2018.1530031, 2018a.

Zaidan, M. A., Haapasilta, V., Relan, R., Paasonen, P., Kerminen, V.-M., Junninen, H., Kulmala, M., and Foster, A. S.: Exploring non-linear associations between atmospheric new-particle formation and ambient variables: a mutual information approach, Atmos. Chem. Phys., 18, 12699-12714, doi:10.5194/acp-18-12699-2018, 2018b.

Zanatta, M., Laj, P., Gysel, M., Baltensperger, U., Vratolis, S., Eleftheriadis, K., Kondo, Y., Dubuisson, P., Winiarek, V., Kazadzis, S., Tunved, P., and Jacobi, H.-W.: Effects of mixing state on optical and radiative properties of black carbon in the European Arctic, Atmos. Chem. Phys., 18, 14037–14057, doi:10.5194/acp-18-14037-2018, 2018.

Zapadinsky, E., Passananti, M., Myllys, N., Kurten, T., and Vehkamäki , H.: Modeling on Fragmentation of Clusters inside a Mass Spectrometer, Journal of Physical Chemistry, A 123 (2), 611-624, https://doi.org/10.1021/acs.jpca.8b10744, 2019.

Zha, Q., Yan, C., Junninen, H., Riva, M., Sarnela, N., Aalto, J., Quéléver, L., Schallhart, S., Dada, L., Heikkinen, L., Peräkylä, O., Zou, J., Rose, C., Wang, Y., Mammarella, I., Katul, G., Vesala, T., Worsnop, D. R., Kulmala, M., Petäjä, T., Bianchi, F., and Ehn, M.: Vertical characterization of highly oxygenated molecules (HOMs) below and above a boreal forest canopy, Atmos. Chem. Phys., 18, 17437–17450, doi:10.5194/acp-18-17437-2018, 2018.

Zhang, J., Liu, C., and Chen, H.: The modulation of Tibetan Plateau heating on the multi-scale northernmost margin activity of East Asia summer monsoon in northern China, Global Planet. Change, 161, 149–161, 2018.

3538 Zhang, S., Zhang, J. H., Bai, Y., Koju, U. A., Igbawua, T., Chang, Q., Zhang, D., and Yao, F. M.: Evaluation
3539 and improvement of the daily boreal ecosystem productivity simulator in simulating gross primary
3540 productivity at 41 flux sites across Europe, Ecol. Model., 368, 205-232,
3541 doi:10.1016/j.ecolmodel.2017.11.023, 2018.

3542 Zhang-Turpeinen, H., Kivimäenpää, M., Aaltonen, H., Berninger, F., Köster, E., Köster, K., Menyailo, O.,
3543 Prokushkin, A., and Pumpanen, J.: Wildfire effects on BVOC emissions from boreal forest floor on
3544 permafrost soil in Siberia, Science of the Total Environment, 134851, doi:10.1016/j.scitotenv.2019.134851,
3545 2020.

3546 Zhao, H., Li, X., Zhang, Q., Jiang, X., Lin, J., Peters, G. P., Li, M., Geng, G., Zheng, B., Huo, H., Zhang, L.,
3547 Wang, H., Davis, S. J., and He, K.: Effects of atmospheric transport and trade on air pollution mortality in
3548 China, Atmos. Chem. Phys., 17, 10367–10381, doi:10.5194/acp-17-10367-2017, 2017.

3549 Zhdanova, E. Y., Chubarova, N. Y., and Lyapustin, A. I.: Assessment of urban aerosol pollution over the
3550 Moscow megacity by the MAIAC aerosol product, Atmos. Meas. Tech., 13, 877–891, doi:10.5194/amt-13-
3551 877-2020, 2020.

3552 Zhou, Y., Dada, L., Liu, Y., Fu, Y., Kangasluoma, J., Chan, T., Yan, C., Chu, B., Daellenbach, K. R.,
3553 Bianchi, F., Kokkonen, T. V., Liu, Y., Kujansuu, J., Kerminen, V.-M., Petäjä, T., Wang, L., Jiang, J., and
3554 Kulmala, M.: Variation of size-segregated particle number concentrations in wintertime Beijing, Atmos.
3555 Chem. Phys., 20, 1201–1216, doi:10.5194/acp-20-1201-2020, 2020.

3556 Zilitinkevich, S., Druzhinin, O., Glazunov, A., Kadantsev, E., Mortikov, E., Repina, I., and Troitskaya, Y.:
3557 Dissipation rate of turbulent kinetic energy in stably stratified sheared flows, Atmos. Chem. Phys., 19, 2489–
3558 2496, doi:10.5194/acp-19-2489-2019, 2019.

3559 Öström, E., Putian, Z., Schurgers, G., Mishurov, M., Kivekäs, N., Lihavainen, H., Ehn, M., Rissanen, M. P.,
3560 Kurtén, T., Boy, M., Swietlicki, E., and Roldin, P.: Modeling the role of highly oxidized multifunctional
3561 organic molecules for the growth of new particles over the boreal forest region, Atmos. Chem. Phys., 17,
3562 8887–8901, doi:10.5194/acp-17-8887-2017, 2017.

3563

Non-stressed conditions

Transpiration draws water from the leaves

Leaves absorb carbon in photosynthesis

The chain of water molecules is pulled upward

Sugars are transported from sources to sinks

Roots take up water from the soil

Water potential

Sugar concentration

Cold soil in spring

Low canopy conductance

Increased stomatal and non-stomatal limitations to photosynthesis

Low sink strength

Low belowground hydraulic conductance

Water potential

Sugar concentration

3564

3565   Figure 1.

3566

3567

3568   Figure 2.

3569
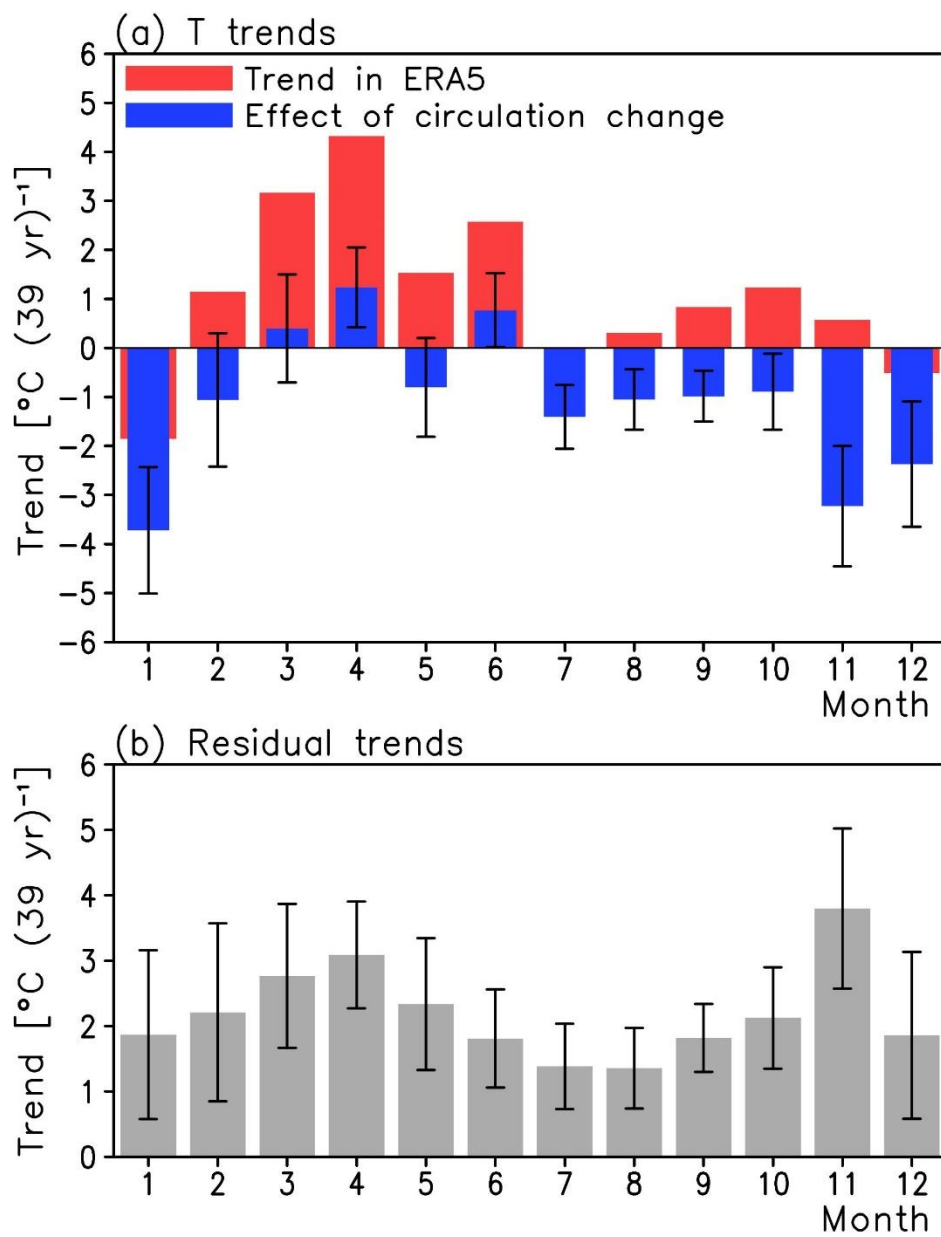
3570

3571   Figure 3.

3572
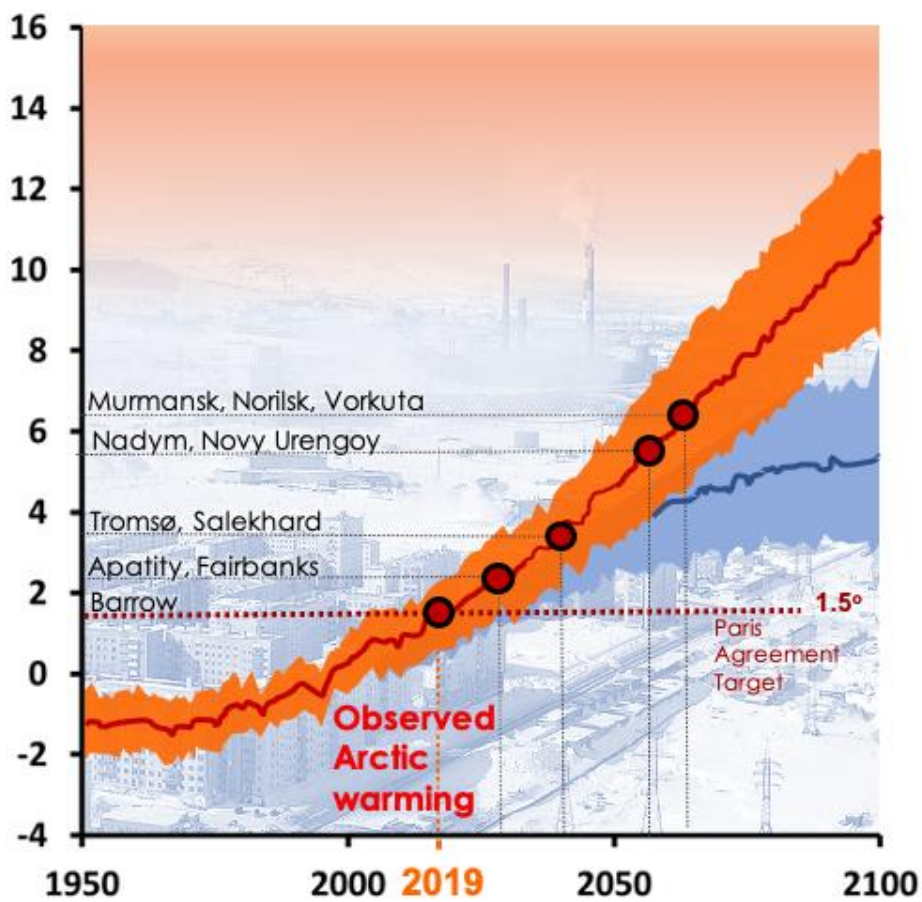
3573

3574   Figure 4.
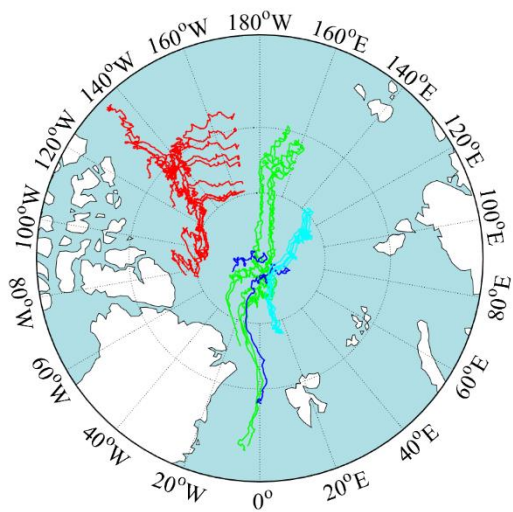
3575

3576   Figure 5.

3577
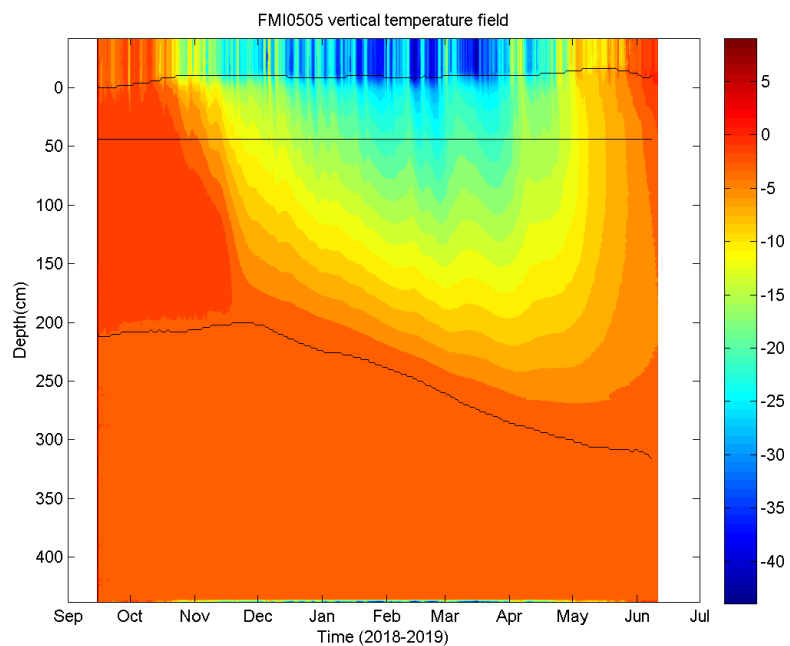
3578

3579   Figure 6.

3580
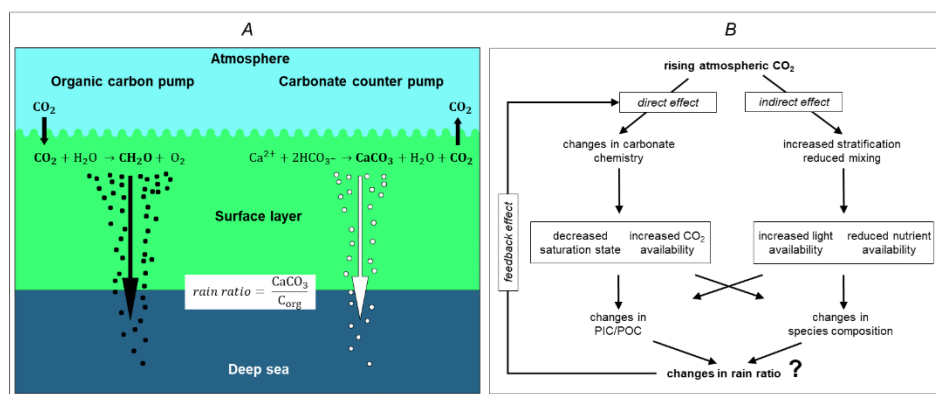
3581

3582   Figure 7.

3583
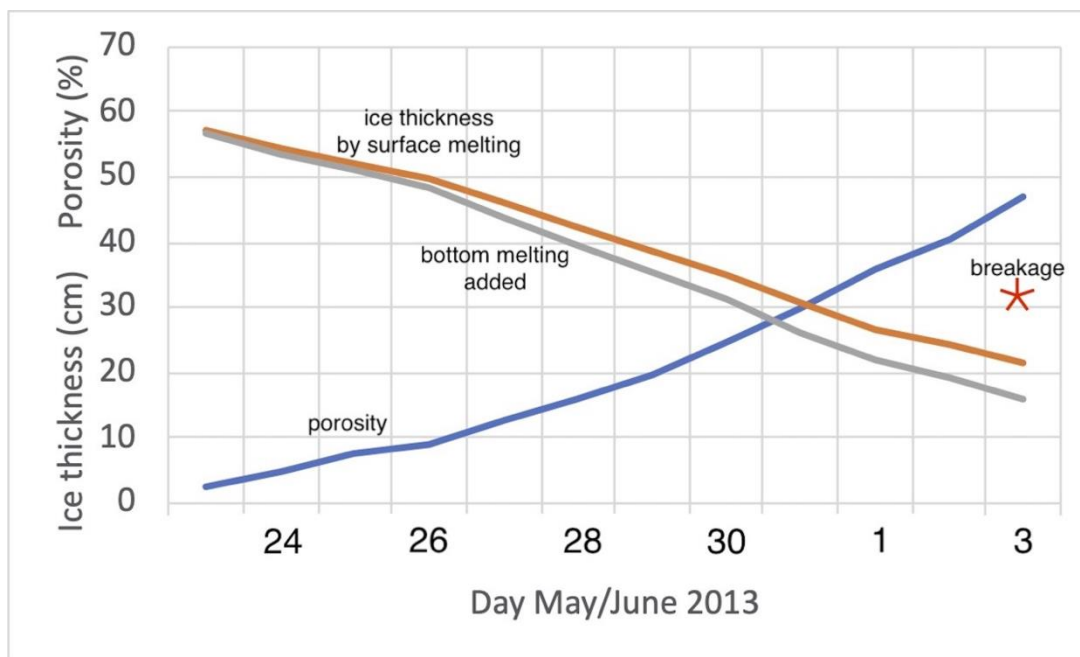
3584

3585   Figure 8.
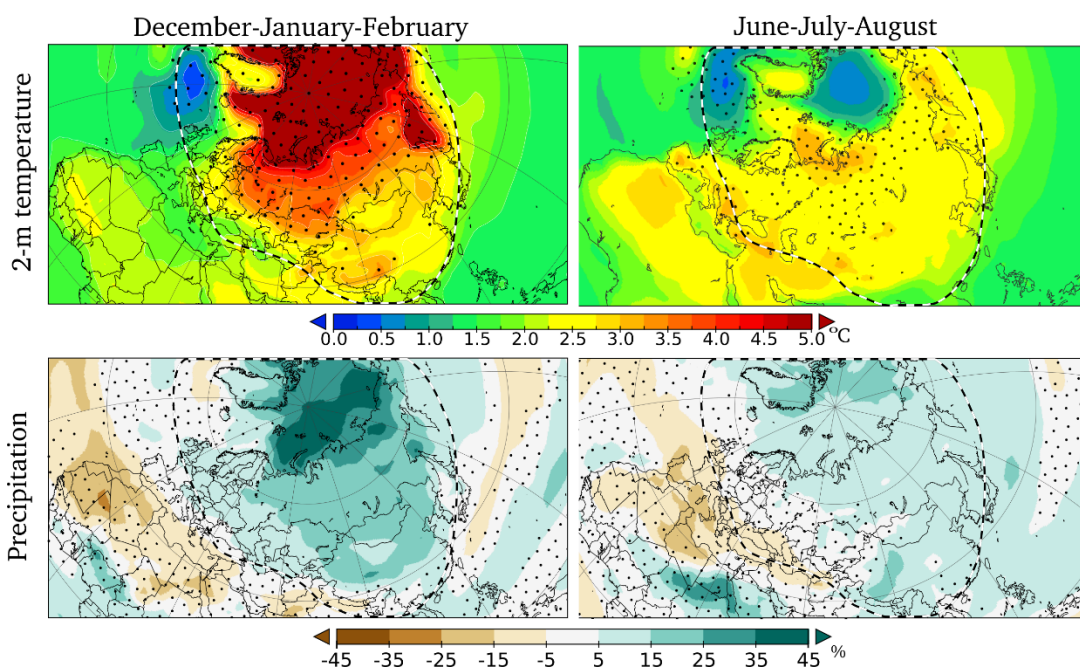
3586

3587   Figure 9.

3588

3589

3590

3591

3592   **Figure 1.** A recent field and modelling study shows that cold soil decreases belowground hydraulic

3593   conductance (i.e. less root water uptake), and further canopy conductance in mature, boreal trees in spring

3594 (Lintunen et al. 2020). Cold temperature also decreases sink strength (i.e. less sugars are needed for

3595 metabolism and growth). Low sink strength increases sugar concentration in leaves, which decreases

3596 photosynthesis due to increased stomatal and non-stomatal limitations for photosynthesis (Hölttä et al., 2017;

3597 Salmon et al., 2020).

3598 **Figure 2.** Example of results from the state-of-the-art aerosol instruments NAIS and PSM displaying NPF

3599 event at Fonovaya station, Siberia, on 22.09.2019. Particles of different polarity, NAIS (a), ions of different

3600 polarity, NAIS (b), particle number distribution at the smallest sizes, PSM (c), number concentration of the

3601 smallest particles in different size bins, PSM (d).

3602

3603 **Figure 3.** Linear trends of monthly mean temperature in Western Siberia (55°-65°N, 65°-90°E) in years

3604 1979-2018. In (a), the red bars show the trend in the ERA5 reanalysis and the blue bars the circulation-

3605 related trend. In (b), the residual trends are shown. The error bars indicate the 5-95% uncertainty range in the

3606 circulation-related trend and the residual trend based on interannual variability. Redrawn from Räisänen

3607 (2021).

3608

3609 **Figure 4.** The northern urban heat islands are forerunners of the global warming. Winter season future

3610 temperatures for the Arctic (60–90°N) averaged over 36 CMIP5 global climate models and expressed as

3611 departures from the means for the 1981–2005 period. The red line is the ensemble mean for RCP8.5, the blue

3612 line is for RCP4.5. Shaded areas denote ± one standard deviation from the ensemble mean (Overland et al.,

3613 2014; and Fig. 2.15 of AMAP, 2017). The observed surface UHIs are shown as red dots collocated with the

3614 expected future Arctic temperature anomalies, e.g., the observed wintertime urban temperature anomaly in

3615 Nadym corresponds to the regional warming as expected to be reached by 2060. Observe that the present

3616 Arctic climate is already 1.5°C warmer than the historical normals 1960-1990.

3617

3618 **Figure 5.** Trajectories of SIMBA buoys deployed in the Arctic in the period 2018-2019. Red: CHINARE (10

3619 buoys), green: NABOS (5 buoys), dark blue: CAATEX (2 buoys), and light blue: MOSAiC (15 buoys).

3620 SIMBA is a thermistor string-based ice mass balance (IMB) buoy. It measures high-resolution (2 cm)

3621 vertical environment temperature (ET) profiles (4 times a day) through the air-snow-sea ice-ocean column.

3622 The heating temperature (HT) measured by the thermistor string once per day is based on the use of a small

3623 identical heater on each sensor. The ET and HT data are used to derive snow depth and ice thickness.

3624 SIMBA uses GPS module to track the buoy location. The Iridium satellite is used for data transmission. A

3625 total 15 SIMBA buoys have been deployed in the Arctic Ocean during the Chinese National Arctic Research

3626 Expedition (CHINARE) 2018 and the Nansen and Amundsen Basins Observational System (NABOS) 2018

3627 field expeditions in late autumn. In 2019 17 SIMBA buoys were deployed during the CAATEX (2) and

3628 MOSAIC expeditions (15, leg 1).

3629

3630 **Figure. 6**. SIMBA observations on the temporal evolution of the snow depth, ice thickness, and the

3631 temperature profile from the ocean through snow and sea ice to air. The results were obtained applying the

3632 algorithm by Liao et al. (2018). The black lines are snow surface (top), Initial freeboard (middle) and ice

3633 base (bottom). 0 level refers to snow/ice interface. The colors indicate the temperature in ºC.

3634 **Figure 7**. **A**: Biological pumps resulting in (i) atmospheric CO_2 sink and(ii) calcium carbonate transport

3635 from surface to deep ocean; **B**: anticipated forward and feedback alterations in ocean ecology driven by

3636 atmospheric CO2 increase. PIC=particulate inorganic carbon; POC=particulate organic carbon (modified

3637 after Rost & Riebesell, 2004).

3638 **Figure 8**. Field data for ice decay in Lake Kilpisjärvi in 2013 showing decrease of ice thickness by surface

3639 melting and bottom melting and increase of porosity until breakage of ice cover.

3640

3641 **Figure 9.** Changes in 2-meter temperature (ºC, upper panels) and precipitation (%, lower panels) during the

3642 21st century. Present-day climatology is averaged over years 1981-2010 and end-of-century climatology

3643 over 2070-2099. Winter (left) and summer (right) are shown separately. Dotted areas indicate high

3644 variability in model ensemble (for temperature: standard deviation of 21st century change exceeds 1ºC; for

3645 precipitation: standard deviation of 21st century change exceeds 100% or present-day precipitation). The

3646 model results are from IPCC AR5, based on 42 individual models in CMIP5 experiments under the RCP4.5

3647 scenario.

3648

3649 **Table 1**. Systems, key topical areas, research question introduced in the PEEX Science Plan (SP) (Kulmala

3650 et al. 2015; 2016a, Lappalainen et al. 2018) connected to the addressed research themes over last 5 yeas by

3651 the PEEX questionary (APPENDIX 1). The addressed research themes and the results are overviewed in

3652 section 3.

3653

3654

PEEX – SP System	PEEX - SP key topical area	PEEX - SP research question (Q-No)	Addressed research themes during the last 5 years
Land	Changing land ecosystem processes	**How could the land regions and processes that are especially sensitive to climate change be identified, and what are the best methods to analyze their responses? (Q-1)**	• high-latitude photosynthetic productivity and vegetation changes (greening, browning) • new methodologies determining Earth surface characteristics
Land	Risk areas of permafrost thawning	**How fast will permafrost thaw proceed, and how will it affect ecosystem processes and ecosystem-atmosphere feedbacks, including hydrology and greenhouse gas fluxes ? (Q-2)**	• soil temperature evolution • changing GHG fluxes, carbon sink-source dynamics due to permafrost thawning

Land	Ecosystem structural changes	**What are the structural ecosystem changes and tipping points in the future evolution of the Pan-Eurasian ecosystem? (Q-3)**	• changes in soil microbial activity e.g. effect of forest fires • changes of the Northern soils and functioning of the Arctic tundra in global carbon cycling context
Atmosphere	Atmospheric composition and chemistry	**What are the critical atmospheric physical and chemical processes with large-scale climate implications in a northern context? (Q4)**	• carbon (C) balance in the boreal forests; methane (CH_4) balance at the Arctic; carbon monoxide (CO), ozone (O_3) at the Northern Eurasian region • Sources and properties of atmospheric aerosols in boreal and Arctic environments • black carbon and dust in the atmosphere and on snow at the Northern high latitudes • methodological and model developments related to atmospheric chemistry and physics
Atmosphere	Urban air quality and megacities, ABL	**What are the key feedbacks between air quality and climate at northern high latitudes and in China? (Q5)**	• recent observations on air quality in China • Anthropogenic emissions and environmental pollution in Russia
Atmosphere	Weather and atmospheric circulation	**How will atmospheric dynamics (synoptic scale weather, boundary layer) change in the Arctic-boreal regions? (Q6)**	• cold & warm episodes • cyclone density dynamics • circulation effect on temperature and moisture • cloudiness in Arctic • atmospheric boundary layer (ABL) dynamics
Water	The Artic Ocean in the climate system	**How will the extent and thickness of the Arctic sea ice and terrestrial snow cover change? (Q-7)**	• Sea ice dynamics and thermodynamics with atmospheric and ocean dynamics • Snow depth/mass and sea ice thickness • Sea ice research supporting navigation • Ocean floor, sediments: composition and fluxes • River runoff effecting the hydrological processes at coastal marine environments in Russia
Water	Arctic marine ecosystem	**What is the joint effect of Arctic warming, ocean freshening, pollution load and acidification on the Arctic marine ecosystem, primary production and carbon cycle? (Q-8)**	• Living marine organisms weaken or even subdue CO_2 accumulation

Water	Lakes and large-scale river systems	**What is the future role of Arctic-boreal lakes, wetlands and large river systems, including thermokarst lakes and running waters of all size, in biogeochemical cycles, and how will these changes affect societies) ? (Q-9)**	• organic carbon, carbon balance, ice cover at lakes in the Northern high latitudes • specific charachteristis of the Lake Baikal and Selenga River delta in Russia • specific charachteristis of Asian water lakes
Society	Anthropogenic impact	**How will human actions such as land-use changes, energy production, the use of natural resources, changes in energy efficiency and the use of renewable energy sources influence further environmental changes in the region? (Q-10)**	• Mitigation e.g method for the natural risk assessment in Russia and new clean energy technologies
Society	Environmental impact	**How do the changes in the physical, chemical and biological state of the different ecosystems, and the inland, water and coastal areas affect the economies and societies in the region, and vice versa? (Q-11)**	• Reindeer grazing effects on the ground vegetation structure and biomass
Society	Natural hazards	**In which ways are populated areas vulnerable to climate change? How can their vulnerability be reduced and their adaptive capacities improved? What responses can be identified to mitigate and adapt to climate change? (Q-12)**	• Emerging zoonotic diseases • UV variation effects on health • Air pollution in different scales and environments (street-level urban air pollution, transported air pollution in urban environments, air pollution at the Arctic) and related health effects;
Feedbacks	Key topics: Atmospheric composition, biogeochemical cycles: water, C, N, P, S	**How will the changing cryospheric conditions and the consequent changes in ecosystems feed back to the Arctic climate system and weather, including the risk of natural hazards? (Q-13)**	• *Research needs:* quantification of the COntinental Biosphere-Aerosol-Cloud-Climate (COBACC) feedback loop at different Northern boreal environments • Gold & high region quantification of BVOC – aerosols feedback loop at the Tibetan /Himalayan Plateau:_
Feedbacks	Key topics: Atmospheric composition, biogeochemical cycles: water, C, N, P, S	**What are the net effects of various feedback mechanisms on (i) land cover changes, (ii) photosynthetic activity, (iii) GHG exchange and BVOC emissions (iv) aerosol and cloud formation and radiative forcing ? How do these vary with climate change on regional and global scales? (Q-14)**	• *Research needs:* The Arctic greening and browning calls for a multi-discipilinary scientific approach together, improved modelling tools and new data in order to solve scientific questions related to the net effects of various feedback mechanisms connecting the biosphere-atmosphere - human activities

Feedbacks	Key topics: Atmospheric composition, biogeochemical cycles: water, C, N, P, S	**How are intensive urbanization processes changing the local and regional climate and environment? (Q-15)**	• *Research needs:* accelerating urbanization calls for studies on the effects of on air pollution, local climate and the effects these changes have on global climate. Integrated studies should lead to services for society, cities helping to mitigate hazards storms, flooding, heat waves, and air pollution episodes (see also 3.2.1)

Table 2. Hydrogeochemical signature of large river system –Selenga River case study. The figure represent metal(loid)s partitioning (Median values) in the Selenga river basin in the upper (Mongolian) and downstream (Russian) part between 20 July -10 August 2011 under dominant high water (A) and 07 June -10 July 2012 under dominant low water conditions. Dark orange fill corresponds to the share of suspended forms of elements > 75% (green), light orange – 75-50% , light blue – 50-25%, dark blue – < 25%. The figure indicate that in the large river system some metals are mostly found in the dissolved form (84–96% of Mo, U, B, and Sb on an average), whereas many others predominantly existed in suspension (66–87% of Al, Fe, Mn, Pb, Co, and Bi). A consistently increasing share of metals in suspended particulate modes (about 2–6 times) is observed under high discharge conditions For details and other hydrological seasons refer to (Kasimov et al., 2020b).

Code/Data availability: This is an review paper and the data availabity is introduced in the original articles.

Author contribution: Co-authors have provided text and/or relevant references. Some of them have been editors of the specific chapters of the manuscript.

Competing interests: no spesific competing interests